8-15-2017

Investigating Core Shale Depositional Environments of Late Pennsylvanian Cyclothems Utilizing Geochemical Proxies to Test the Superestuarine Model

Bryce A. Mathis
Louisiana State University and Agricultural and Mechanical College

INVESTIGATING CORE SHALE DEPOSITIONAL ENVIRONMENTS OF LATE PENNSYLVANIAN CYCLOTHEMS UTILIZING GEOCHEMICAL PROXIES TO TEST THE SUPERESTUARINE MODEL

A Thesis

Submitted to the Graduate Faculty of
Louisiana State University and
College of Science
In partial fulfillment of the
Requirements for the degree of
Master of Science

in

The Department of Geology and Geophysics

by
Bryce A. Mathis
B.S., Texas Tech University, 2012
December 2017

ACKKNOWLEDGEMENTS

I would like to thank my advisor Dr. Achim Herrmann for his guidance and the opportunity to work on this NSF funded research. This gratitude is also extended to my committee members, Dr. Samuel Bentley and Dr. Carol Wilson, for their time and feedback on this project. I would also like to thank my friend and research group partner Adam Turner for his assistance in the lab collecting and organizing data, and for all his helpful advice. I want to thank all the close friends I made at LSU for their generous support, and making my time here exciting and unforgettable. And lastly, I want to give a special thanks to my family for their never-ending love, encouragement, and support throughout my education and all other aspects of my life; without which, none of this would have been possible.

TABLE OF CONTENTS

ACKNOWLEDGMENTS…….. ii

ABSTRACT……. iv

CHAPTER

1. INTRODUCTION…… 1

2. GEOLOGIC BACKGROUND……. 8
   - 2.1 Paleogeographic Setting…….. 8
   - 2.2 Paleoclimate and Regional Hydrology……..10
   - 2.3 Cyclothem Deposits and Lateral Facies Variations…….. 11

3. METHODS AND MATERIALS…… 24
   - 3.1 Sampling……... 24
   - 3.2 Nitrogen Isotope Analysis……. 26
   - 3.3 Elemental Analysis……... 26

4. RESULTS……... 26
   - 4.1 Internal Stratigraphy and Correlation of Hushpuckney Shale…….. 29
   - 4.2 Nitrogen Isotope and Organic Carbon Trends…….. 35
   - 4.3 Elemental Trends…….. 37

5. DISCUSSION……. 39
   - 5.1 Isotopic Fractionation of Nitrogen in Core Shales……... 39
   - 5.2 Texas Eastern Shelf: Depositional Environment of the Upper Salesville Shale……. 42
   - 5.3 LPMS: Depositional Environments of the Hushpuckney Shale……... 47

6. CONCLUSIONS…… 57

REFERENCES……. 60

APPENDIX: GEOCHEMICAL DATA……... 71

VITA……..87

ABSTRACT

The Late Paleozoic Midcontinent Sea (LPMS) inundated vast areas of the North American interior during glacio-eustatic transgressions, depositing widespread black shales facies within the core shale intervals of major cyclothems. These black shale deposits are unique because no modern analogs can adequately explain the depositional environments and model for organic matter preservation across such vast ancient epicontinental settings. One possible explanation is that a *superestuarine circulation* system developed across the LPMS during humid interglacial phases, which promoted strong water column stratification and benthic anoxia.

The goal of this research was to test the validity of *the superestuarine estuarine model* and its key features. Specifically, whether preconditioned (i.e. oxygen-poor and intermittently denitrified) waters from the eastern tropical Panthalassic Ocean (etPan) laterally advected into epicontinental settings in tandem with large-scale, quasi-estuarine circulation and pycnocline formation, resulting in stronger reducing conditions in locations proximal to the paleoshoreline. Samples were collected from one Late Pennsylvanian cyclothemic core shale, the Hushpuckney Shale Member of the Swope Formation, and its lateral equivalents across five locations. This research utilized $\delta^{15}N$ values, elemental, and TOC-S concentrations as spatio-temporal proxies for evaluating redox gradients and paleocirculation patterns across the study sites.

Analysis revealed that samples from Eastern Shelf of Texas are organic-poor, maintain background $\delta^{15}N$ values, and express no enrichments in paleoredox proxies. In contrast, samples from the Midcontinent Shelf and Illinois Basin of the LPMS show an increasing gradient in TOC, $\delta^{15}N$, U, and Mo approaching the paleoshoreline. These results support the hypothesis that superestuarine circulation produced stronger reducing conditions in shallow, proximal locations of the LPMS. However, this model does not appear to be applicable for core shale deposits on

the Eastern Shelf of the Permian Basin Seaway, where sediment dilution and depth-stratification may have influenced organic preservation and redox conditions. The data also does not support the idea that preconditioned seawater advected from the etPan to epicontinental environments during core shale deposition. Instead, it appears that widespread benthic anoxia across the LPMS was a function of strong water column stratification associated with continental runoff, combined with large settling fluxes of both terrestrial and marine organic detritus.

1. INTRODUCTION

During the Middle Pennsylvanian to Early Permian, the North American interior was repeatedly inundated by a vast and relatively shallow epicontinental sea known as the Late Paleozoic Midcontinent Sea (LPMS) (Figure 1; Heckel, 1977, 1991, 1994). At its maximum extent, the LPMS covered an area of ~2.1 x 10^6 km^2 making it larger than any modern epicontinental seas such as the Baltic Sea (0.42 x 10^6 km^2), Gulf of Carpentaria (0.51 x 10^6 km^2), and Hudson Bay (1.2 x 10^6 km^2) (Algeo et al., 2008a; Algeo and Heckel; 2008). However, unlike these modern seas, which have either permanently or intermittently oxic deepwaters, the LPMS bottomwaters were subjected to extended intervals of anoxia during glacioeustatic highstands, resulting in the accumulation of organic-rich black shales (Heckel, 1977, 1991; Algeo et al., 2004, 2008a). These "core shales," named for their central position within the vertical succession of major cyclothems, are laterally extensive and can be traced from Texas, Oklahoma, and Kansas northeastward to Iowa and Illinois (Figure 2; Heckel, 1977, 1994; Youle et al., 1994; Watney et al., 1995; Algeo and Heckel, 2008). The black shale intervals are characterized by fine grain size, abundant phosphatic granule layers, lack of biota other than nektic and pelagic organisms (Heckel, 1977), and enriched with high concentrations of organic matter and redox-sensitive trace-metals (Coveney et al., 1991; Hoffman et al., 1998; Algeo et al., 2004a). These features are commonly thought to reflect slow accumulation rates in sediment-starved, distal offshore settings with oxygen-depleted (and possibly euxinic) bottomwaters (Heckel, 1977, 1994, 2008; Algeo et al., 2004b; Algeo and Heckel, 2008).

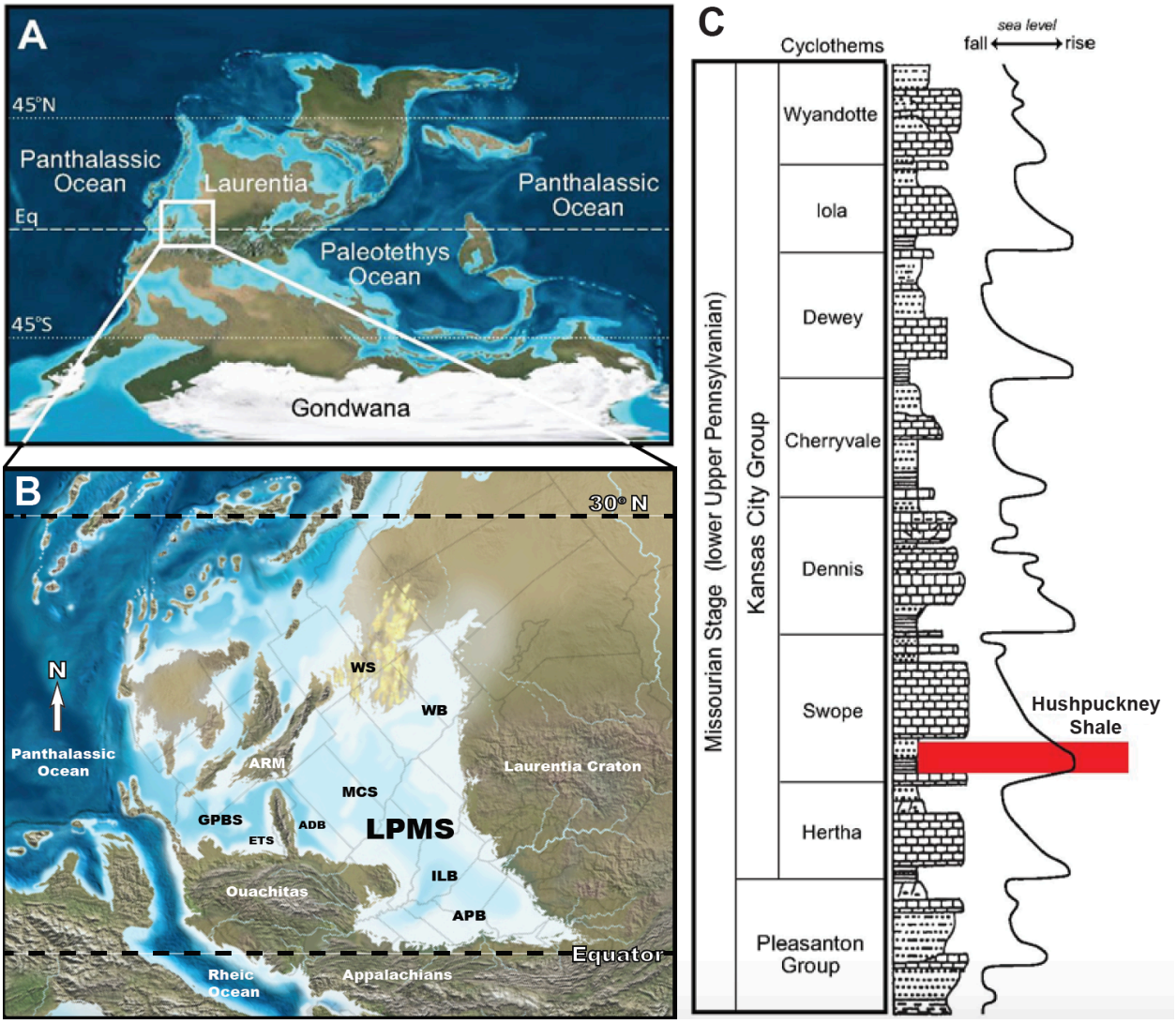

Figure 1: Paleogeographic setting of the Late Paleozoic Midcontinent Sea (LPMS) and stratigraphy of the Hushpuckney Shale. (A) Global paleogeographic rendering of the Pennsylvanian (courtesy of R. Blakey; http://jan.ucc.nau.edu/rcb7/300Marcet.jpg). The LPMS (white box) was situated within the tropical to subtropical latitudes at the western margin of Laurentia. (B) Regional paleogeography of the LPMS displaying its internal and external constituents: ADB = Anadarko Basin, APB = Appalachian Basin, ARM = Ancestral Rocky Mountains, ETS = Texas Eastern Shelf (i.e. Eastern Shelf of Midland Basin), GPBS = Greater Permian Basin Seaway, ILB = Illinois Basin, MCS = Midcontinent Shelf, WB = Williston Basin, WS = Wyoming Shelf. (C) Stratigraphy of the Missourian Stage in North America. The Hushpuckney Shale is the "core shale" of the Swope Formation in the Midcontinent-type cyclothems. Modified from *Algeo et al.* (2004, 2008a).

The black shale deposits of Late Paleozoic cyclothems are unique in that no modern analogs can adequately explain the depositional environments and the model for organic matter preservation across such vast ancient epicontinental settings (Arthur and Sageman, 1994; Algeo and Heckel, 2008). Modern systems conducive to black shale deposition are primarily located in oceanic or continent-margin settings and classified either as *silled basins*, such as the Black Sea, Cariaco Basin, and Santa Barbara Basin; or continental margin *upwelling zones*, such as the Namibian and Peruvian Shelf (Demaison and Moore, 1980; Thiede and Suess, 1983; Wignall, 1994; Arthur and Sageman, 1994; Hay, 1995). Upwelling systems tend to produce patchy concentrations of organic-rich deposits along a linear trend reflecting localized zones of upwelling on a continental margin (Calvert and Price 1983; Arthur and Sageman, 1994). Silled basins generally exhibit gradual depletions in trace-metal enrichments under prolonged periods or intensification of benthic anoxia due to restricted watermass renewal (Algeo and Lyons, 2006; Algeo and Tribovillard, 2009). Paleogeographic reconstructions and temporal trace element data from cyclothemic black shales suggest that the LPMS had sufficient watermass exchange with the open ocean (Algeo et al., 2004; Algeo and Maynard, 2008; Algeo and Tribovillard, 2009), which precludes the silled basin model. The widespread deposition of thin black shales across a broad epicontinental sea also implies that the upwelling model is not fittingly applicable.

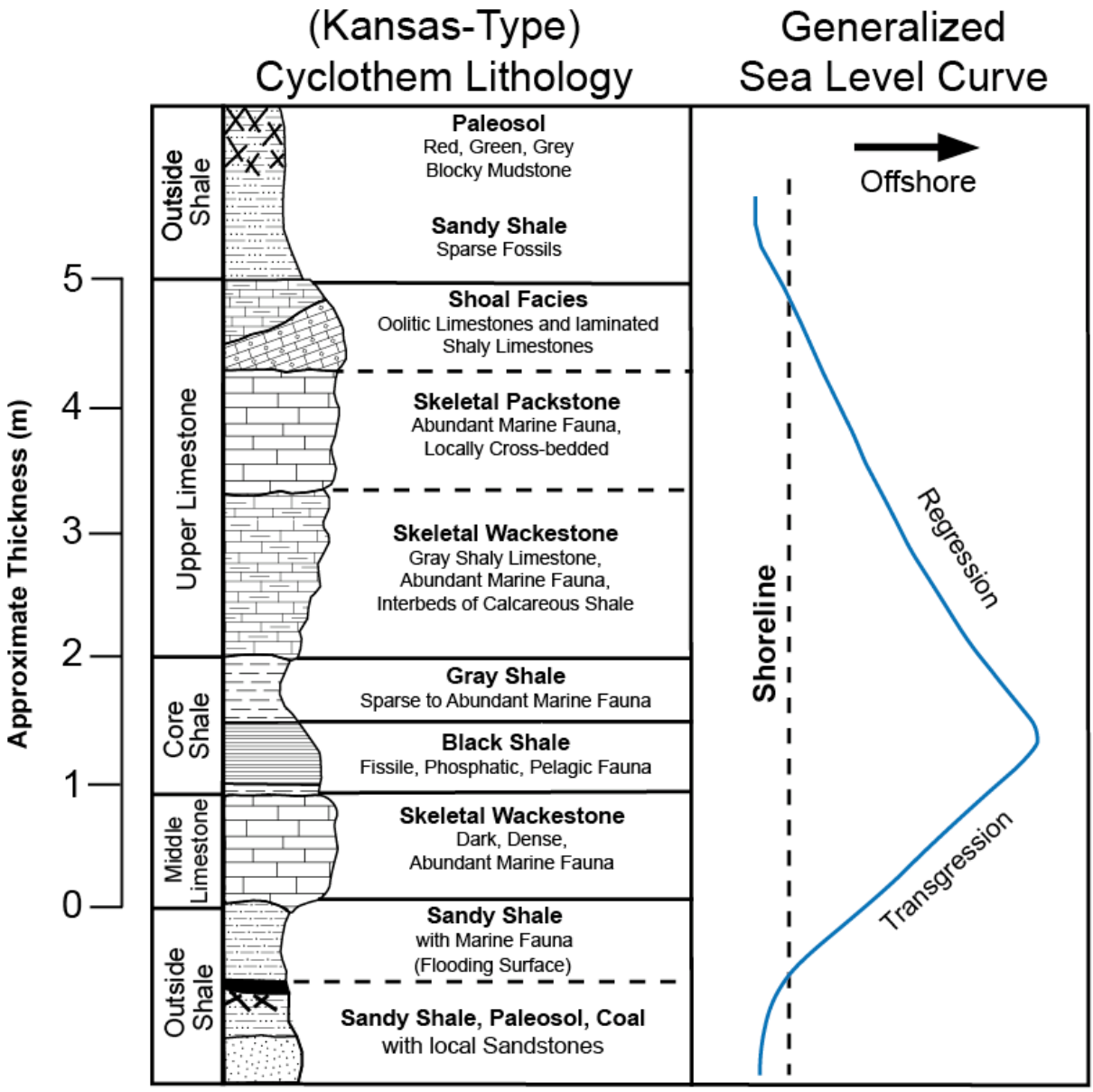

Figure 2: A basic vertical succession of a Midcontinent (Kansas) type major cyclothem showing the average thickness for each unit deposited during a single transgressive-regressive cycle. Modified from *Heckel* (1994).

Because no modern epicontinental seas or anoxic marine settings adequately apply to the LPMS, it has been proposed that it become the type example of a *superestuarine circulation system* characterized by large-scale quasi-estuarine circulation and pycnocline formation, unrestricted deepwater exchange, and lateral advection of "preconditioned" (i.e. oxygen-

depleted, intermittently denitrified) deepwaters facilitating the development of benthic anoxia and black shale deposition (Figure 3; Algeo et al., 2008a; Algeo and Heckel, 2008). Key boundary conditions promoting superestuarine circulation and benthic anoxia in the LPMS were (1) a humid paleoclimate resulting in enhanced precipitation with strong continental runoff, (2) a mostly landlocked setting, (3) shallow seafloor bathymetry (<100 m), (4) a deepwater connection to the global ocean, and (5) location of the entrance to this deepwater connection in a region of extreme shallowing of the oxygen-minimum zone (OMZ) in the eastern tropical Panthalassic Ocean (etPan) (Algeo and Heckel, 2008). In this model, intermediate waters from the OMZ of the etPan delivered oxygen-depleted and intermittently denitrified waters directly into the deepwater corridor of the Permian Basin Seaway (Algeo et al., 2008a). Slow transit of these bottomwaters through the ~1000-km-long, stratified seaway maintained the oxygen-deficient status of the water mass prior to low-intensity upwelling out of the deep basins and onto the shallow epicontinental shelf environments. At the same time, strong continental runoff from surrounding landmasses (associated with wet climate conditions) produced an extensive freshwater lens, which yielded a strong regional pycnocline and generated a large-scale quasi-estuarine circulation system (Algeo et al., 2008a; Algeo and Heckel, 2008). The preconditioned waters that were welled up onto the shelf margin became entrained in the shoreward-flowing bottomwaters of the estuarine circulation, and laterally advected across extensive portions of the epicontinental sea beneath this pycnocline. Benthic anoxia was maintained and intensified as the bottomwaters advected further inland due to pycnoclinal strengthening proximal to sources of freshwater runoff. The strength of this pycnocline varied spatially (with distance from the shoreline) and temporally (with changes in freshwater input as climate conditions varied during

cyclothem deposition), resulting in geochemical gradients across the LPMS (Hoffmann et al., 1998; Algeo et al., 2008; Algeo and Heckel, 2008).

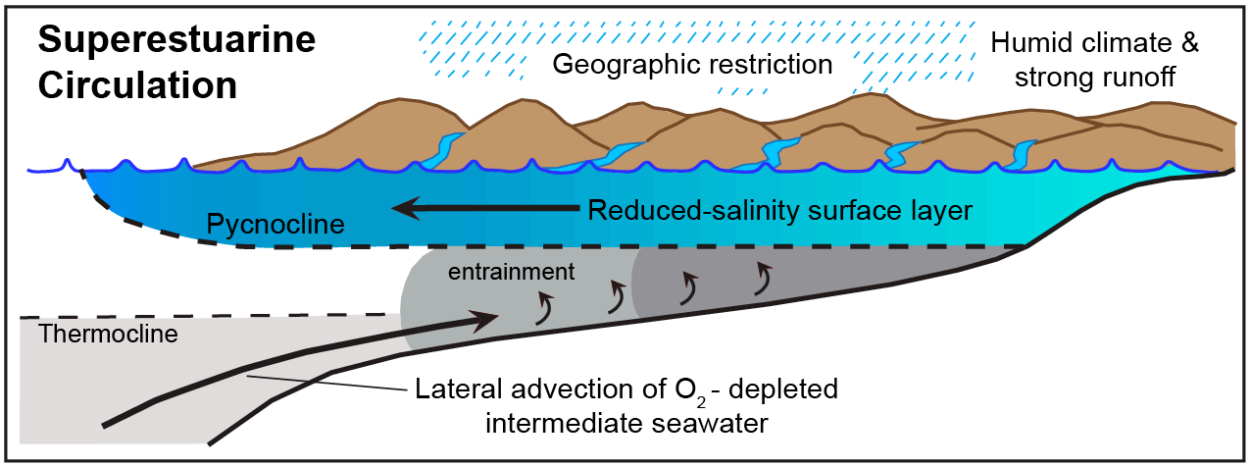

Figure 3: Model of the environmental and boundary conditions for marine anoxia in superestuarine circulation systems of epicontinental seas. Modified from *Algeo et al.* (2008b).

In order to establish the parameters under which a dynamic system of this type could exist, the *superestuarine circulation model* requires tests against a range of paleoceanographic and biogeochemical conditions to support its validity as a type analog for benthic anoxia and black shale deposition in ancient epicontinental seas. This study utilizes geochemical data (nitrogen isotopes, major-element, trace-element, and total organic carbon and sulfur (TOC-TS) concentrations for bulk sediment samples) as spatiotemporal proxies for determining the variations in redox gradients and oceanographic conditions during core shale deposition.

The goal of this study is to test the hypothesis that preconditioned intermediate waters from the etPan were laterally advected into shallow, North American cratonic-interior seas where superestuarine circulation and pycnocline formation resulted in intensely reducing bottomwaters, thus facilitating extensive black shale deposition across various depths during glacio-eustatic highstands of the Pennsylvanian (Figure 3). Unlike previous cyclothemic core shale studies which analyze multiple sections from individual cratonic regions (i.e. Midcontinent Shelf,

Illinois Basin, and Texas Eastern Shelf), this research analyzes samples acquired in all these regions from one laterally extensive and correlatable core shale, the Hushpuckney Shale Member of the Swope Cyclothem and its stratigraphic equivalents, forming a transect that ties together constituent regions of the Permian Basin Seaway with the LPMS.

2. GEOLOGIC BACKGROUND

2.1 PALEOGEOGRAPHIC SETTING

The LPMS was a mostly enclosed epicontinental sea, surrounded by landmasses that varied greatly in character (Figure 1B and 4). To the south and southeast, the Appalachian-Ouachita orogenic belt was a long and nearly continuous mountain arc system that formed through the tectonic collisions of Laurentia and Gondwana during the creation Pangea. One of the outliers to this orogenic complex was the ~500-km-long Amarillo-Wichita Uplift, which was active during the Middle to Late Pennsylvanian, and separated the LPMS from the Texas Eastern Shelf and Palo Duro, Midland, Delaware, and Val Verde basins to the southwest (i.e. the Greater Permian Basin Seaway; Handford et al., 1981; Budnick, 1989). Another outlier to the Ouachita orogenic belt was the low-lying Ozark Uplift (consisting of the Ozark Dome and Plateau) that remained active throughout the Pennsylvanian, and projected towards the Illinois Basin (Houseknecht et al., 1993). To the east and northeast of the LPMS, the Laurentian Craton was emergent but considered mostly low-relief (Algeo et al., 2008a). The northern, arid region of the LPMS consisted of the Wyoming Shelf and Wyoming Straits where lithofacies associations indicate evaporitic lagoons, shoals, and migrating dune fields prevailed in this area (Desmond et al., 1984; Maughan, 1993; Algeo et al., 2008a). Water depths through this passage were shallow, perhaps ~10 meters or less, during maximum eustatic highstands (Desmond et al., 1984; Maughan, 1993; Garfield et al., 1988). To the northwest, the LPMS was bordered by the Ancestral Rocky Mountains, which rose to moderate elevations during the Middle-Late Pennsylvanian to Early Permian (Kluth, 1986; Miller et al., 1992). The only significant connection the LPMS had to the open ocean, via the Permian Basin Seaway, was a deep (> 100 m) and narrow (~ 30 – 40 km) passage way known as the “Panhandle Strait” located at the

western end of the Amarillo-Wichita Uplift (Handford et al., 1981; Budnik, 1989; Algeo et al., 2008a).

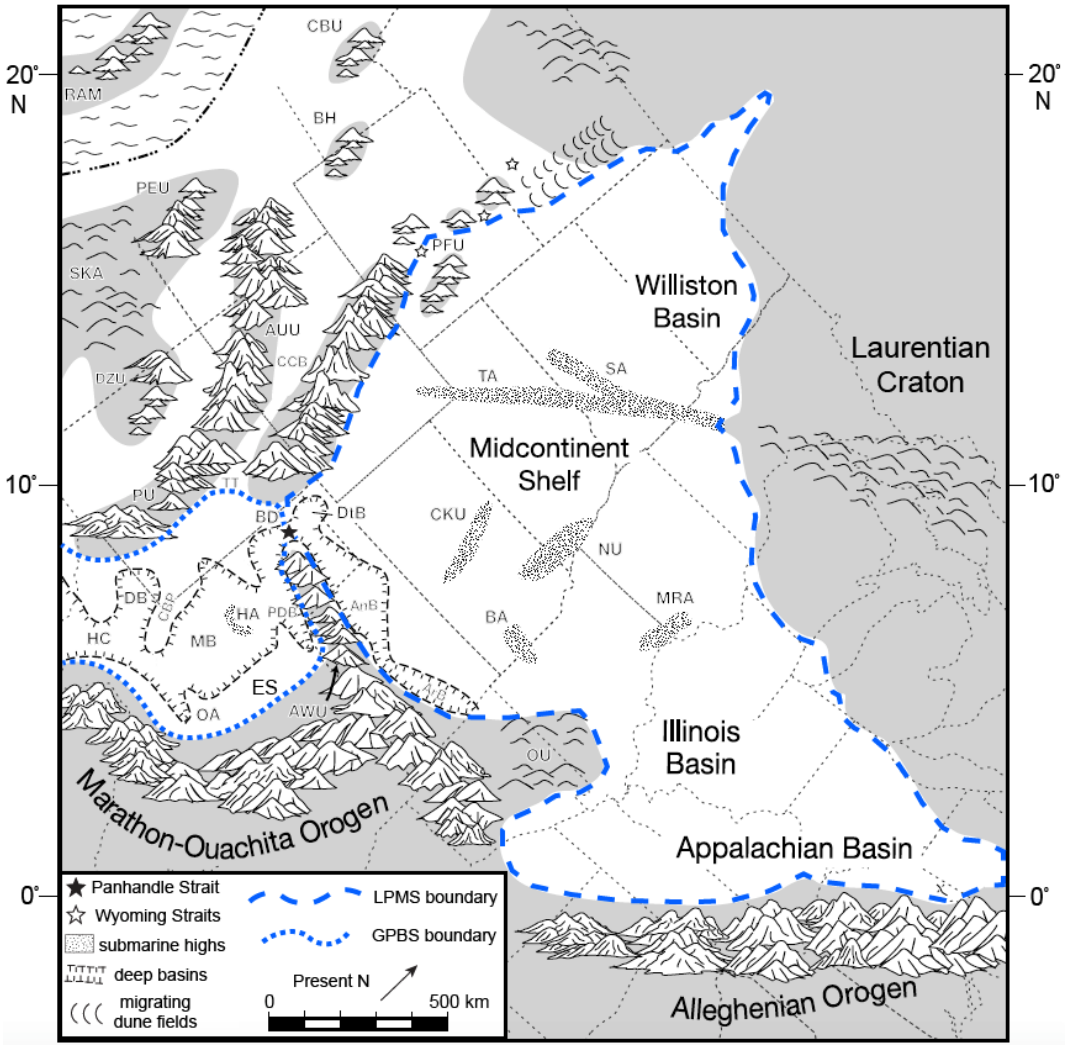

Figure 4: Paleogeographic features of the Late Paleozoic Midcontinent Sea (LPMS) and Greater Permian Basin Seaway (GPBS) of North America. Abbreviations: AnB = Anadarko Basin, ArB = Arkoma Basin, AUU = Ancestral Uncompahgre Uplift, AWU = Amarillo–Wichita Uplift, BA = Bourbon Arch, BD = Bravo Dome, BH = Bannock High, CBP = Central Basin Platform, CBU = Copper Basin Uplift, CCB = Central Colorado Basin, CKU = Central Kansas Uplift, DB = Delaware Basin, DtB = Dalhart Basin, DZU = Defiance–Zuni Uplift, ES = Eastern Shelf, HA = Horseshoe Atoll, HC = Hovey Channel, MB = Midland Basin, MRA = Mississippi River Arch, NU = Nemaha Uplift, OA = Ozona Arch, OU = Ozark Uplift, PDB = Palo Duro Basin, PEU = Piute-Emery Uplift, PFU = Pathfinder Uplift, PU = Pedernal Uplift, RAM = Remnant Antler Mountains, SA = Siouxian Arch, SKA = Sedona-Kaibab Arches, TA = Transcontinental Arch, TT = Taos Trough. Modified from Algeo et al. (2008a).

2.2 PALEOCLIMATE AND REGIONAL HYDROLOGY

The LPMS extended from the humid tropical zone at paleolatitudes of ~0–5°N to the dry tropical zone at paleolatitudes of ~15–20°N (Heckel, 1977, 1980; Algeo et al., 2008). Along the southern margin, the periequatorial Appalachian-Ouachita orogenic belt was situated within the paleo-Intertropical Convergence Zone (ITCZ) (Scotese, 1998). This produced a monsoonal climate with moisture-laden air masses drawn from the proto-Tethyan embayment to the east (Crowley et al., 1989; Parish, 1993; Scotese, 1998; Poulsen et al., 2007; Montanez et al., 2007), resulting in high levels of rainfall and fluvial discharge into the LPMS. It is commonly hypothesized that Pennsylvanian climate conditions in the equatorial-tropical regions became warmer and more humid during interglacial phases of eustatic rise (transgressive to highstand systems tracts), followed by a transition to cooler and drier climate conditions in the next glacial phases of eustatic fall (regressive to lowstand systems tracts) (Cecil, 1990; Heckel, 1995; West et al., 1997; Soreghan et al., 2002; Feldman et al., 2005; Falcon-Lang et al., 2004, 2011

During interglacial cycles, it is estimated that the LPMS received ~800-1500 km^3 of freshwater influx per year; comparable to the modern Baltic Sea (~485 km^3/yr) and Hudson Bay (~975 km^3/yr) when normalized to drainage area (Algeo et al., 2008). Continental runoff to the LPMS was sourced from (1) many short, steep streams emanating from the Appalachian and Ouachita orogens, (2) several major foreland basin rivers with headwaters in the northern Appalachians, and (3) several rivers draining large areas of the Laurentian Craton (Wells et al., 2007; Algeo et al., 2008). It is assumed that most of the freshwater input was derived from the major foreland basin drainage system entering the eastern portion of the LPMS, which would have resulted in a westward net flow of surface waters (Heckel, 1977, 1980; Algeo and Heckel, 2008). This strong influx of continental runoff into the LPMS would have produced a reduced-

salinity layer of surface waters extending from the eastern interior towards at least the Midcontinent Shelf (Algeo et al., 2008; Algeo and Heckel, 2008). Beneath this reduced-salinity layer, or "pycnocline," the watermass was likely close to normal-marine salinity owing to good exchange with Panthalassic ocean waters in the westward connection (Algeo et al., 2008a; Algeo and Heckel, 2008). Evidence for strong continental runoff into the LPMS during core shale deposition includes: (1) large concentrations of terrigenous organic matter (which can reach 80% or more of the total organic matter) within the black shale facies of core shales, suggesting strong export from coastal peat swamps in the east (c.f. Watney et al., 1989; Greb et al., 2003; Algeo et al., 2004b); (2) strong lateral variation in the redox proxies of black shale units, indicative of regional gradients in pycnocline strength, i.e, greater reducing conditions in the east and weaker towards the west (c.f. Coveney et al., 1991; Algeo et al., 1997; Hoffmann et al., 1998); and (3) uniformity of sediment ε_{Nd} values from the Appalachian to Anadarko basins, suggesting extensive reworking and transport of sediment westward across the midcontinent region (c.f. Gleason et al., 1994; Patchett et al., 1999).

2.3 CYCLOTHEM DEPOSITS AND LATERAL FACIES VARIATIONS

The Pennsylvanian stratigraphic successions of the Late Paleozoic Ice Age are well known for their strong cyclic character of intercalated marine, paralic, and terrestrial strata (Wanless and Weller, 1932; Wanless and Shepard, 1936; Ross and Ross, 1985, 1988; Veevers and Powell, 1987). These successions, referred to as "cyclothems," represent glacial-interglacial cycles of approximate Milankovich durations of 100,000 and 400,000 years (Heckel, 1986, 2008; Horton et al., 2012), and an exceptionally high-resolution stratigraphic record of these deposits is preserved on the North American midcontinent (Figure 5; Heckel, 1997, 1986, 2008).

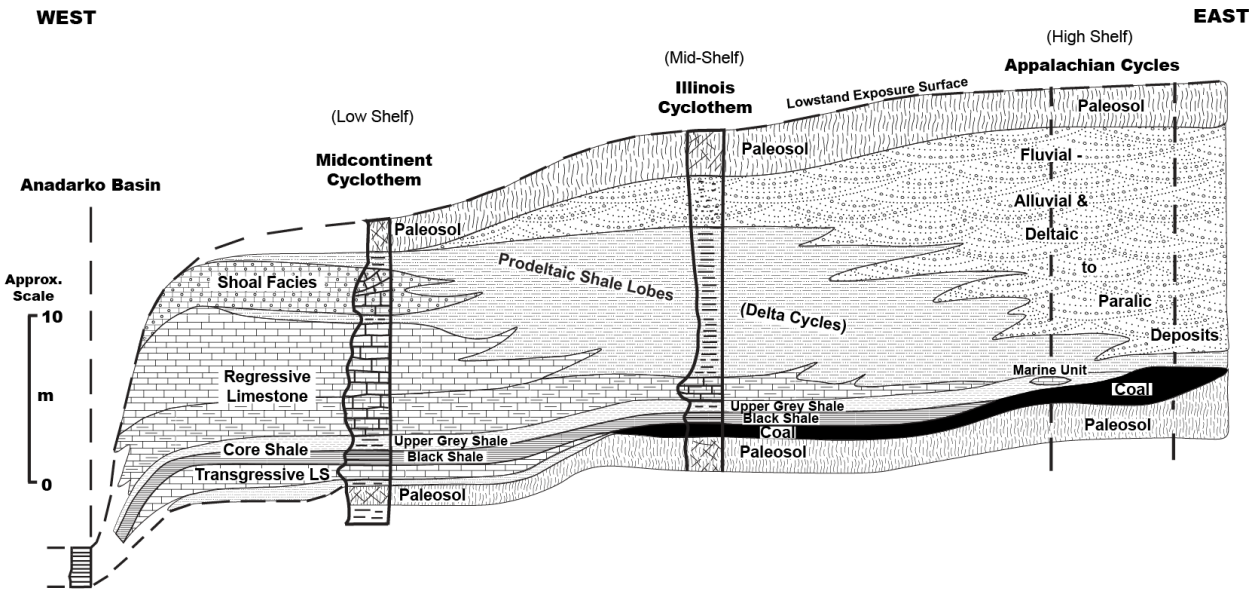

Figure 5: General lithofacies preserved in major cyclothem from the Anadarko Basin (where deep marine deposition of anoxic shale facies was continuous) onto the Midcontinent Shelf through the Illinois and Appalachian basins where cyclothems are typically bound by exposure surfaces (i.e. paleosols). Sequences are characterized from west to east by decreasing amounts of marine limestone, thicker coal beds, and increasing siliciclastics. Modified from *Heckel* (2008).

Each 3 to 10 meter-thick cyclothem contains a stratigraphic sequence that records covarying changes in relative sea level, climate, and sedimentation patterns within a given basin (Cecil et al., 1990, 2003; Heckel, 1990, 2008; Tandon and Gibling, 1994; Cecil and Dulong, 2003). Cyclothem deposits can also show considerable compositional variability, both regionally and temporally, but generally consist of repetitive lithologies that can be classified under specific type models based on the lithofacies preserved within each succession. The most commonly recognized cyclothem type models include the Midcontinent (Kansas)-type, Illinois-type, and Appalachian-type cyclothems (Wanless and Shepard, 1936; Wellar, 1958; Heckel, 1977, 1980, 1986, 1994). Facies relationships and stratigraphic successions observed between the Midcontinent-type to the Appalachian-type have been interpreted as a reflection of the starting point, direction of eustatic transgression, and degree of sea level expansion during each

glacioeustatic cycle and implies that the Midcontinent Shelf, Illinois, and Appalachian basins occupied ancient low-shelf, mid-shelf, and high-shelf depositional environments, respectively (Figure 5; Heckel, 1980, 1994, 2008; Rosenau et al., 2014). Sediment compaction and tectonic activity across the various lowland basins occurred at sufficient rates during the Pennsylvanian to provide the net accommodation space necessary for multiple cyclothems to develop across the US midcontinent (Heckel, 1994).

2.3.1. Midcontinent (Kansas) Cyclothems: Low Shelf

The Midcontinent Shelf of the LPMS extended from the Transcontinental Arch in the west to the Illinois Basin in the east (Figure 4; Algeo et al., 2008a). Water depths across the shelf generally shallowed towards the northeast (proximal to the highlands of the Laurentian Craton) and deepened towards the southwest (into the deepwater Anadarko Basin), however, bathymetric relief was probably fairly limited across broad areas of the Midcontinent Shelf (Herrmann et al., 2015). The Midcontinent or "Kansas"-type cyclothems were deposited in a setting well removed from any major clastic sourcing regions, and as a result, these cyclothems are largely dominated by carbonates and lesser amounts of siliciclastics (Heckel, 1977, 1986, 1994). The basic or "ideal" Kansas-type cyclothem is characterized by four depositional members in ascending order: an outside shale, middle limestone, core shale, and upper limestone (Figure 2 and 5).

Outside Shale – This member is composed of highly variable shale lithofacies with localized occurrences of sandstone and coal units, which forms most or all the shale formations that separate or lie "outside" the marine limestone members (Heckel, 1977, 1994). It consists largely of prodeltaic to deltaic, paralic, and fluvial clastics in northern Kansas and Missouri, and often grades southward to thick prodeltaic shales along the shelf margin in southern Kansas and

northern Oklahoma (Heckel, 1977, 1994, 2008). Commonly at the top of this member, and often forming the entire unit along the northern shelf, are gray to mottled reddish, blocky mudstone paleosols (0.2 to 2.0 m thick) that formed under prolonged periods of subaerial exposure (Schutter and Heckel, 1985; Joeckel, 1989; Heckel, 1994). These paleosol horizons usually extend for hundreds of kilometers along outcrop (e.g. Joeckel, 1994, 1999), and are often disconformably overlain by thin, sandy shale with marine fossils representing the base of the next sea level transgression (Heckel, 1994; Feldman et al., 2005).

Middle Limestone – Deposited atop the outside shale, this member is typically a thin (0.3 to 1.0 m) dark colored, and dense marine limestone. It is composed of mostly skeletal wackestone containing abundant and diverse marine biota (e.g. echinoderms, bryozoans, brachiopods, corals, mollusks, sponges, and algae) that were deposited below effective wave base, and exhibit an overall deepening-upward sequence (Irwin, 1965; Heckel, 1977). These limestones are laterally extensive across the Midcontinent Shelf, and are thought to have undergone slow compaction before cementation under decreasingly oxygenated conditions (Heckel, 1983), allowing for the preservation of fine-grained organic matter (Heckel, 1994).

Core Shale – This marine unit is consists of a thin (0.5 to 2.0 m), gray to black, phosphatic clay shale that was deposited as a condensed section under dysoxic to anoxic conditions of near sediment starvation in a water mass that inhibited the production and/or preservation of carbonate mud (Heckel, 1977, 1994, 2008). The shales that are gray typically carry diverse open-marine benthic fauna along with many invertebrate phyla (Heckel, 1977, 1994). Within the lower to lower-mid portion of the core shale unit, a distinctive black, organic-rich, fissile shale (< 1 m thick) containing abundant pelagic fauna (e.g. conodonts and fish remains) was deposited under prolonged periods of bottomwater anoxia that eliminated any

benthic organisms (Heckel, 1977, 1994; Algeo and Heckel, 2008). Centimeter-scale compositional cycles within the black shale facies have shown it to be correlatable over distances of at least a few hundred kilometers (e.g. Algeo et al., 1997, 2004). The lateral continuity of fine sediment layers at this scale implies uniformity of environmental conditions and synchroneity of changes in the watermass properties over extensive areas during black shale deposition (Algeo and Heckel, 2008). TOC percentages within the black shale facies generally range between 5 – 30 weight % (max. 40 wt.%), and large concentrations of terrigenous OM reflect strong export from coastal peat swamps (c.f. Greb et al., 2003; Algeo et al., 2004, 2008).

Upper Limestone – The fourth member of the ideal Midcontinent-type cyclothem consists of a variably thick (1.5 to 10 m), shallowing-upward carbonate sequence that overlies the upper grey shale facies of the previous core shale member with an abrupt but conformable contact (Heckel, 1977, 1994, 2008). The basal portion of the upper limestone member consists of a wavy-bedded, skeletal mudstone to wackestone containing calcitic invertebrates (e.g. crinoids, brachiopods, echinoderms, and bryozoans), and thin partings of grey calcareous shale (Heckel, 1977, 1994; Butler, 2010). It often displays evidence of grain corrosion and lacks algal fragments, micrite envelopes, or cross bedding suggesting that it formed in water as deep as the underlying core shale below the effective wave base and perhaps below the effective photic zone (Heckel, 1977, 1994; Heckel and Pope, 1992). This open-marine, argillaceous limestone represents proliferation of invertebrates in a deepwater environment as sufficient oxygen levels again circulated to the seafloor (Heckel and Pope, 1992; Heckel, 1994). The limestone then grades upward into skeletal packstone characterized by abundant marine biota, algal fragments, and local cross-bedding which suggests it was deposited within shallower waters well within the photic zone, and near or within the effective wave base (Heckel, 1977, 1983, 1994). The top of

the upper limestone member, particularly in shallower northern region (i.e. Iowa and Nebraska), often includes sparsely fossiliferous, lagoonal to peritidal carbonates, or oolitic shoals that were deposited above the wave base in shoreface environments (Heckel, 1977; Heckel and Pope, 1992). This vertical succession records first an open-marine, low-energy, offshore environment in the lower portion of the limestone, which becomes shallower and increasingly agitated by wave action as sea level regressed through time (Heckel, 1977, 1994, 2008; Strasser et al., 2006).

2.3.2. Illinois Cyclothems: Mid Shelf

The Illinois Basin is an oval-shaped, intracratonic basin that originally formed in response to rifting events in the eastern midcontinent during the late Precambrian to Early Cambrian (Kolata and Nelson, 1991, 1997). During the Pennsylvanian, the greatest degree of subsidence and sedimentation occurred in the southern portion of the Illinois Basin due to flexural loading effects in the neighboring Appalachian foreland basin (Willman et al., 1975; Klein and Willard, 1989). In the Illinois-type cyclothems, widespread coal deposits unconformably overlie paleosols (underclays), and represent the start of a new cyclothem (Figure 5; Cecil et al., 2003; Heckel, 2008; Rosenau et al., 2013). Many sequence stratigraphic interpretations suggest these laterally extensive coal beds (formerly coastal peat swamps) were established primarily during phases of glacio-eustatic transgression due to a combination of increasingly wet climate conditions and a coeval rise in sea level that backed up and ponded freshwater drainage in low-gradient intracratonic basins, which elevated the regional water table (Heckel and Pope, 1992; Tandon and Gibling, 1994, Flint et al., 1995; Pashin, 1998; Martino, 2004; Greb et al., 2008; Falcon-Lang and DiMichelle, 2010).

The top of coal bed deposits are often marked by a widespread erosional or "ravinement" surface that reflects shoreline erosion as the LPMS transgressed into the Illinois Basin (Archer and Kvale, 1993; Cecil et al., 2003; 2014). Immediately above this surface, a very thin transgressive limestone may be present in local occurrences; however, it is often reduced to a thin shell hash layer of pyritized brachiopod and bivalve fragments, probably because the carbonate mud-producing algae were inhibited or dissolved by the acidic environment created by the underlying peat (Heckel, 2008; Rosenau et al., 2013). More typically, the transgressive ravinement surface is directly overlain by a black, highly fissile, phosphatic shale that lacks benthic organisms, and possesses the same conodont fauna observed in the core shales of the Midcontinent Shelf (Heckel, 1994, 2008; Rosenau et al., 2013; Cecil et al., 2014). Regional correlations show that black shales typically pinch out near the Illinois Basin margins or onto tectonic highs, whereas, the upper gray shale facies and overlying limestone (i.e. upper limestone member) persists farther paleo-landward (Nelson et al., 2010; Rosenau et al., 2013).

Overlying the core shale unit is a thin, fossiliferous, marine limestone (wackestone to packstone) containing a diverse array of open-marine fauna that favored oxygenated water close to normal salinity, and without a large amount of suspended sediment (Rosenau et al., 2013). The marine limestone then gives way to a coarsening-upward succession of clastic rocks that were deposited by rapidly prograding deltas as sea level began to fall (Heckel, 2008; Rosenau et al., 2013). In most cases, deltas filled nearly all the available accommodation space in the Illinois Basin (Rosenau et al., 2013). As sea level continued to regress, the deltaic sediments in the basin became exposed to the processes of subaerial weathering, where soil formation (pedogenesis) and fluvial incision completed the Illinois-type cyclothem sequence (Heckel, 1994, 2008; Rosenau et al., 2013).

2.3.3. Appalachian Cyclothems: High Shelf

Appalachian-type cyclothems were deposited within a tectonically subsiding foreland basin in proximity to a major clastic source (Appalachian orogen), and are dominantly non-marine sequences with thick sandstone and coal beds with minimal limestones and shales (Figure 5; Heckel, 1986, 1994; Klein and Willard, 1989). During the late-Middle through Late Pennsylvanian, cyclothem deposition was largely confined to the northern part of the Appalachian Basin (i.e. western Pennsylvania, eastern Ohio, and northern West Virginia) because the southern portion of the basin experienced rapid detrital infilling during the early-Middle Pennsylvanian (Heckel, 2008). Although significant tectonic activity was affecting this basin, deposition largely kept pace with crustal subsidence during this time period (Greb et al., 2003; Algeo et al., 2008a).

The beginning sequence of the Appalachian-type cyclothems is noted by incised valley-fill deposits of thick fluvial sandstones, along with lacustrine deposits and minor stream channel sandstones that formed on interfluves outside the paleovalleys (Belt et al., 2011. Above these units, well-developed paleosols and underclays formed over large portions of the basin, and they are generally superimposed by coals beds of varying thickness (Figure 5; Fahrer, 1996; Heckel, 2008, 2012). Marine units in the succession overlie coals and paleosols (Heckel, 1994, 2008). These shallow-water marine units are typically thin and lithologically heterogeneous ranging from argillaceous/silty/sandy skeletal limestones (wackestones to packstones) to fossiliferous, dark to light grey shales, and calcareous siltstones and sandstones (Heckel, 1994, 2008). Skeletal limestones within these marine units commonly contain phosphorite, glaucony, and abundant normal-marine fauna (e.g. mollusks, brachiopods, echinoderms, bryozoans, corals, and sponges) that favored oxygenated waters, and thus represent condensed sections that developed away from

or between deltaic influxes during sea level highstands (Fahrer and Heckel, 1992; Heckel, 1994, 2008; Stamm and Wardlaw, 2003). The same fauna associated with the marine units in the Appalachian Basin are also found within the grey shales and argillaceous limestones deposited in the Illinois Basin and Midcontinent Shelf (Malinky and Heckel, 1998; Algeo and Heckel, 2008). These condensed marine units were eventually buried by a coarsening-upward sequence of siliciclastics as prograding deltas and alluvial fans began filling the remaining accommodation space in the Appalachian Basin during late highstand to sea level regression. The phosphatic, black shale facies of the Illinois and Midcontinent Shelf core shale sequences are absent from the Appalachian-type cyclothems, possibly due to very shallow water depths and proximity to significant deltaic influences which impeded water column stratification (Heckel, 1994, 2008; Broach, 2014). Although there is no development of core shale intervals or middle/upper limestones within the Appalachian Basin, correlations have been made between the marine units and individual major cyclothems of the Midcontinent using conodont-based biostratigraphy (Heckel et al., 2011; Heckel, 2012).

2.3.4. Texas Cyclothems

The Eastern Shelf of the Permian Basin in Texas formed at the beginning of the Missourian when subsidence in the Midland Basin was sufficient to form a distinct hinge-line between the basin and the Ouachita structural belt (Figure 4; Cleaves and Erxleben, 1985; Yancey, 1986). The region maintained an inclined shelf morphology throughout the Pennsylvanian and Permian where water depths shallowed towards the Ouachita orogen and deepened towards the steep shelf margin into the Midland Basin (Yancey, 1986). In the deep Midland Basin of western Texas, the entire succession of Pennsylvanian strata is composed of basinal, sediment-starved black shale that continued to accumulate as the basin began subsiding

during the Missourian in response to the tectonic forces of the Ouachita-Marathon orogen (Cleaves and Erxleben, 1985; Yancey and Cleaves, 1990; Heckel, 1994). Eastward and up-dip from the Midland Basin, Pennsylvanian outcrops along the Eastern Shelf contain cyclic deposits with similar lithologies observed in the Illinois and Appalachian Basins (Heckel, 1994), however, a wide range of depositional patterns occurs both down dip and along strike of the shelf because deposition of carbonates and siliciclastics were not mutually exclusive (Figure 6; Cleaves and Erxleben, 1985; Yancey, 1986; Boardman and Malinky, 1985). The controls of mixed carbonate-siliciclastic deposition observed in the Texas cyclothems have been attributed to a combination of both glacio-eustatic sea level fluctuations and deltaic progradation/abandonment (Cleaves and Erxleben, 1985; Boardman and Malinky, 1985; Boardman and Heckel; 1989). During the early Missourian (the focused time period of this study) depositional settings across the Eastern Shelf consisted of four deltaic depocenters, two carbonate banks, one carbonate platform, and an embayment-strandplain complex (Figure 7; Cleaves, 1975; Cleaves and Erxleben, 1982, 1985).

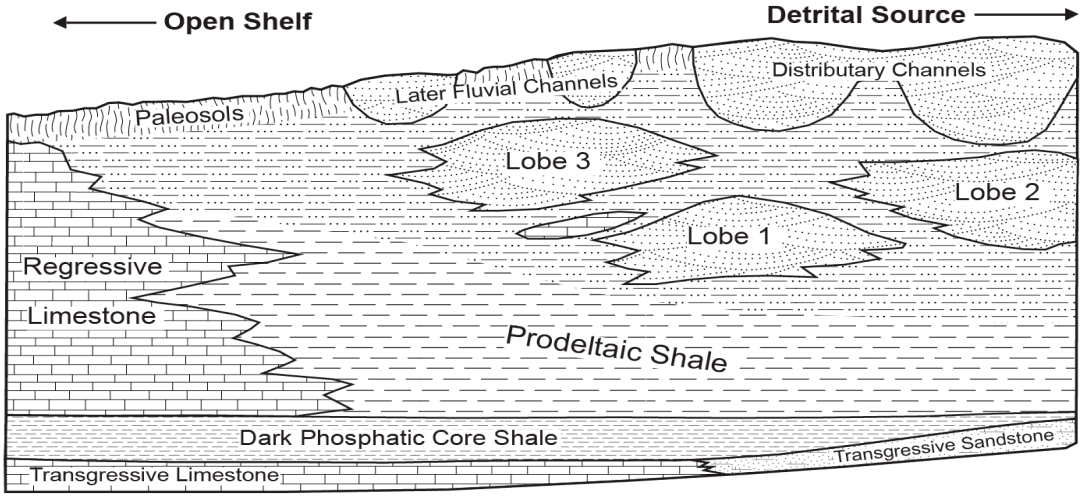

Figure 6: Depositional model for mixed carbonate – siliciclastic cyclothems across the Eastern Shelf of Texas during the Pennsylvanian. Figure modified from *Boardman and Heckel* (1989).

In Texas cycles, deltaic/terrestrial shales and sandstones overlie extensive marine units and typically contain well-developed paleosols at their tops (Boardman and Heckel, 1989; Yancey and Cleaves, 1990; Heckel, 2008). Lithofacies of the marine units varied across the shelf from limestones, shales, or sandstones depending on their proximity to the paleoshoreline and/or areas of strong detrital influx such as prograding delta systems (Cleaves and Erxleben, 1985; Boardman and Malinky, 1985; Yancy, 1986). Marine units preserved in the Eastern Shelf cyclothems have been readily correlated with those in the Midcontinent Shelf and other basins using conodont biostratigraphy (c.f. Boardman and Heckel, 1989; Heckel et al., 2011), however, the abundance of conodonts is usually lower in the Texas shelf samples due to greater sediment dilution caused by the invasion of deltaic siliciclastics (Boardman and Heckel, 1989). Another difference noted by several workers (e.g. Boardman and Malinky, 1985; Brown et al., 1987; Boardman and Heckel, 1989; Yancey and Cleaves, 1990; Boardman et al., 1995) is that outcrops of core shale intervals in Texas cycles are typically non-fissile and contain less organic matter compared to their correlative counterparts located along the Midcontinent Shelf and Illinois Basin. Instead, the more typical core shale interval observed in outcrops consists of a dark grey, slightly phosphatic, bioturbated shale with a fossil content suggestive of dysaerobic to near aerobic benthic conditions, which grades upwards into a shale deposited under fully aerobic conditions (Boardman and Malinky, 1985; Brown et al., 1987; Teo, 1991; Boardman et al., 1995).

In a generalized ascending order, Texas cyclothems are comprised of: (1) lowstand terrestrial/nearshore deltaic sandy-shales, fluvial sandstones, paleosols, and thin local occurrences of coal, (2) transgressive limestones that developed away from siliciclastic input or transgressive, shoreface sandstones, (3) a marine “core” shale composed of dark phosphatic shale

that varies in color across the shelf from black, dark gray, to light gray, and (4) thick shoaling-upward limestones or coarsening-upward siliciclastics depending on the proximity to prograding deltas (Figure 6; Boardman and Malinky, 1985; Yancey, 1986; Boardman and Heckel, 1989; Heckel, 1994). The Upper Salesville major cycle of north-central Texas correlates with the Swope Cyclothem and Hushpuckney Shale member of the midcontinent (Boardman and Heckel, 1989). It consists of a fining-upward, transgressive sandstone (Devil's Hollow Sandstone) overlain by a dark phosphatic shale, which is overlain by a thick grey-brown prodeltaic shale incised by the fluvial Turkey Creek Sandstone, and capped by the terrestrial Keechi Creek Shale (Boardman and Heckel, 1989; Yancey and Cleaves, 1990). The lack of limestone units and dominance of siliciclastic material in the outcrops of the Upper Salesville cycle have been interpreted by some workers (e.g. Yancey, 1986; Rosscoe and Bader, 2010) as an indication for a "high-shelf" depositional environment proximal to the paleoshoreline and detrital sources.

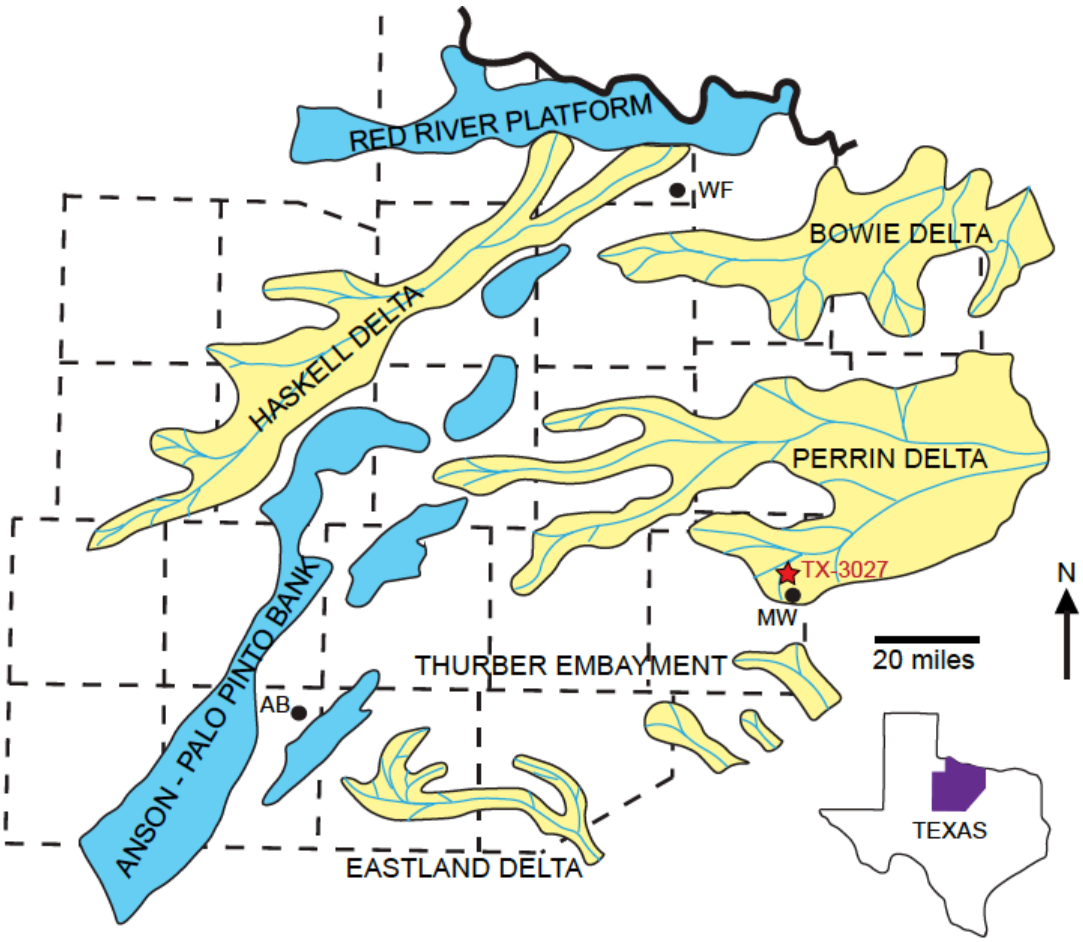

Figure 7: Major depositional systems and their approximate paleogeographic extent across the Eastern Shelf in north-central Texas during the early Missourian. Black dots with abbreviations represent locations of present-day cities: AB = Abilene, MW = Mineral Wells, WF = Wichita Falls. The red star labeled TX-3027 denotes the outcrop location of the Upper Salesville Shale sampled in this study. Dashed lines are geographic boundaries of Texas counties. Figure modified from *Cleaves* (1975).

3. METHODS AND MATERIALS

3.1 SAMPLING

This study utilizes both drillcore and outcrop sample data collected from one laterally extensive cyclothemic core shale: the Hushpuckney Shale Member of the Swope Cyclothem and its correlative equivalents (Figure 1C). Five sample locations were chosen for geochemical analysis that represent a depositional transect across the Texas Eastern Shelf, the Midcontinent Shelf, and Illinois Basin (Figure 8). These study sites represent coeval cyclothem deposition between the Texas Eastern Shelf and constituent areas within the LPMS that shared a marine connection with Greater Permian Basin Seaway.

The north-central Texas outcrop section (TX-3027) is located on the south side of Texas Highway 3027 about 2.6 miles (~4.2 km) northwest of Mineral Wells, Texas (Figure 7 and 8). Samples were taken from the upper Mineral Wells Formation in the Hushpuckney equivalent "Upper Salesville Shale" at 5 centimeter (cm) intervals within the grey to dark grey shale facies. The core shale interval at this location on the Eastern Shelf was deposited above the Devil's Hollow Sandstone unit (the base of the cyclothem; Cleaves, 1975), and is overlain by a thick sequence yellow-brown prodeltaic shale (Boardman and Heckel, 1989). TX-3027 is situated within the paleo-depocenter of the Perrin multilateral delta system (Figure 7; Brown et al., 1973; Cleaves and Erxleben, 1985), which prograded in an east-to-west direction throughout the Missourian, and supplied silica-rich detritus from a source area in the northernmost part of the Ouachita structural belt in Texas (Cleaves, 1975; Cleaves and Erxleben, 1985).

The drillcore samples Clarkson, KEX, and ILH are located on the Midcontinent Shelf of the LPMS (Figure 8), and occupied distinct locations along the shelf slope: Clarkson is located proximal to the shelf margin in southeastern Kansas, KEX is located in the mid-shelf area of

northeastern Kansas, and ILH is located on the mid-high shelf area of southwestern Iowa. The Hushpuckney Shale is situated between the lower Middle Creek Limestone and upper Bethany Falls Limestone, and shale samples were taken at 1 – 3 cm intervals for all three core sites.

The drillcore sample ELY-1 is located within the Illinois Basin region of the LPMS. This study site is situated near the central portion of the basin in southeastern Illinois. The Hushpuckney Shale at this sample location was deposited directly above a sharp contact with the Womac Coal, and is overlain by the Macoupin Limestone. Samples near the lithofacies transition from the underlying coal and lowermost black shale were taken at 1 – 2 cm intervals, while the remainder of the Hushpuckney Shale was sampled at 1 – 5 cm intervals.

Figure 8: Regional paleogeography of North America during Late Pennsylvanian glacio-eustatic highstands. Red stars indicate sample locations of the Hushpuckney Shale and its correlative units collected for analysis in this study. TX-3072 is situated on the Eastern Shelf of the Greater Permian Basin Seaway. Clarkson, KEX, and ILH are located on the Midcontinent Shelf, and ELY-1 is located within the Illinois Basin of the LPMS.

3.2 NITROGEN ISOTOPE ANALYSIS

Samples used for geochemical analyses were powdered using a tungsten carbide ball mill and stored in plastic vials for later chemical analysis. Measurements of the nitrogen isotopic composition of all study units were performed at the Stable Isotope Laboratory in the Department of Geosciences at Boise State University. Powdered samples were measured against the standard isotopic ratio of atmospheric N_2, and data from the sampled intervals are represented in delta (δ) notation as defined by the equation:

$\delta^{15}N_{air} = [(^{15}N/^{14}N)_{sample}/(^{15}N/^{14}N)_{standard} - 1]*1000$. All values are reported as a per mil (‰) variation in $\delta^{15}N_{air}$ in which atmospheric N_2 is 0‰. Adjusted mass measurements, based on the estimated organic content for the lithofacies of each sample location, were applied to powdered samples so that approximately 100 μg of nitrogen were weighed into tin capsules. Each tin capsule (filled to the appropriate mass) was combusted using a Thermo Scientific TC/EA elemental analyzer interfaced with a ThermoFisher Delta V Plus continuous flow isotope ratio mass spectrometer.

3.3 ELEMENTAL ANALYSIS

Powdered samples of approximately 500 mg from all study locations were measured for total carbon and sulfur concentrations at the University of Cincinnati using an Eltra 2000 C-S analyzer. Total organic carbon (TOC) was measured on an acidified aliquot of each sample. Approximately 4 – 5 grams of powdered samples from the Midcontinent Shelf study units (Clarkson, KEX, and ILH) were taken for XRF elemental analysis at the University of Cincinnati. A wavelength-dispersive Rigaku 3070 XRF spectrometer was used for determining concentrations of major and trace elements. Both U.S. Geological Survey (USGS) shale standards (SDO-1, SCO-1, and SGR-1) and internal black shale standards (analyzed by XRAL)

were used for sample calibrations. Replicate analyses demonstrated that analytical precision was better than ± 5% for all trace elements. Detection limits for trace elements were ~2 ppm for U and Mo.

For the study locations that lacked the appropriate 4 – 5 grams of powdered sample for XRF analysis (Texas outcrop TX-3072, and Illinois drillcore ELY-1), an alternate method using the relative abundance of select elemental ratios was applied for general comparisons with XRF data. These relative abundances were measured using an LSX-213 (G2) Laser Ablation System with an iCap Qc Inductively Coupled Plasma Mass Spectrometer (ICP-MS) at Louisiana State University. The data collected from LA-ICP-MS analysis was measured in counts per second (cps). Powdered samples of approximately 500 mg were measured into a 13mm tungsten carbide die, and pressed into consolidated pellets using a Carver 10-ton hydraulic press. These pellets were then mounted onto thin section slides and analyzed using the LA-ICP-MS system. Each sample pellet was ablated twice by a single line scan that was approximately 2,000 microns long by 50 microns wide with a laser energy of 10%, laser shot frequency of 10 Hz, and scan rate of 20 microns/second. The ICP-MS was set to a 30 second purge and an acquisition time of 140 seconds. The data acquired from the two-line ablations for each sample was then averaged to provide the mean value. Powdered samples of the USGS shale standards SBC-1, SDO-1, SCo-1, and SGR-1 were also pressed into 13mm pellets and used for sample calibrations during analysis.

In shales, aluminum (Al) is generally regarded as the main conservative proxy for aluminosilicates which dominate the insoluble component of weathered terrigenous clastics; therefore, elemental concentrations were normalized to Al (expressed as element/Al ratios) in order to correct for variable dilution caused by OM and authigenic minerals such as carbonates,

pyrite, and apatite (Arthur et al., 1985, 1990; Arthur and Dean, 1991; Calvert et al., 1996). For samples that were analyzed using XRF, ratio units for major elements are in (weight %) / (Al weight %) and trace elements in (ppm) / (Al weight %). The ratio units for samples analyzed using LA-ICP-MS express both major and trace elements in (cps) / (Al cps). Mo was not measured during LA-ICP-MS analysis; however, the elemental ratios of U/Al and Fe/Al were measured for abundances and relative comparison to the sample sets analyzed with XRF.

4. RESULTS

4.1. INTERNAL STRATIGRAPHY AND CORRELATION OF HUSHPUCKNEY SHALE

In order to correlate any variations that may have occurred in the depositional environment of the Hushpuckney Shale across the North American midcontinent, an effort was made to subdivide the sampled sections into four stratigraphic intervals using lithofacies distinctions and geochemical characteristics, primarily nitrogen isotopes, that were defined by *Herrmann et al.* (2012) using samples from the Edmonds #1A (KEX) drillcore near Kansas City, Kansas (Figure 9). These subdivisions have been applied to correlative sections of the Hushpuckney Shale in Iowa, Missouri, and southeastern Kansas (Herrmann et al., 2012, 2015).

Interval 1, the lower black shale (LBS), is characterized by a rapid upsection increase in $\delta^{15}N$ from background values of 4-6‰ to peak values ranging from 12 to 15‰ (Figure 9). Interval 2, the middle black shale (MBS), is marked by the peak $\delta^{15}N$ excursion at its base and a gradual decrease in $\delta^{15}N$ values towards lower values. The black shale within intervals 1 and 2 is normally dense and fissile. Interval 3, the upper black shale (UBS), begins at the inflection point where the decreasing $\delta^{15}N$ trend stabilizes towards background values around 4‰, and consists of black shale that is less dense and fissile. The MBS/UBS boundary also lies near peak TOC values, and may correspond to the maximum flooding surface (MFS) during cyclothem deposition (Algeo et al., 2004, 2008; Herrmann et al., 2012). Interval 4, the upper grey shale (UGS), exhibits a stable trend of $\delta^{15}N$ values around 4 to 6‰, and is recognized by an observable transition from black to grey shale and/or where TOC percentages sharply decline to much lower values ($\leq$ 2% TOC).

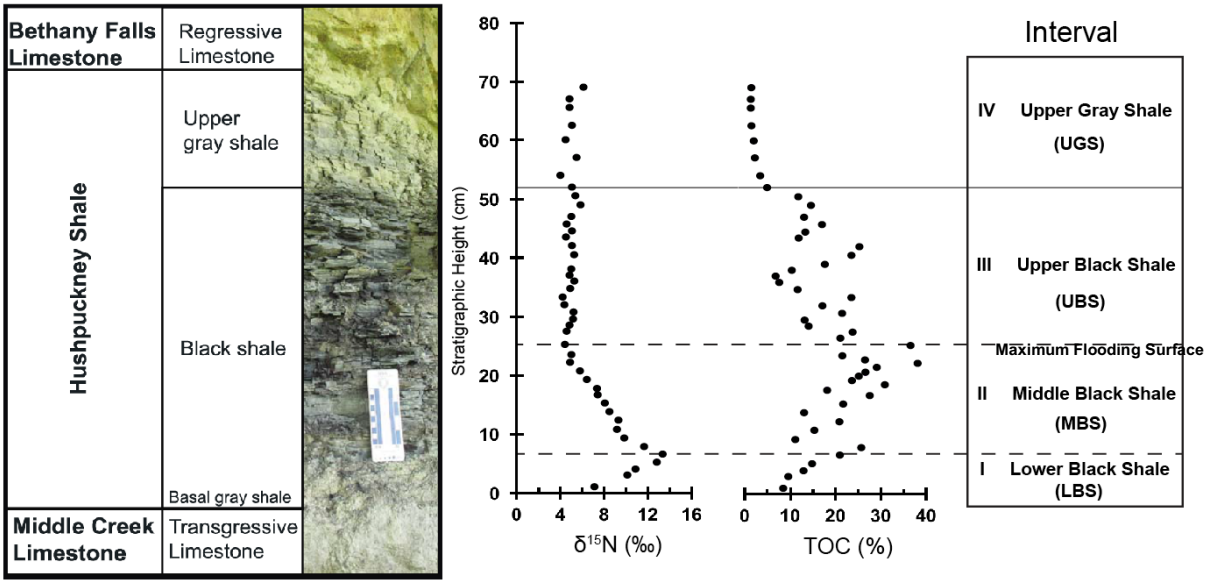

Figure 9: Core shale subdivision scheme based on N-isotope and TOC trends. Geochemical data presented is from KEX drillcore, and outcrop photo is from Xenia, Kansas. Modified from *Herrmann et al.* (2015).

Stratigraphic plots of the δ^{15}N-isotopes for each study unit were compared with measured stratigraphy of each sample location to determine if the subdivision scheme, as described above, is applicable for samples in the Illinois Basin and Eastern Shelf of Texas (Figure 10). Stratigraphic thicknesses, bounding lithologies, and isotopic profiles of correlative Hushpuckney Shale units are highly variable. In the Texas outcrop section, the core shale interval is much thicker (~ 1.9 meters) than the average Midcontinent Shelf thickness (≤ 1 meter), and is much lighter in color compared to the study units located on the Midcontinent Shelf and Illinois Basin. More importantly, there is no distinguishable δ^{15}N-isotopic excursion that occurs within the core shale interval in the Texas unit, and δ^{15}N values are sustained at background values with an average of +4.03‰ and a standard deviation of 0.31. These results indicate the core shale unit in Texas cannot be subdivided into correlative intervals based on N-isotopes.

In the Illinois drillcore sample ELY-1, a distinct positive $\delta^{15}N$-isotopic excursion occurs within the lower half of the black shale unit that may be compared to the Hushpuckney samples of the Midcontinent Shelf. The difference, however, is that the peak $\delta^{15}N$ value is greater in the Illinois Basin study site (+15.3‰) than the Midcontinent Shelf locations (+13.4 to +14.6‰), and the isotopic excursion occurs sharply in ELY-1 after the lithofacies transition from coal to black shale. The entire core shale interval of ELY-1 is also much thicker (~2.1 meters) than the average Midcontinent Shelf core shale thicknesses (≤ 1 meter). Aside from the aforementioned stratigraphic variations, it is still possible to subdivide the Hushpuckney Shale of ELY-1 into correlative intervals based on the recorded N-isotopic patterns.

For all study units that can be appropriately subdivided, the data results are presented in a normalized fashion such that intervals 1 to 4 are equally scaled (Herrmann et al., 2015). This permits a more direct comparison of abundance trends between the sampled sections of individual study units. Conceptually, this normalization method transforms the y-axis of data plots from stratigraphic thicknesses (Figures 11-14) to a relative timescale (Figure 16). This transformation is based on the assumption that transitions between different intervals across the study areas were approximately simultaneous, and that variations in thickness of intervals 1- 4 (LBS to UGS) were due primarily to local variations in either sedimentation rate or accommodation space (Herrmann et al., 2015).

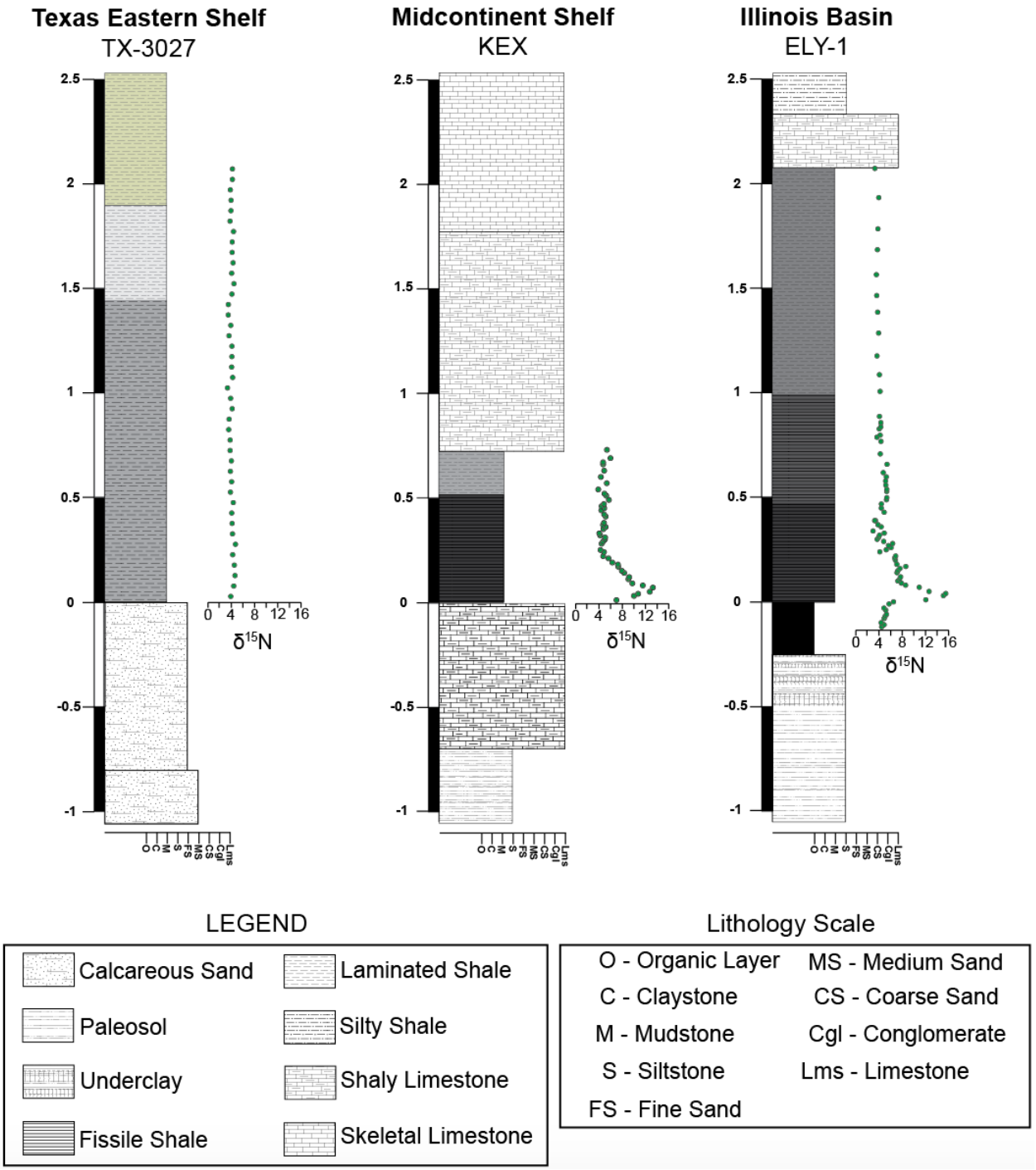

Figure 10: Select measured stratigraphy from sample sections TX-3072 (Upper Salesville Shale), KEX (Swope Cyclothem – Hushpuckney Shale), and ELY-1 (Macoupin Cyclothem – Hushpuckney Shale). Results from nitrogen isotope analysis are plotted to the right of the corresponding stratigraphic column, and the $\delta^{15}N$ values are reported as permil (‰) AIR. Shading of shale intervals are approximate colors of the sediment.

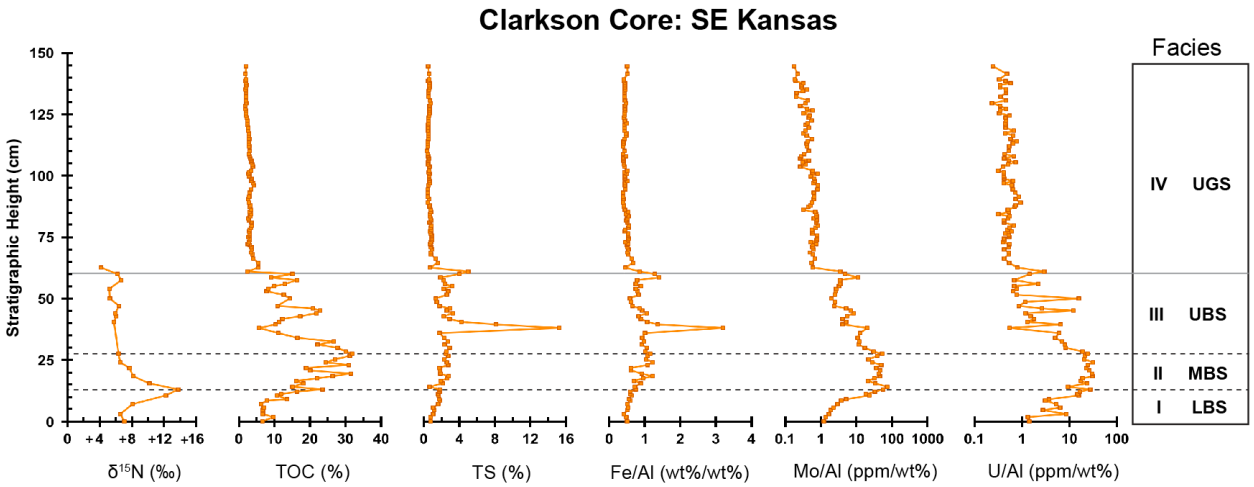

Figure 11: Geochemical data of the Hushpuckney Shale measured from the Clarkson drillcore in southeast Kansas. Data results plotted against the stratigraphic height. Dotted lines across plots represents black shale facies subdivisions based on geochemical characteristics outlined in *Herrmann et al.* (2012, 2015).

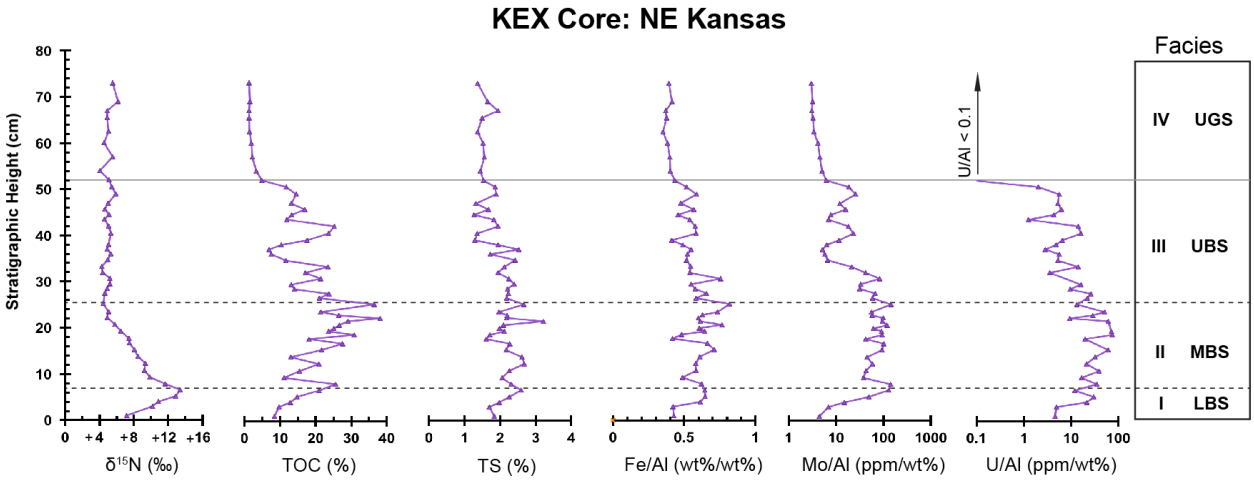

Figure 12: Geochemical data of the Hushpuckney Shale measured from the KEX drillcore in northeast Kansas. Data results plotted against the stratigraphic height. Dotted lines across plots represents black shale facies subdivisions based on geochemical characteristics outlined in *Herrmann et al.* (2012, 2015).

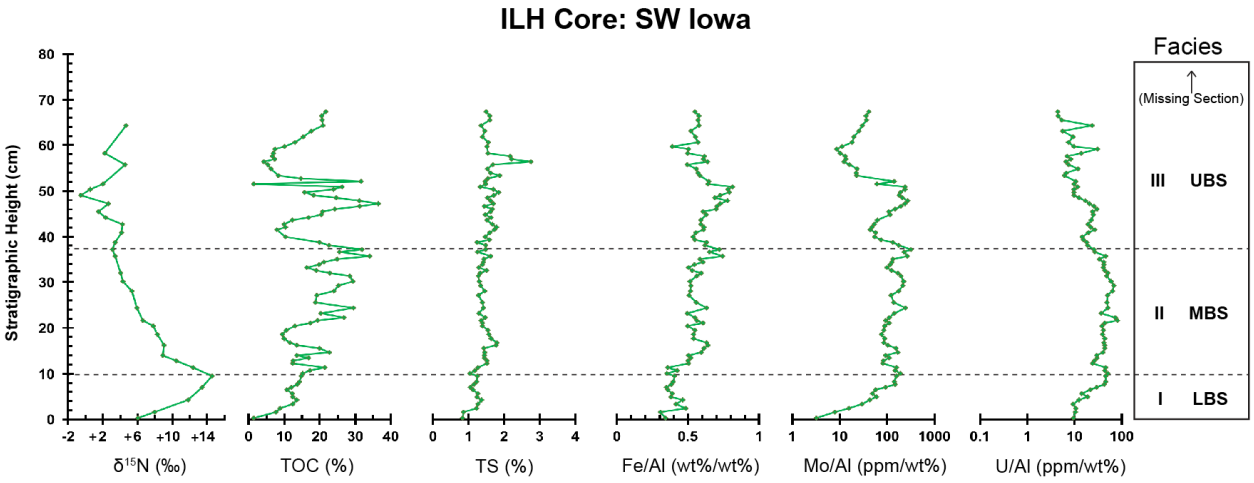

Figure 13: Geochemical data of the Hushpuckney Shale measured from the ILH drillcore in southwest Iowa. Data results plotted against the stratigraphic height. Dashed lines across the top of the plots indicate missing section. The uppermost portion of the black shale and upper grey shale were missing in core for analysis. Dotted lines across plots represents black shale facies subdivisions based on geochemical characteristics outlined in *Herrmann et al.* (2012, 2015).

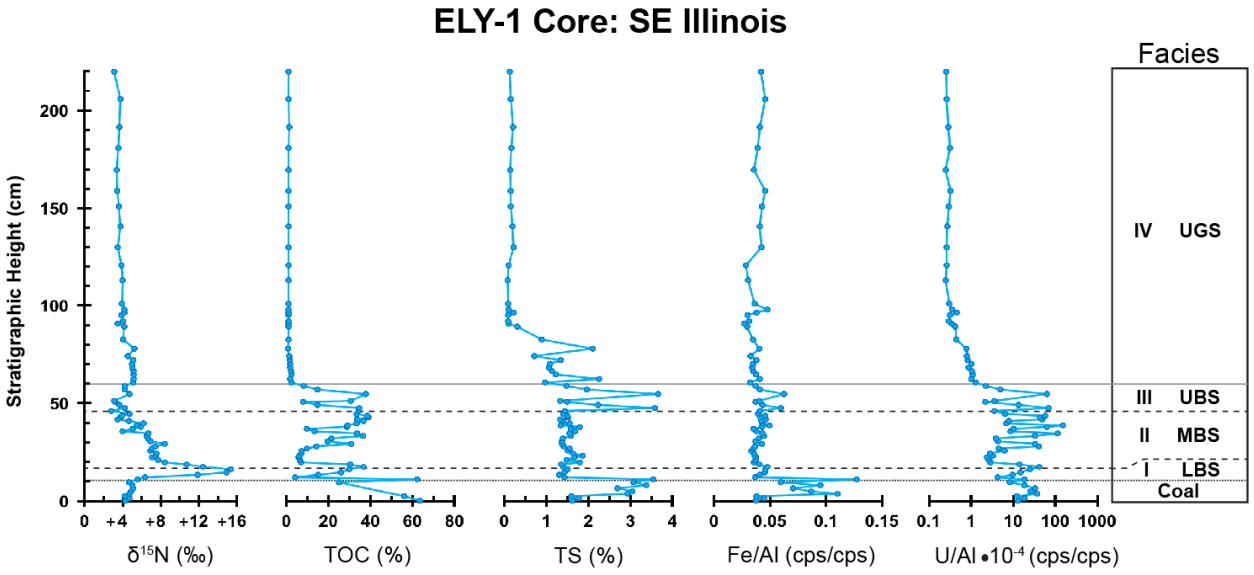

Figure 14: Geochemical data of the Hushpuckney Shale and underlying Womac Coal measured from the ELY-1 drillcore in southeast Illinois. Elemental data was acquired using LA-ICP-MS analysis and elemental ratios are presented in counts-per-second (cps/cps). Data results plotted against the stratigraphic height. Dotted lines across plots represents black shale facies subdivisions based on geochemical characteristics outlined in *Herrmann et al.* (2012, 2015).

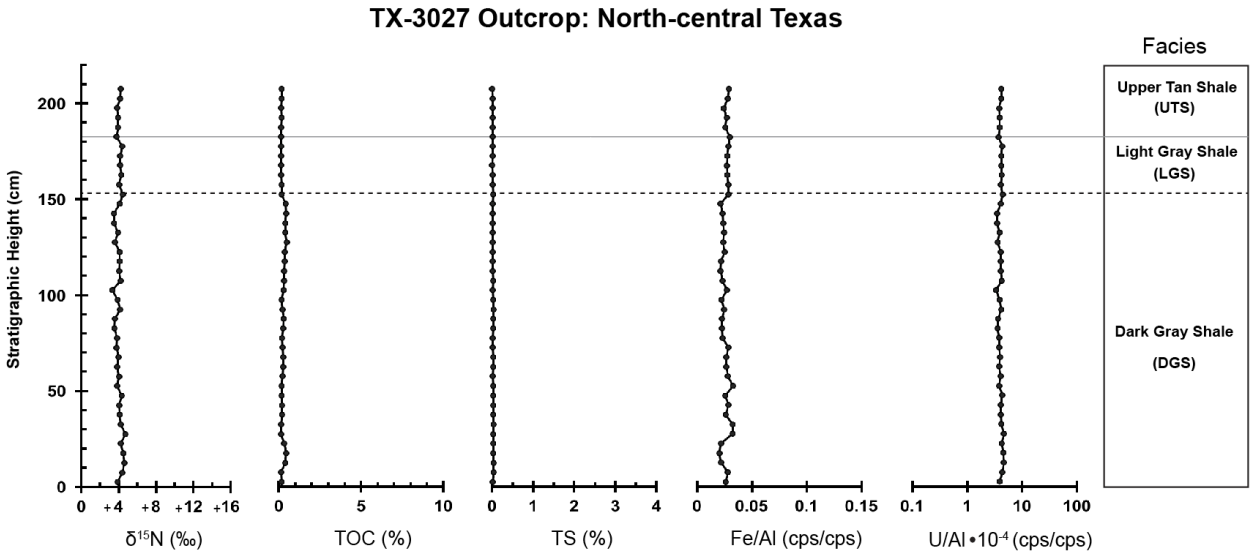

Figure 15: Geochemical data of the Upper Salesville Shale (i.e. Hushpuckney Shale equivalent) measured from the TX-3027 outcrop in north-central Texas. Elemental data was acquired using LA-ICP-MS analysis and elemental ratios are presented as counts-per-second (cps/cps). Data results are plotted against the stratigraphic height.

4.2 NITROGEN ISOTOPE AND ORGANIC CARBON TRENDS

The N-isotopic composition ($\delta^{15}N$) and total organic carbon (TOC) exhibit regular patterns of stratigraphic and geographic variation across the Hushpuckney Shale and its correlative units (Figures 11-16). TOC concentrations reflect the redox conditions of the water column and underlying sediments during organic matter (OM) accumulation, and can also indicate the relative flux of OM during deposition (Zonneveld et al., 2010). In all the LPMS study units, excluding TX-3027, both $\delta^{15}N$ and TOC increase rapidly upsection in the LBS interval after transitioning from the transgressive limestone in the Midcontinent Shelf samples, and the underlying transgressive coal in the Illinois Basin samples (Figure 16). The maximum $\delta^{15}N$ values slightly deviate across the LPMS with lesser values occurring in the Kansas samples (~13.4 and 13.8‰), intermediate values in Iowa (~14.6‰), and higher values in Illinois (~15.3‰). The overall trend, however, is that maximum $\delta^{15}N$ values increase towards the

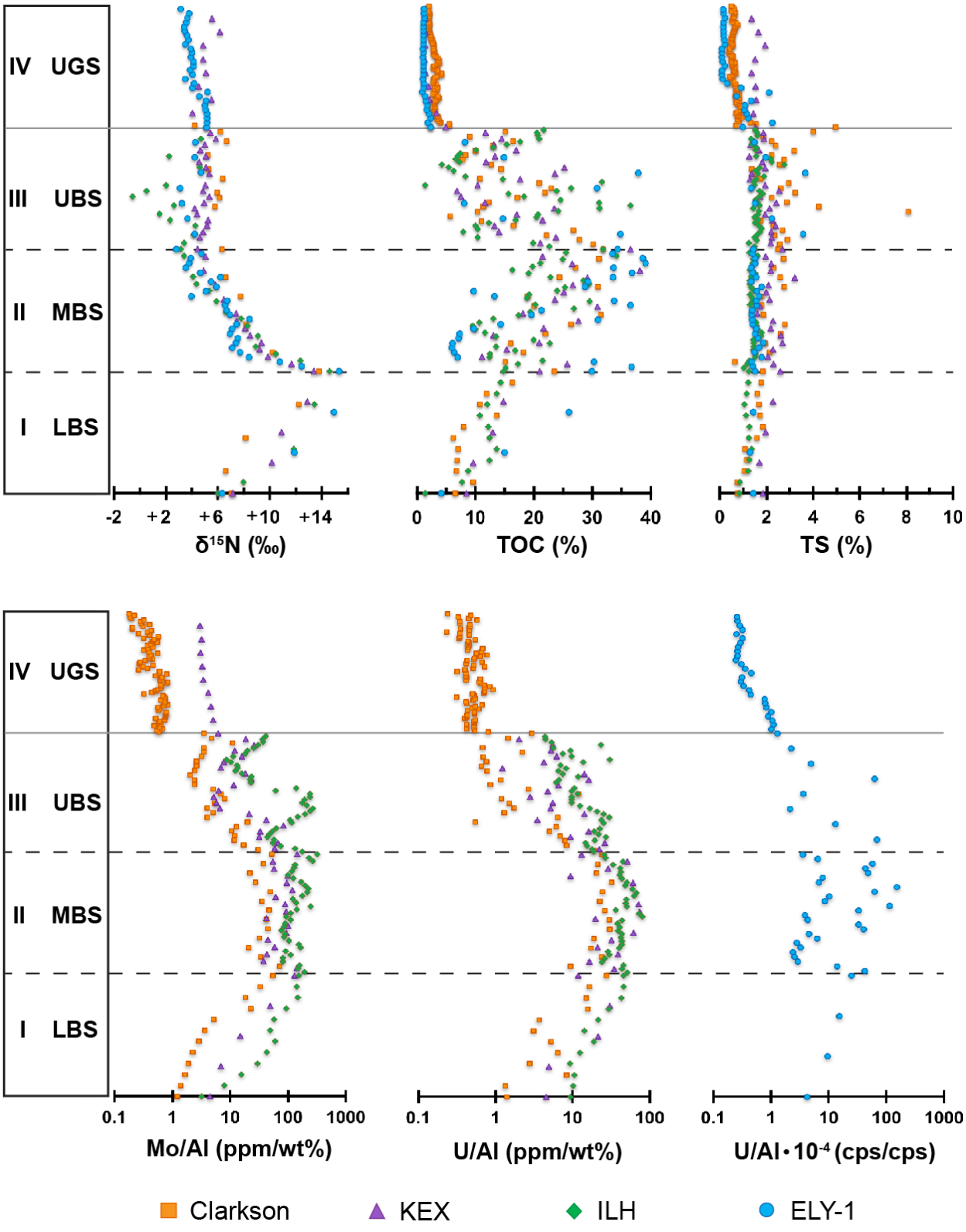

Figure 16**:** Geochemical gradient comparisons for the Hushpuckney Shale across the Midcontinent Shelf (Clarkson, KEX, and ILH) to the Illinois Basin (ELY-1).

shallower eastern interior of the LPMS. After the peak ^{15}N excursion, both $\delta^{15}N$ and TOC concentrations begin to vary spatially within the MBS interval across the LPMS. $\delta^{15}N$ begins to decline towards lower background values (4-5‰), and an overall increasing TOC trend in the MBS towards peak values is observed for Clarkson (~32%), KEX (~38%), ELY-1 (~39%). $\delta^{15}N$ at both ILH and ELY-1 decline past background values reaching minimum $\delta^{15}N$ values of +2.8‰ for ELY-1 at the MBS/UBS contact, and -0.5‰ for ILH in the middle part of the UBS interval. Within the UBS interval, TOC values exhibit an overall decreasing trend at both the Clarkson and KEX locations, but TOC reaches peak values in the middle portion of the UBS interval for ILH (~36%), and approaches peak values for ELY-1 (~38%). After the spikes in TOC at ILH and ELY-1, TOC then declines modestly along with Clarkson and KEX trends to values ≤ 2% during the UGS interval (Figure 16).

4.3 ELEMENTAL TRENDS

The total sulfur content (TS) is representative of both the inorganic fraction produced by sulfide forming minerals (e.g. pyrite) under sulfate-reducing conditions, and the organic fraction of sulfur that is assimilated to sedimentary organic material during early diagenesis (Kasten and Jorgensen, 2000). Fe/Al represents the normalized fraction of iron present within samples, and it is sensitive to reductive leaching processes within marine environments. Both TS and Fe/Al follow very similar trends in all study units throughout the core shale intervals. In the TX-3027 outcrop (Figure 15), TS and Fe/Al remain fairly constant with only small deviations in Fe/Al, and very low TS values that measure below 0.05%. For the Midcontinent Shelf region, these values are highest near the shelf margin at Clarkson (especially in the UBS), and decrease towards the north, showing no discernible spatial gradients across the study locations (Figure 16). TS exhibits an overall increasing trend from the LBS to the UBS, and drops to lower values

in the UGS. In Illinois, however, TS remains fairly constant and low (between 1 – 2%) in the LBS and MBS intervals of the ELY-1 section. In the UBS interval for ELY-1, TS percentages increase sharply to peak values of ~3.6% with Fe/Al reflecting coeval increases.

Molybdenum and uranium may serve as useful proxies for interpreting the evolving paleo-redox conditions of a marine depositional environment. The Hushpuckney equivalent Upper Salesville Shale sample TX-3027 displays low and stable U abundances throughout the core shale unit (Figure 15) similar to the other geochemical data sets measured at this location (i.e. $\delta^{15}N$, TOC, and TS). Mo was not measured during LA-ICP-MS analysis for this sample location. In contrast, Mo and U contents show systematic variation both stratigraphically and geographically across the Midcontinent Shelf and Illinois Basin study units of the LPMS (Figure 16). In general, Mo and U rapidly increase upsection within the LBS and into the MBS, and then steadily decline in the UBS towards lower enrichments in the UGS. For the Midcontinent Shelf samples, the greatest Mo and U content in the black shale facies occur in Iowa at ILH (~316 for Mo/Al and ~81 for U/Al) and decline towards the south in Kansas (~72 for Mo/Al and ~31 for U/Al at Clarkson). The spatial gradient for Mo/Al records greater values than U/Al across the Midcontinent Shelf, reflecting stronger enrichments of Mo relative to U in areas proximal to the paleoshoreline. Mo was not measured for the Illinois Basin sample ELY-1; however, peak U abundances appear to be relatively high in the MBS interval of ELY-1 according to U/Al measurements from LA-ICP-MS. Until XRF analysis is conducted on the black shale facies of ELY-1, it will remain unclear whether maximum U and Mo contents are greater or less than those observed in Iowa.

5. DISCUSSION

5.1 ISOTOPIC FRACTIONATION OF NITROGEN IN CORE SHALES

Sedimentary organic nitrogen typically reflects the isotopic signature of fixed-N, primarily in the form of nitrate (NO_3^-), from the overlying watermass, which is transferred to the sediment by the sinking flux of organic matter (Altabet and Francois, 1994; Sigman et al., 2009; Algeo et al. 2008b). Likewise, the $\delta^{15}N$ values preserved in the OM reflect the weighted isotopic average of mixed ^{15}N sources imparted to the local watermass from both large fixed-N source pools (i.e. seawater and terrigenous runoff), and any enrichments/depletions associated with biological N-cycling in the water-column (Figure 17; Brandes and Devol, 2002; Capone et al., 2008). The two major N-cycle processes that strongly alter the size and isotopic composition of the fixed-N reservoir at any location are nitrogen fixation and water-column denitrification, with both processes generating distinct $\delta^{15}N$ signatures (Brandes and Devol, 2002; Deutsch et al., 2004; Capone et al., 2008; Sigman et al., 2009; Junium, 2010).

Nitrogen fixation, the process where N_2 gas is converted by cyanobacteria into a bioavailable form, has a very small isotopic fractionation effect (ε = -1 to -3‰), and tends to lower the overall $\delta^{15}N$ of seawater nitrate while increasing the size of the fixed-N pool (Dippner and Montoya, 2001; Sigman et al., 2009). The biomass produced in water columns with active N_2-fixation typically have $\delta^{15}N$ values ranging between -2‰ to +2‰ (Thunnel et al., 2004; Quan and Falkowski, 2008; Junium, 2010). In contrast, denitrification, the process where bacteria reduce NO_3^- to N_2 for metabolizing OM under suboxic conditions, ultimately removes fixed-N from the marine environment, and strongly discriminates (ε = 20 to 30‰) against the heavier ^{15}N-isotope. In modern pelagic oxygen minimum zones (i.e. Arabian Sea and Eastern Tropical

Pacific), water-column denitrification partially consumes the available nitrate pool, resulting in significant enrichment ($\delta^{15}N \geq +15‰$) of the residual nitrate (Gruber and Sermiento, 1997; Brandes and Devol, 2002; Voss et al., 2001; Sigman et al., 2009; Prokopenko et al., 2011). This heavy nitrate source is then utilized by other organisms to produce OM with high $\delta^{15}N$ values, which is preserved in the sediment record (Sigman et al., 2009; Quan et al., 2013).

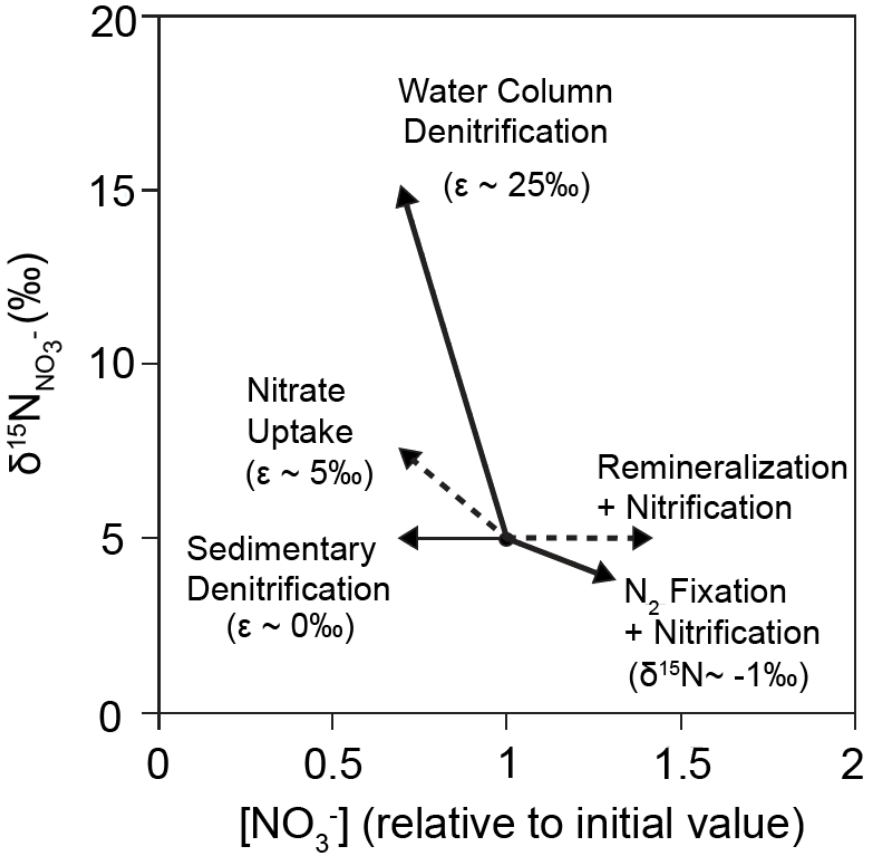

Figure 17: Effects of different marine N-cycle processes on nitrate concentration and $\delta^{15}N$ values, assuming an initial nitrate pool with a $\delta^{15}N$ of 5‰ (black circle). Solid arrows indicate process that adds/removes fixed N from seawater, while dashed arrows indicate internal cycling process of fixed N. Estimates of isotope fractionation effects (ε) are based on values presented in *Sigman et al.* (2009). Large isotope effects are associated with nitrate uptake and nitrification; however, these processes are typically complete reactions with no effect on N-isotope dynamics, similar to sedimentary denitrification. Figure modified from *Montoya et al.* (2002).

The N-isotopic composition of OM in cyclothemic core shales is determined by the $\delta^{15}N$ composition of both allochthonous terrigenous OM and autochthonous marine OM (Herrmann et al., 2015). The $\delta^{15}N$ values of Pennsylvanian coals ranges between -0.2‰ and +4.7‰ (Whiticar, 1996; Rimmer et al., 2006), and diagenesis during coal maturation has no significant influence on the $\delta^{15}N$ signal (Ader et al., 1998). Therefore, terrigenous OM in the black shales, which can reach up to 80% of the total organic content in the LBS and MBS (Algeo et al., 2004, 2008), may have contributed $\delta^{15}N$ values not exceeding more than ~ +5‰. The bulk nitrogen content and isotopic signal throughout cyclothemic core shales, however, is considered to be dominantly marine sourced (Algeo et al., 2008b; Herrmann et al., 2015). This is because the C_{org}:N ratio of terrigenous OM (20-80:1) is far greater than marine algal matter (4-10:1) (Meyers, 1994), and lignin, the compound that is most refractory in terrigenous OM and survives more readily during transport to the marine environment, contains no N (Sjostrom, 1993). Therefore, the primary contribution of marine OM to the $\delta^{15}N$ signal in cyclothemic core shales should reflect the isotopic composition of the original watermass. The major factors controlling the $\delta^{15}N$ signal within the paleo-epicontinental settings of this study include mixed inputs from: (1) mean Panthalassic Ocean $\delta^{15}N$ with estimated values ranging from +4‰ to +6‰ (Algeo et al., 2008b), (2) continental runoff with an estimated mean $\delta^{15}N$ of +4‰ (Sigman et al., 2009), and (3) regional water-column $\delta^{15}N$ enrichment or depletion relative to the ambient fixed-^{15}N pool due to denitrification or nitrogen fixation (Capone et al., 2008; Sigman et al., 2009; Junium, 2010).

The positive $\delta^{15}N$ excursion observed in all the LPMS black shale samples, excluding TX-3027, towards maximum values of ~ +14 to +16‰ are very similar to what is recorded in contemporary denitrifying systems. Spatial and temporal variations in $\delta^{15}N$ values across the study sites were likely due to differences in the contribution of isotopically distinct fixed-N

source pools, and the dynamics of N-cycle fractionation processes within the water-column. Diagenetic alteration of the $\delta^{15}N$ signal due to outcrop exposure in the TX-3027 study site is considered unlikely because the positive excursion event is preserved within several outcrop samples on the Midcontinent Shelf (c.f. Algeo et al., 2008b; Herrmann et al., 2015).

5.2 TEXAS EASTERN SHELF: DEPOSITIONAL ENVIRONMENT OF THE UPPER SALESVILLE SHALE

Since the Hushpuckney equivalent Upper Salesville Shale in north-central Texas displays too many contrasts in N-isotopes and lithofacies (Figure 10 and 15), it was determined for this study that the shale unit cannot be subdivided into the four correlative intervals that are applicable to the Hushpuckney Shale in both the Midcontinent Shelf and Illinois Basin. Instead, geochemical data sampled from the Texas unit is plotted against the stratigraphic height of the outcrop, and individual stratigraphic intervals are referenced by their associated color facies in ascending order: dark grey shale (DGS), light grey shale (LGS), and upper tan shale (UTS). The transgressive core shale interval is represented by the condensed (~1.8 meter) section of dark gray to light gray shale comprised of the DGS and LGS facies, while the thicker (~10 meters) UTS facies represents the prodeltaic shale that was deposited as deltas began prograding across the shelf during sea level regression (Boardman and Heckel, 1989; Yancey and Cleaves, 1990; Boardman et al., 1995).

The entire core shale interval in TX-3027 maintains background $\delta^{15}N$ values of ~ 4‰, and there is no evidence that reducing conditions were ever significant due to the lack of OM preservation (< 1% TOC), very low sulfur content (< 0.5%), and the absence of authigenic uranium enrichment throughout the sampled section (Figure 15). The results for this study location on the Eastern Shelf indicate that both the sediment and bottomwater conditions retained

enough dissolved oxygen content, i.e. weakly to fully oxic (>2 mL O_2/L H_2O; Tyson and Pearson, 1991; Capone et al. 2008), throughout core shale deposition to prevent a sustained reducing environment. Higher redox potentials within the water column and/or seafloor would have caused extensive oxidation of any OM that was supplied to the sediments, inhibited microbial reduction processes such as denitrification and sulfate reduction, and suppressed any authigenic effects of uranium precipitation and preservation within the sediment (Algeo et al., 2004; Potter et al., 2005; Tribovillard et al., 2006; Algeo and Tribovillard, 2009).

The apparent absence of bottomwater anoxia and subsequently higher paleo-redox conditions exhibited for this area on the Eastern Shelf suggests that (1) preconditioned (i.e. oxygen-poor, nutrient-rich, denitrified) waters were not upwelled and advected across the shelf from the nearby Midland Basin, (2) water column stratification was not strong enough to fully restrict vertical circulation of dissolved oxygen from the surface waters down to the seafloor, and (3) the influx of OM likely did not exceed the capacity of aerobic respiration within the water column or sediment pore-waters to sustain a prolonged anoxic/reducing environment throughout core shale deposition. Weak water column stratification could be attributed to lower rates of freshwater runoff from the surrounding Ouachita orogen to produce a sufficient halocline and quasi-estuarine circulation system, or possibly by the absence of a permanent thermocline due to potentially shallower water depths at this location on the inner shelf (Yancey, 1986; Teo, 1991; Rosscoe, 2010). The low concentrations of organic carbon and redox sensitive trace elements in the Upper Salesville Shale may also be ascribed to the effects of sediment dilution (Demaison and Moore, 1980; Teo, 1991; Hentz, 1994; Boardman et al., 1995), because TX-3027 was located within the paleo-depocenter of the Perrin delta system (Figure 7; Brown et al., 1973; Cleaves and Erxleben, 1985) and very proximal to a major detrital source (i.e. the Ouachita

orogen; Figure 8). Sediment dilution occurs when the rate of clastic influx is relatively higher than the rate of OM supplied to the depositional setting. As a result, the OM becomes more spatially dispersed throughout the sediments, and may not be concentrated enough for its decomposition to lower the overall redox conditions on the seafloor. This idea of sediment dilution is also supported by lower concentrations of conodont fauna observed throughout several Texas core shale units, compared to their counterparts on the Midcontinent Shelf, and has been attributed to proximal influences from encroaching deltaic muds (c.f. Boardman and Heckel, 1989). Additionally, the Eastern Shelf lacked any significant inputs of terrestrial OM from surrounding landmasses that could possibly counter the effects of sediment dilution and help surpass aerobic respiration within the water column and sediment porewaters to foster an anoxic environment. Unlike the LPMS, which received a large supply of terrestrial OM from extensive peat swamps in the Illinois and Appalachian basins (Greb et al., 2003; Algeo et al., 2004), only thin localized coals have been observed within deltaic deposits on the Eastern Shelf (Brown et al., 1973; Cleaves and Erxleben, 1985; Cleaves, 1996), suggesting the primary source of OM supplied during Texas core shale deposition was derived from marine organics (Teo, 1991).

Although geochemical data from TX-3027 indicates core shale deposition occurred under oxic conditions in this inner shelf setting, black, organic-rich core shales deposited under anoxic settings have been observed in the Pennsylvanian cycles of the Eastern Shelf (Boardman and Malinky, 1985; Yancey, 1986; Boardman and Heckel, 1989; Cleaves, 1993, 1996). This facies, however, is primarily documented in the subsurface by well logs, and located along the deeper, outer shelf region proximal to the Midland Basin (Jackson, 1964; Boardman and Malinky, 1985; Brown, 1989; Cleaves, 1993; Wright, 2011). The high gamma-ray neutron values, which

characterize these black shales in the subsurface well logs, also diminish up-dip along the shelf towards the paleoshoreline (Boardman and Malinky, 1985; Cleaves, 1993) indicating less organic, uranium, and clay content in the shales (Asquith and Krygowski, 2004). These lateral facies changes in core shale characteristics across the Eastern Shelf (i.e. organic-rich, black shales deposited in a deep, anoxic setting on the outer shelf; and organic-poor, gray shales deposited in a shallow, oxic setting on the inner shelf) suggest that depth-controlled stratification played a primary role in black shale deposition for this epicontinental setting; not quasi-estuarine circulation as *Algeo and Heckel* (2008) hypothesized.

In the depth-stratification model, an anoxic environment developed when the well-established OMZ (beneath a stable thermocline) of the Midland basin rose above the shelf edge and intruded upon the Eastern Shelf during times of maximum sea level transgression (Figure 18; Boardman and Malinky, 1985; Yancey, 1986; Cleaves, 1993, 1996; Bradshaw and Mazzulo, 1996). Along the outer-shelf region, organic-rich muds accumulated in a deep, offshore setting under oxygen deprived and sediment starved conditions to form black shales. Further inshore, the shelf environment likely shallowed above the thermocline where bottomwaters were more oxygenated, and proximal deltaic influences diluted the seafloor OM that survived oxidation through the water column. It was in this setting that organic-poor muds lacking redox-sensitive elemental enrichments accumulated to form dark – light gray shales, corresponding to what is observed at the TX-3027 study location. Sea level regression would have resulted in delta progradation across the shelf (depositing the thick UTS facies at TX-3027), and caused the thermocline and OMZ to recede from the shelf margin area back into the Midland basin allowing carbonate production to resume on the shelf edge banks under oxic conditions (Boardman and

Malinky, 1985; Cleaves and Erxleben, 1985; Yancey, 1986; Cleaves, 1996; Yang and Kominz, 2002).

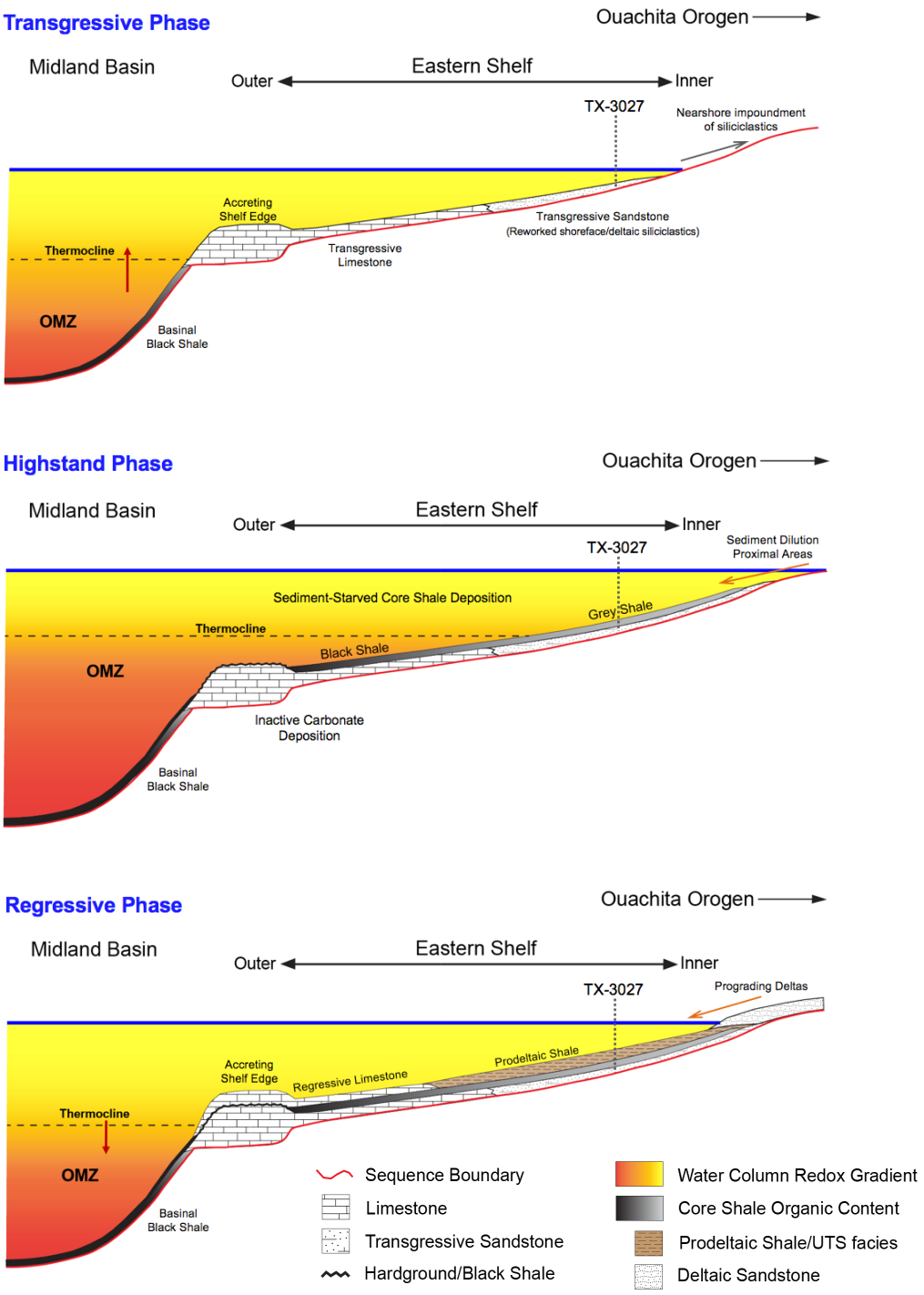

Figure 18**:** Conceptual model illustrating how changes in glacio-eustatic sea level and depth-stratification affected cyclothem deposition on the Eastern Shelf of the Permian Basin Seaway.

5.3 LPMS: DEPOSITIONAL ENVIRONMENTS OF THE HUSHPUCKNEY SHALE

5.3.1. Interval 1: Lower Black Shale

The LBS for the Midcontinent Shelf samples Clarkson, KEX, and ILH overlie the middle limestone unit, while the LBS in the Illinois Basin sample (ELY-1) directly overlies coal bed deposits with a sharp erosional contact. This contrast in the underlying lithofacies (marine limestone vs. terrestrial peat swamps) between the two basins suggests that black shale deposition likely occurred in both nearshore and offshore environments, and that the unit likely progressed from relatively shallow water in the Illinois Basin to relatively deeper water along the Midcontinent Shelf (Heckel, 1991; Coveney et al., 1991; Bisnett and Heckel, 1996). Much of the OM preserved in the LBS and overlying MBS interval is derived from terrigenous (humic) sources with lesser proportions of marine algal matter, reflecting strong export from coastal peat swamps (c.f. Greb et al., 2003; Algeo et al., 2004, 2008). The erosional surface that scours the top of extensive coal beds in the Illinois Basin has been interpreted in previous studies (c.f. Bauer and Demaris, 1982; Demaris et al., 1983; Rosenau et al., 2013) as the transgressive "ravinement" surface, upon which the marine facies (i.e. black shale) was deposited during sea level transgression (Olszewski, 1996; Rosenau et al., 2013; Cecil et al., 2014; DiMichele, 2014). It is likely that ravinement during shoreline transgression of coastal peat swamps in the east helped remobilize large quantities of humic organic debris into the overlying seawater for dispersal (Wenger and Baker, 1986; Olszewski, 1996; Rosenau et al., 2013). The fact that large concentrations of terrestrial OM can be found in black shales deposited far offshore on the Midcontinent Shelf supports the idea that humic detritus may have been dispersed seaward by freshwater surface plumes emanating from humid, equatorial climates of the eastern interior (Coveney et al., 1991, Algeo et al., 2004; Algeo and Heckel, 2008). A terrigenous source of

organic carbon delivered by freshwater runoff would be consistent with the contribution of a halocline to water column stratification in quasi-estuarine systems (Witzke, 1987; Heckel, 1991; Algeo and Heckel, 2008).

Geochemical data collected from the LBS interval reveals an upsection trend of increasing TOC, $\delta^{15}N$, TS, Mo/Al, and U/Al values, signifying that the marine depositional environments in both the Midcontinent Shelf and Illinois Basin became increasingly hypoxic/reducing to facilitate both enhanced OM preservation and enrichments in redox-sensitive elements (Figure 19). The *superestuarine circulation model* predicts that these environmental conditions were stimulated across the LPMS by the incursion of oxygen-depleted, denitrified bottomwaters that were laterally advected from the OMZ of the etPan (Algeo et al., 2008; Algeo and Heckel, 2008). However, the lack of ^{15}N, OM, and redox-sensitive element enrichments observed in the Hushpuckney equivalent Upper Salesville Shale (TX-3027) of north-central Texas challenges the idea that advection of "preconditioned" seawater from the etPan was necessary for (1) introducing the ^{15}N-enriched isotopic signal during core shale deposition, or (2) facilitating intensely reducing bottomwaters across North American epicontinental environments. In modern marine systems, oxygen deprivation and reducing conditions may develop when excessive OM delivery causes aerobic consumers to utilize dissolved O_2 for their metabolism faster than it is replenished, or insufficient circulation in the water column prevents O_2 renewal at depth (Demaison and Moore, 1980; Potter et al., 2005; Tribovillard et al., 2006). For the LPMS, these environmental conditions were likely initiated by large settling fluxes of organic detritus (both allochthonous terrestrial OM and autochthonous marine OM) in conjunction with halocline stratification, which would have limited vertical mixing by separating oxygenated surface waters from the oxygen-depleted bottomwaters and

sediments below. *Algeo and Heckel* (2008) assumed that primary productivity was too low to help stimulate benthic O_2 demand across the LPMS. However, this is considered highly unlikely due to the potential eutrophication effects stemming from fluvial-derived nutrients (Coveney et al., 1991; Hatch and Leventhal, 1992; Olszewski and Patowski, 2003, 2009).

Rising $\delta^{15}N$ values in the Midcontinent Shelf and Illinois Basin study units are interpreted as extensive water column denitrification that was initiated across the LPMS during the onset of black shale accumulation, which intensified throughout LBS deposition to peak $\delta^{15}N$ enrichments. This microbial process of OM degradation commences when dissolved O_2 becomes depleted in the subsurface waters towards suboxic conditions, and denitrifying organisms utilize seawater nitrate (preferentially consuming $^{14}NO_3^-$) as on oxidant for their metabolism (Capone et al., 2008; Galbraith et al., 2008; Robinson et al., 2012). Previous studies of the Hushpuckney Shale have suggested that bottomwaters became increasingly euxinic during LBS deposition (e.g. Algeo and Maynard, 2004; Algeo et al., 2004) based on strong concurrent enrichments observed in U and Mo values, which typically reflect greater fixation under euxinic conditions (Tribovillard et al., 2009). This scenario, however, conflicts with the environmental conditions necessary for water column denitrification to occur. Under strongly reducing settings, essentially all seawater nitrate is consumed, erasing the ^{15}N-enrichment associated with incomplete denitrification in the water column (Capone et al., 2008; Junium, 2010). Thus, bottomwater conditions are interpreted as becoming increasingly suboxic throughout LBS deposition to facilitate extensive denitrification across the LPMS study area, but not fully anoxic.

Decreasing O_2 levels commonly result in greater OM preservation (hence, increasing TOC values), and greater export of trace elements to the sediment in association with the organic flux (Algeo and Maynard, 2004). At the same time, depleted O_2 levels generally cause the zone

of sulfate (SO_4^{2-}) reduction to rise toward the sediment-water interface, creating an environment where anoxic/euxinic pore-waters exist beneath suboxic bottomwaters (Algeo and Maynard, 2004; Tribovillard et al., 2006; Piper and Calvert, 2009). Sediments deposited under such conditions are commonly enriched in redox-sensitive elements such as U and Mo because the reduced ionic species of these elements are either readily adsorbed onto OM (especially to humic substances) or form insoluble chemical precipitates (Pratt and Davis, 1992; Calvert and Pedersen, 1993; Hoffmann et al., 1998). Authigenic enrichment for both these elements is considered to take place primarily within the sediments and not in the water column (Tribovillard et al., 2006; Algeo and Tribovillard, 2008). Therefore, the simultaneous enrichments in U and Mo across the LPMS study sites may be attributed to increasingly euxinic porewaters near the sediment-water interface, beneath a suboxic water-column.

Spatial gradients are also observed in the increasing $\delta^{15}N$, TOC, U/Al, and Mo/Al values throughout the LBS interval with greater values moving north across the Midcontinent Shelf and east towards the Illinois Basin (Figure 16). These lateral variations seem to reflect greater oxidant depletion and stronger reducing conditions towards the shallower eastern interior of the LPMS, approaching major sources of terrestrial OM (i.e. peat swamps) and freshwater runoff. Depositional environments in closer proximity to these sources likely experienced stronger halocline stratification to restrict oxygen from circulating down to the bottomwaters and sediments (Algeo and Heckel, 2008), along with an increased flux of settling OM (Coveney et al, 1987; Hatch and Leventhal, 1992), resulting in greater consumption of oxidants (e.g. O_2, NO_3^-, SO_4^{2-}) by microbial communities. Thus, stronger reducing conditions towards the paleoshoreline resulted in more intense denitrification in the water column, along with enhanced fixation of U and Mo in the sediments. These spatial gradients in redox proxies across the LPMS study area

are consistent with benthic redox variations facilitated by a large-scale, quasi-estuarine circulation system (c.f. Coveney et al., 1991; Hoffman et al., 1998; Algeo and Heckel, 2008).

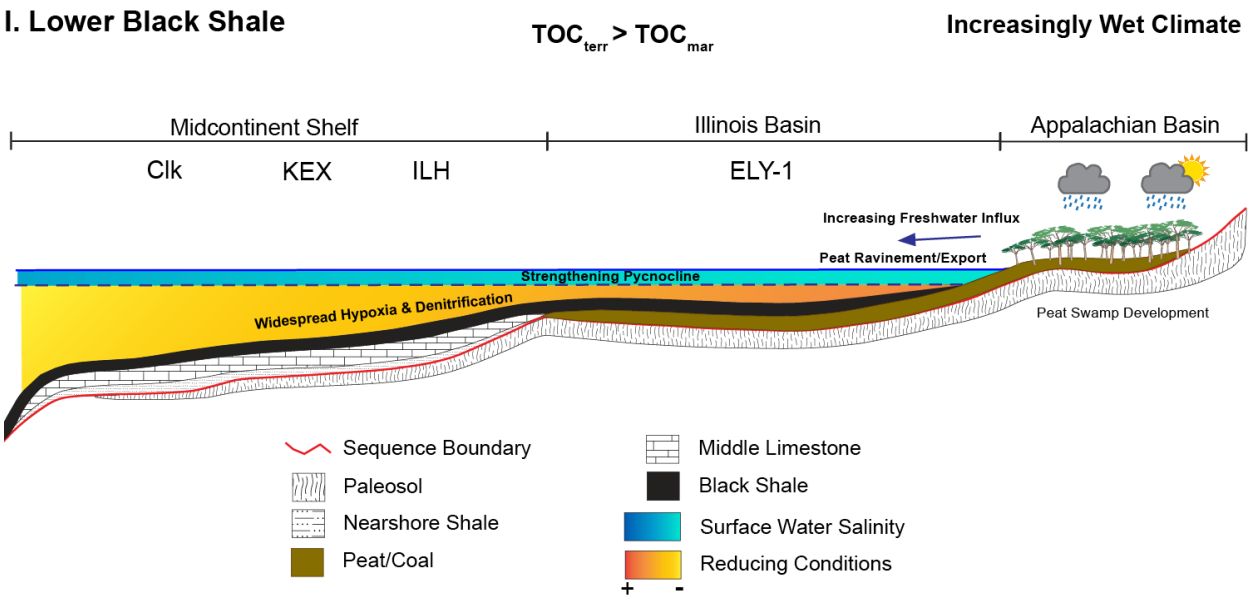

Figure 19**:** Interpreted depositional environment for the Lower Black Shale (LBS) facies of the Hushpuckney Shale during late transgression.

5.3.2. Interval 2: Middle Black Shale

The MBS interval across the LPMS study area is characterized by maximum $\delta^{15}N$ values at its base, followed by an upsection decline in $\delta^{15}N$ towards lower background values (Figure 16). This relaxation phase of the $\delta^{15}N$ excursion occurs in conjunction with increasing TOC, TS, U/Al, and Mo/Al trends signifying that the LPMS became more reducing across the study transect with greater OM delivery and preservation. Organic content in the MBS is predominately comprised of terrigenous material exported from coastal peat swamps (Algeo and Heckel, 2008; Algeo et al., 2008b), and peak TOC values near the top of the MBS boundary may correspond to the maximum flooding surface (Algeo et al., 2004). The overall increase in reducing conditions during late eustatic transgression was likely attributed to stronger water

column stratification, which may be related to enhanced precipitation and freshwater runoff to the LPMS from its equatorial watersheds (Figure 20; Algeo et al., 2004, 2008b; Algeo and Heckel, 2008). $\delta^{15}N$, TOC, TS, U/Al, and Mo/Al values exhibit patterns of geographic and stratigraphic variability across the LPMS (Figure 16), suggesting that lateral gradients in water mass conditions became more pronounced in the MBS relative to the LBS. Differences in these spatial gradients may have been controlled by the supply of OM and nutrients, biogeochemical processes of local microbes, and surface water salinities with respect to pycnoclinal strength.

The cause of declining $\delta^{15}N$ values in cyclothemic black shales has been interpreted in previous studies as the input of less denitrified seawater advected from the etPan (Algeo and Heckel, 2008; Algeo et al., 2008b; Herrmann et al., 2015). However, a more plausible explanation may be attributed to changes in regional N cycling within the LPMS, considering that no change is recorded in the isotopic signal of the coeval Texas shale sample (TX-3027) that was located more proximal to the etPan. Changes in the $\delta^{15}N$ record of marine sediments are usually associated with imbalances to the N-budget in the overlying waters (Brandes et al., 2007; Junium, 2010). Under strongly reducing (anoxic/euxinic) water columns, essentially all the subsurface nitrate is consumed in the zone of active denitrification near the suboxic/anoxic interface, thereby, erasing the ^{15}N-enrichment associated with incomplete denitrification (Thunnel et al., 2004; Junium, 2010). These environmental conditions effectively minimize and/or eliminate the isotopic signal of denitrification occurring in the water column, and cause the $\delta^{15}N$ signal to decrease toward the oceanic mean value (Thunnel et al., 2004; Deutsch et al., 2004; Quan and Falkowski, 2009; Gibson et al., 2015), which is estimated to be ~ +4 to +6‰ during the Late Pennsylvanian (Algeo et al., 2008b). Excessive denitrification can also lead to N-poor conditions in the water column that favor the growth of N-fixing cyanobacteria (Deutsch et

al., 2004; Meyers et al., 2009; Sigman et al., 2009). In geographic regions where N-fixing biomass become prominent, the input of isotopically light N (δ15N = -2 to +2‰) will further lower the δ15N signal of the marine sediments below the oceanic mean (Thunnel et al, 2004; Quan et al., 2008; Meyers et al., 2009). In the Hushpuckney Shale, evidence for nitrogen fixation compensating the effects of intense denitrification is supported by the receding $\delta^{15}N$ trends in ELY-1 and ILH that surpass below background values (< 4‰) near the MBS/UBS contact and within the UBS interval.

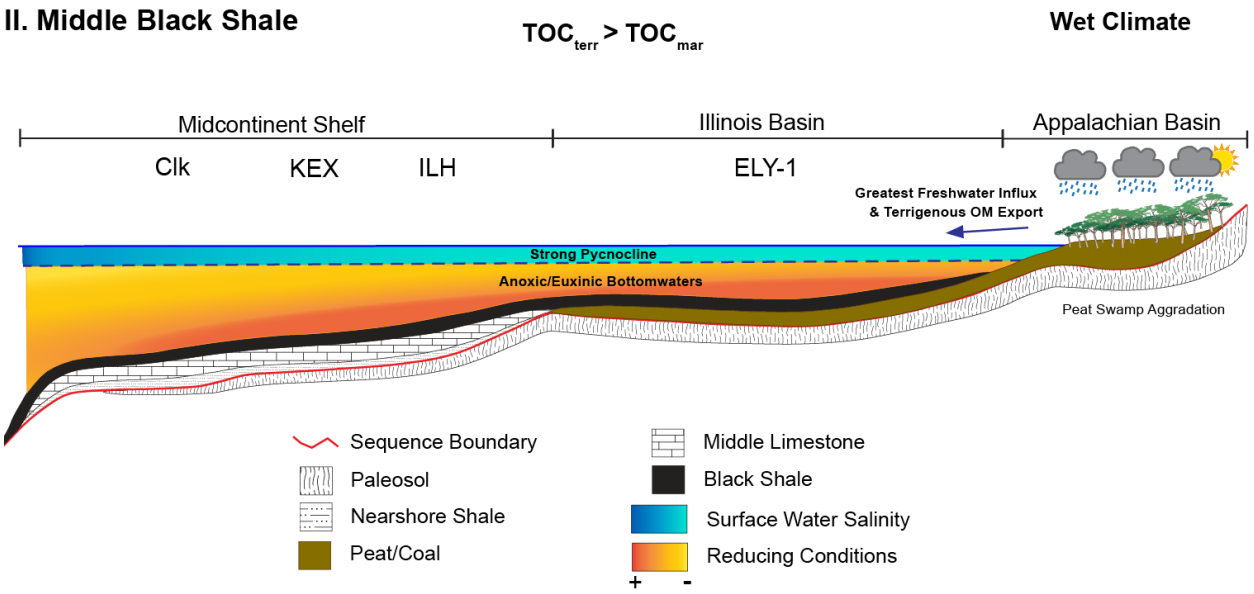

Figure 20: Interpreted depositional environment for the Middle Black Shale (MBS) facies of the Hushpuckney Shale during early highstand.

5.3.3. Interval 3: Upper Black Shale

The UBS is generally characterized by the overall up-section stabilization of $\delta^{15}N$ towards background values, diminishing TOC, U/Al and Mo/Al values (Figure 16), and a shift in dominance from terrestrial- to marine-derived OM (Algeo et al., 2004; 2008b; Algeo and Heckel, 2008). Patterns of spatial and temporal variation are exhibited for all of these proxies across the

LPMS. For instance, $\delta^{15}N$ for both the ILH and ELY-1 sections remain below background values (< 4‰) through the lower half of the UBS interval indicating that these areas likely experienced higher rates of N-fixation compared to the KEX and Clarkson locations. Spatial gradients continue to be exhibited in TOC, Mo/Al, and U/Al across the study transect despite the overall declining trend in these proxies, suggesting that the eastern interior regions of the LPMS experienced relatively greater reducing benthic conditions.

Taken together, the geochemical data presented in this research and other studies (e.g. Hoffman et al., 1998; Algeo et al., 2004, 2008a; Herrmann et al., 2012, 2015) support the inference that the LPMS bottomwaters became less anoxic/reducing during the late highstand to early regressive phase of the glacioeustatic cycle (Figure 21). The progressive shift to higher redox potentials in the UBS along with reduced input of terrigenous OM were likely influenced by climatic changes towards the next glacial phase. As the global climate began to cool and Gondwanan icesheets grew, sea level fall commenced and climate conditions became increasingly arid within the paleotropics (West et al., 1997; Soreghan et al., 2002; Olszewski and Patzkowsky, 2003; Algeo et al., 2004, 2008a; Falcon-Lang et al., 2009). A transition to drier climate conditions would result in both a loss of coastal peat swamps and less freshwater runoff to the LPMS, contributing to a reduced flux of terrigenous OM and a weakened pycnocline (Algeo et al., 2004). A weakening pycnocline also would have allowed increased vertical mixing in the water column, causing benthic redox conditions to fluctuate, and enhance marine OM production through upward mixing of bottomwater nutrients (Algeo et al., 2004, 2008a).

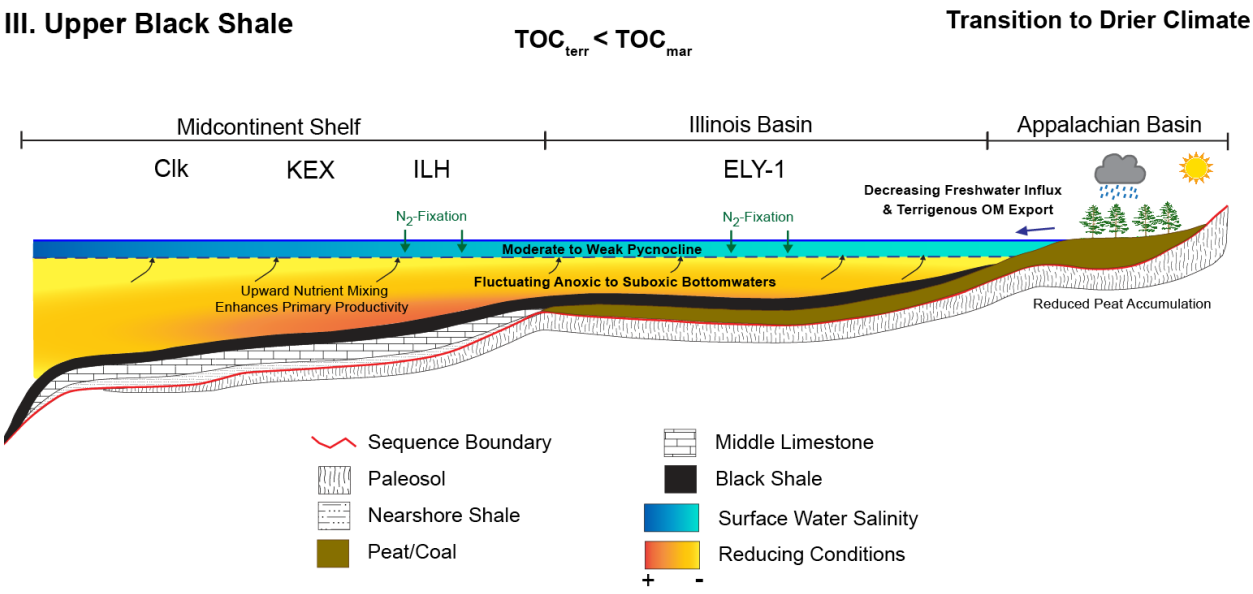

Figure 21: Interpreted depositional environment for the Upper Black Shale (UBS) facies of the Hushpuckney Shale during late highstand.

5.3.4. Interval 4: Upper Grey Shale

The UGS facies across all LPMS sections is characterized by low TOC values (< 2%), sustained $\delta^{15}N$ at background values (~ 4 to 6‰), no authigenic enrichment of U or Mo, and varying degrees of bioturbation with sparse to abundant marine benthic fauna (Heckel, 1994; Algeo et al., 2004). These characteristics of the upper grey shale indicate that bottomwater conditions had become increasingly oxygenated, and that dissolved oxygen levels on the seafloor had risen high enough to support benthic dwelling fauna (Heckel, 1977, 1994; Algeo et al., 2004). Therefore, the UGS facies marks a transition between the underlying black shale facies, which was deposited under mostly anoxic benthic conditions beneath a stratified water column, and the overlying regressive limestone facies, which was deposited in a well-oxygenated watermass across most of the LPMS (Heckel, 1977, 1994; Algeo et al., 2004). The UGS facies thus represents the time in which the stratified water column of the LPMS deteriorated, and

downward mixing of O_2-rich surface waters progressively increased towards the seafloor (Heckel, 1994; Algeo et al., 2004).

These environmental conditions during UGS deposition were likely influenced by both climatic and eustatic changes (Figure 22). Increasingly arid climate conditions would further reduce the amount of freshwater runoff to the LPMS, causing the pycnocline to significantly weaken and allow for greater mixing in the water column (Algeo et al., 2004; Algeo and Heckel, 2008). Eustatic regression associated with Gondwanan icesheet buildup would also cause water depths to shallow across the LPMS, which would reduce the vertical mixing distance between oxygenated surface waters and the seafloor.

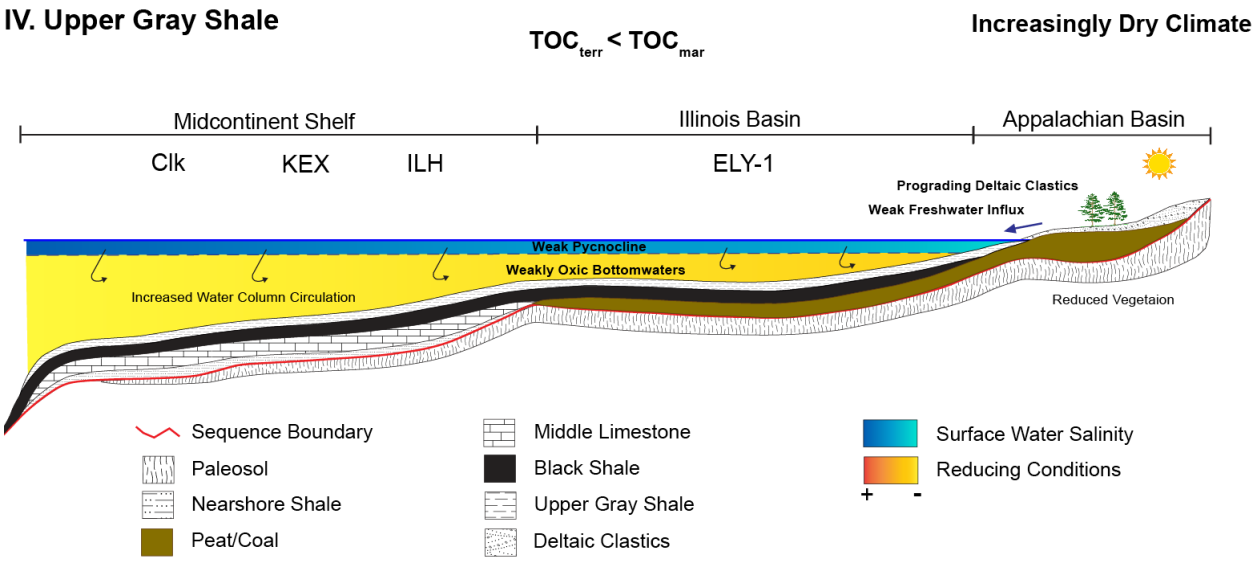

Figure 22: Interpreted depositional environment for the Upper Gray Shale (UGS) facies of the Hushpuckney Shale during early regression.

6. CONCLUSIONS

The *superestuarine circulation* model for black shale deposition in cyclothemic core shales was tested by comparing the spatial and temporal variations of geochemical proxies in the Hushpuckney Shale and its lateral equivalents across a wide geographic range of the North American midcontinent. An important discovery from the data collected in this study was the lack of $\delta^{15}N$, OM, and redox-sensitive element enrichment on the Eastern Shelf of the Permian Basin Seaway, while, progressively greater enrichments are observed in the LPMS moving north across the Midcontinent Shelf and east towards the Illinois Basin. These results challenge the notion that "preconditioned" seawater advected from the etPan was responsible for (1) introducing the ^{15}N-enriched isotopic signal, or (2) facilitating benthic anoxia across North American epicontinental environments during core shale deposition. Instead, it appears that separate but unique paleoenvironmental conditions were responsible for the compositional variation in sediments between the Eastern Shelf and the LPMS.

The higher paleo-redox conditions inferred for the Eastern Shelf study site (TX-3027) suggest that water column stratification was not strong enough to prevent vertical mixing of dissolved oxygen to the benthic environment, nor was there a high enough influx of OM to exceed oxidative capacity in the water column or sediment pore-waters during core shale deposition. Weak water column stratification may be attributed to: (1) lower rates of freshwater runoff from the surrounding Ouachita orogen to produce a sufficient halocline; and (2) the absence of a stable thermocline due to potentially shallow water depths at this inner shelf location (Yancey, 1986; Teo, 1991; Rosscoe, 2010). Although not directly observed in this study, lateral gradients in organic-richness and enrichment of redox-sensitive elements have been reported in Pennsylvanian core shale intervals across the Eastern Shelf, where stronger

enrichments occur towards the deep, outer-shelf region proximal to the Midland Basin (c.f. Boardman and Malinky, 1985; Yancey, 1986; Boardman and Heckel, 1989; Cleaves, 1993, 1996; Write, 2011). This trend implies that depth-stratification may have been the primary mechanism responsible for black shale deposition in this epicontinental setting; not quasi-estuarine circulation as *Algeo and Heckel* (2008) hypothesized (c.f. Algeo et al., 2008a, Figure. 8a). In this model, benthic anoxia developed when the well-established OMZ (beneath a stable thermocline) of the Midland basin rose above the shelf edge and intruded upon the Eastern Shelf during glacio-eustatic highstands (Boardman and Malinky, 1985; Yancey, 1986; Cleaves, 1993, 1996; Bradshaw and Mazzulo, 1996). Organic-rich, black shales were deposited in a deep, anoxic setting along the outer shelf, while organic-poor, gray shales were deposited in a shallow, dysoxic to oxic setting along the inner shelf.

For the LPMS study transect, lateral gradients in redox proxies (e.g. U/Al, Mo/Al, and $\delta^{15}N$) indicate that reducing conditions intensified towards the shallow eastern interior of the sea, suggesting stronger oxidant depletion occurred in that direction. This pattern is consistent with large-scale, quasi-estuarine circulation, in which strong freshwater drainage into the eastern region of the LPMS resulted in strong density stratification. Widespread benthic anoxia appears to have been controlled by the vertical density gradient in the water column associated with continental runoff combined with large settling fluxes of organic detritus (both allochthonous terrestrial OM and autochthonous marine OM) to the basinal environments. The $\delta^{15}N$ excursions observed in the black shale facies of the LPMS study sites are interpreted as local N-cycling and fractionation processes (e.g. denitrification and N_2-fixation) that occurred within the basin. Spatial and temporal variations in the $\delta^{15}N$ signal were likely caused by imbalances to the fixed-

N reservoir of the local watermass, which seem to have been a function of changing redox conditions in the water column.

7. REFERENCES

Ader, M., Boudou, J. P., Javoy, M., Goffé, B., & Daniels, E. (1998). Isotope study on organic nitrogen of Westphalian anthracites from the Western Middle field of Pennsylvania (USA) and from the Bramsche Massif (Germany). *Organic Geochemistry*, *29*(1), 315-323.

Algeo, T. J., Hoffman, D. L., Maynard, J. B., Joachimski, M. M., Hower, J. C., & Watney, W. L. (1997). Environmental reconstruction of anoxic marine systems: core black shales of Upper Pennsylvanian Midcontinent cyclothems. In *Cyclic Sedimentation of Appalachian Devonian and Midcontinent Pennsylvanian Black Shales: Analysis of Ancient Anoxic Marine Systems—A Combined Core and Field Workshop. Joint Meeting of Eastern Section AAPG and The Society for Organic Petrography (TSOP), Lexington, Kentucky* (pp. 103-147).

Algeo, T. J., & Maynard, J. B. (2004a). Trace-element behavior and redox facies in core shales of Upper Pennsylvanian Kansas-type cyclothems. *Chemical geology*, *206*(3), 289-318.

Algeo, T. J., Schwark, L., & Hower, J. C. (2004b). High-resolution geochemistry and sequence stratigraphy of the Hushpuckney Shale (Swope Formation, eastern Kansas): implications for climato-environmental dynamics of the Late Pennsylvanian Midcontinent Seaway. *Chemical Geology*, *206*(3), 259-288.

Algeo, T. J., Heckel, P. H., Maynard, J. B., Blakey, R., & Rowe, H. (2008a). Modern and ancient epeiric seas and the super-estuarine circulation model of marine anoxia. *Dynamics of Epeiric seas: sedimentological, paleontological and geochemical perspectives. Geological Association Canada Special Publication*, 7-38.

Algeo, T., Rowe, H., Hower, J. C., Schwark, L., Herrmann, A., & Heckel, P. (2008b). Changes in ocean denitrification during Late Carboniferous glacial–interglacial cycles. *Nature Geoscience*, *1*(10), 709-714.

Algeo, T. J., & Heckel, P. H. (2008). The Late Pennsylvanian midcontinent sea of North America: a review. *Palaeogeography, Palaeoclimatology, Palaeoecology*, *268*(3), 205-221.

Altabet, M. A., & Francois, R. (1994). Sedimentary nitrogen isotopic ratio as a recorder for surface ocean nitrate utilization. *Global Biogeochemical Cycles*,*8*(1), 103-116.

Arbenz, J. K. (1989). The Ouachita system. *The geology of North America—An overview: Geological Society of America, The Geology of North America, v. A*, 371-396.

Archer, A. W., Kuecher, G. J., & Kvale, E. P. (1995). The role of tidal-velocity asymmetries in the deposition of silty tidal rhythmites (Carboniferous, Eastern Interior Coal Basin, USA). *Journal of Sedimentary Research*, *65*(2).

Archer, A. W., & Kvale, E. P. (1993). Origin of gray-shale lithofacies ("clastic wedges") in US midcontinental coal measures (Pennsylvanian): an alternative explanation. *Geological Society of America Special Papers*, *286*, 181-192.

Arthur, M. A., & Sageman, B. B. (1994). Marine shales: depositional mechanisms and environments of ancient deposits. *Annual Review of Earth and Planetary Sciences*, *22*, 499-551.

Belt, E. S., Heckel, P. H., Lentz, L. J., Bragonier, W. A., & Lyons, T. W. (2011). Record of glacial–eustatic sea-level fluctuations in complex middle to late Pennsylvanian facies in the Northern Appalachian Basin and relation to similar events in the Midcontinent basin. *Sedimentary Geology*, *238*(1), 79-100.

Bishop, J. W., Montañez, I. P., & Osleger, D. A. (2010). Dynamic Carboniferous climate change, Arrow Canyon, Nevada. *Geosphere*, *6*(1), 1-34.

Bisnett, A. J., & Heckel, P. H. (1996). Sequence stratigraphy helps to distinguish offshore from nearshore black shales in the Midcontinent Pennsylvanian succession. *SPECIAL PAPERS-GEOLOGICAL SOCIETY OF AMERICA*, 341-350.

Blakey, R.C. (2007). Carboniferous–Permian palaeogeography of the Assembly of Pangae. In: Wong, Th.E. (Ed.), Proceedings of the XVth International Congress on Carboniferous and Permian Stratigraphy. Utrecht, 10–16 August 2003. Royal Dutch Academy of Arts and Sciences, (Amsterdam), pp. 443–456.

Bjølykke, K. (1998). Clay mineral diagenesis in sedimentary basins—a key to the prediction of rock properties. Examples from the North Sea Basin. *Clay minerals*, *33*(1), 15-34.

Boardman, D. R., & Heckel, P. H. (1989). Glacial-eustatic sea-level curve for early Late Pennsylvanian sequence in north-central Texas and biostratigraphic correlation with curve for midcontinent North America. *Geology*, *17*(9), 802-805.

Boardman, D. R., & Malinky, J. M. (1985). Glacial-Eustatic Control of Virgilian Cyclothems in North Central Texas.

Boardman II, D. R., Nestell, M. K., & Knox, L. W. (1995). Depth-related microfaunal biofacies model for late Carboniferous and Early Permian cyclothemic sedimentary sequences in Mid-Continent North America.

Brandes, J. A., & Devol, A. H. (2002). A global marine‐fixed nitrogen isotopic budget: Implications for Holocene nitrogen cycling. *Global Biogeochemical Cycles*, *16*(4).

Brown, L. F., Cleaves, A. W., & Erxleben, A. W. (1973). *Pennsylvanian depositional systems in North-Central Texas: a guide for interpreting terrigenous clastic facies in a cratonic basin* (No. 14). Bureau of Economic Geology, University of Texas at Austin.

Brown, L. F., Raúl Fernando Solís I., & Johns, D. A. (1987). *Regional stratigraphic cross sections, Upper Pennsylvanian and Lower Permian strata (Virgilian and Wolfcampian Series), north-central Texas*. Bureau of Economic Geology, University of Texas at Austin.

Budnik, R. T. (1986). Left-lateral intraplate deformation along the Ancestral Rocky Mountains: implications for late Paleozoic plate motions. *Tectonophysics*, *132*(1-3), 195-214.

Calvert, S. E., Bustin, R. M., & Ingall, E. D. (1996). Influence of water column anoxia and sediment supply on the burial and preservation of organic carbon in marine shales. *Geochimica et Cosmochimica Acta*, *60*(9), 1577-1593.

Cecil, C. B. (1990). Paleoclimate controls on stratigraphic repetition of chemical and siliciclastic rocks. *Geology*, *18*(6), 533-536.

Cecil, C. B., & Dulong, F.T. (2003). Precipitation models for sediment supply in warm climates. Climate Controls on Stratigraphy: Society for Sedimentary Geology (SEPM) Special Publication 77, p. 21–28.

Cecil, C.B., Dulong, F.T., West, R.R., Stamm, R., Wardlaw, B., and Edgar, N.T. (2003) Climate controls on the stratigraphy of a Middle Pennsylvanian cyclothem in North America, in Cecil, C.B., and Edgar, N.T., eds., Climate Controls on Stratigraphy: Society for Sedimentary Geology (SEPM) Special Publication 77, p. 151–180.

Cecil, C. B., DiMichele, W. A., & Elrick, S. D. (2014). Middle and Late Pennsylvanian cyclothems, American Midcontinent: Ice-age environmental changes and terrestrial biotic dynamics. *Comptes Rendus Geoscience*, *346*(7), 159-168.

Cleaves, A. W. (1975). *Upper Desmoinesian-Lower Missourian Depositional Systems (Pennsylvanian), North-Central Texas*. Unpubl. Ph.D. dissertation, The University of Texas at Austin.

Cleaves, A. W. (1993). Sequence Stratigraphy, Systems Tracts, and Mapping Strategies for the Subsurface Middle and Upper Pennsylvanian of the Eastern Shelf, North-Central Texas.

Cleaves, A. W., & Erxleben, A. W. (1982). Upper Strawn and Canyon depositional systems, surface and subsurface, north-central Texas: Society of Economic Paleontologists and Mineralogists. *Permian Basin Section, Publication*, 82-21.

Cleaves, A. W., & Erxleben, A. W. (1985). Upper Strawn and Canyon Cratonic Depositional Systems of Bend Arch, North-Central Texas: ABSTRACT. *AAPG Bulletin*, *69*(1), 142-143.

Crowley, T. J., Hyde, W. T., & Short, D. A. (1989). Seasonal cycle variations on the supercontinent of Pangaea. *Geology*, *17*(5), 457-460.

Crowley, T. J., & Baum, S. K. (1991). Estimating Carboniferous sea-level fluctuations from Gondwanan ice extent. *Geology*, *19*(10), 975-977.

Crowley, T. J., Yip, K. J., Baum, S. K., & Moore, S. B. (1996). Modelling Carboniferous coal formation. *Paleoclimates*, *2*, 159-177.

Coveney, R. M., & Shaffer, N. R. (1988). Sulfur-isotope variations in Pennsylvanian shales of the midwestern United States. *Geology*, *16*(1), 18-21.

Coveney, R. M., Watney, W. L., & Maples, C. G. (1991). Contrasting depositional models for Pennsylvanian black shale discerned from molybdenum abundances. *Geology*, *19*(2), 147-150.

Cruse, A. M., & Lyons, T. W. (2004). Trace metal records of regional paleoenvironmental variability in Pennsylvanian (Upper Carboniferous) black shales. *Chemical Geology*, *206*(3), 319-345.

Demaison, G. J., & Moore, G. T. (1980). Anoxic environments and oil source bed genesis. *AApG Bulletin*, *64*(8), 1179-1209.

DiMichele, W. A., Falcon-Lang, H. J., Nelson, W. J., Elrick, S. D., & Ames, P. R. (2007). Ecological gradients within a Pennsylvanian mire forest. *Geology*, *35*(5), 415-418.

DiMichele, W. A., & Falcon-Lang, H. J. (2011). Pennsylvanian 'fossil forests' in growth position (T0 assemblages): origin, taphonomic bias and palaeoecological insights. *Journal of the Geological Society*, *168*(2), 585-605.

DiMichele, W. A. (2014). Wetland-dryland vegetational dynamics in the Pennsylvanian ice age tropics. *International Journal of Plant Sciences*, *175*(2), 123-164.

Desmond, R. J., Steidtmann, J. R., & Cardinal, D. F. (1984). Stratigraphy and depositional environments of the middle member of the Minnelusa Formation, central Powder River Basin, Wyoming.

Druce, E. C. (1973). Upper Paleozoic and Triassic conodont distribution and the recognition of biofacies. *Conodont Paleozoology. Geological Society of America Special Paper*, *141*, 191-237.

Eble, C. F. (2003). Desmoinesian coal beds of the Eastern Interior and surrounding basins: the largest tropical peat mires in earth history. *Extreme Depositional Environments: Mega End Members in Geologic Time*, *370*, 127.

Elrick, S. D., & Nelson, W. J. (2010, April). Facies relationships of the Middle Pennsylvanian Springfield Coal and Dykersberg Shale: Constraints on sedimentation, development of coal splits and climate change during transgression. In *Geological Society of America Abstracts with Programs* (Vol. 42, No. 2, p. 51).

Fahrer, T. R. (1996). *Stratigraphy, Petrography and Paleoecology of Marine Units Within the Conemaugh Group (Upper Pennsylvanian) of the Appalachian Basin in Ohio, West Virginia and Pennsylvania*. Unpubl. Ph.D. dissertation, University of Iowa

Fahrer, T. R., & Heckel, P. H. (1992). Petrology and depositional significance of Conemaugh marine units in the Appalachian Basin. *Geological Society of America, Abstracts with Programs;(United States)*, *24*(CONF-921058--).

Falcon-Lang, H. J. (2004). Pennsylvanian tropical rain forests responded to glacial-interglacial rhythms. *Geology*, *32*(8), 689-692.

Feldman, H. R., Franseen, E. K., Joeckel, R. M., & Heckel, P. H. (2005). Impact of longer-term modest climate shifts on architecture of high-frequency sequences (cyclothems), Pennsylvanian of Midcontinent USA. *Journal of Sedimentary Research*, *75*(3), 350-368.

Genger, D., & Sethi, P. (1998). A geochemical and sedimentological investigation of high-resolution environmental changes within the Late Pennsylvanian (Missourian) Eudora core black shale of the Mid-Continent region, USA.

Gleason, J. D., Patchett, P. J., Dickinson, W. R., & Ruiz, J. (1994). Nd isotopes link Ouachita turbidites to Appalachian sources. *Geology*, *22*(4), 347-350.

Greb, S. F., Eble, C. F., & Hower, J. C. (1999). Depositional history of the Fire Clay coal bed (Late Duckmantian), eastern Kentucky, USA. *International Journal of Coal Geology*, *40*(4), 255-280.

Gruber, N. (2008). The marine nitrogen cycle: overview and challenges. *Nitrogen in the marine environment*, 1-50.

Gruber, N., & Sarmiento, J. L. (1997). Global patterns of marine nitrogen fixation and denitrification. *Global Biogeochemical Cycles*, *11*(2), 235-266.

Handford, C. R., Dutton, S. P., & Fredericks, P. E. (1981). Regional cross sections of the Texas Panhandle: Precambrian to mid-Permian: The University of Texas at Austin. *Bureau of Economic Geology cross sections*, *8*.

Hatch, J. R., & Leventhal, J. S. (1992). Relationship between inferred redox potential of the depositional environment and geochemistry of the Upper Pennsylvanian (Missourian) Stark Shale Member of the Dennis Limestone, Wabaunsee County, Kansas, USA. *Chemical Geology*, *99*(1), 65-82.

Hay, W.W. (1995). Paleoceanography of marine organic-carbon-rich sediments. In: Huc, A.-Y. (Ed.), Paleogeography, Paleoclimate, and Source Rocks. Am. Assoc. Petrol. Geol., Studies in Geology, vol. 40, pp. 21-59.

Heckel, P. H. (1977). Origin of phosphatic black shale facies in Pennsylvanian cyclothems of mid-continent North America. *AAPG Bulletin*, *61*(7), 1045-1068.

Heckel, P. H. (1980). Paleogeography of eustatic model for deposition of Midcontinent Upper Pennsylvanian cyclothems. Rocky Mountain Section (SEPM).

Heckel, P. H. (1986). Sea-level curve for Pennsylvanian eustatic marine transgressive-regressive depositional cycles along midcontinent outcrop belt, North America. *Geology*, *14*(4), 330-334.

Heckel, P. H. (1991). Thin widespread Pennsylvanian black shales of Midcontinent North America: a record of a cyclic succession of widespread pycnoclines in a fluctuating epeiric sea. *Geological Society, London, Special Publications*, *58*(1), 259-273.

Heckel, P. H. (1994). Evaluation of evidence for glacio-eustatic control over marine Pennsylvanian cyclothems in North America and consideration of possible tectonic

effects. *Tectonic and Eustatic Controls on Sedimentary Cycles: SEPM, Concepts in Sedimentology and Paleontology*, *4*, 65-87.

Heckel, P. H. (1995). Glacial-eustatic base-level--Climatic model for late Middle to Late Pennsylvanian coal-bed formation in the Appalachian basin. *Journal of Sedimentary Research*, *65*(3).

Heckel, P. H. (Ed.) (1999), Field Trip #8: Middle and Upper Pennsylvanian (Upper Carboniferous) cyclothem succession in Midcontinent Basin U.S.A. Kansas Geol. Surv. Open File Rep., 99–27, 236 pp.

Heckel, P. H. (2003), Conodont-rich Pennsylvanian dark shales of the Kansas City region, in Geological Field Trips in the Greater Kansas City Area (Western Missouri, Northeastern Kansas, and Southwestern Nebraska), Missouri Department of Natural Resources, Geological Survey, and Resource Assessment Division, Special Publication, vol. 11, edited by T. M. Niemi, pp. 53–97, Missouri Department of Natural Resources, Geological Survey, and Resource Assessment Division, Jefferson City.

Heckel, P. H. (2008). Pennsylvanian cyclothems in Midcontinent North America as far-field effects of waxing and waning of Gondwana ice sheets. *Geological Society of America Special Papers*, *441*, 275-289.

Heckel, P. H., & Baesemann, J. F. (1975). Environmental interpretation of conodont distribution in Upper Pennsylvanian (Missourian) megacyclothems in eastern Kansas. *AAPG Bulletin*, *59*(3), 486-509.

Heckel, P. H., Barrick, J. E., & Rosscoe, S. J. (2011). Conodont-based correlation of marine units in lower Conemaugh Group (Late Pennsylvanian) in Northern Appalachian Basin. *Stratigraphy*, *8*(4), 253.

Heckel, P. H., & Pope, J. P. (1992). *Stratigraphy and cyclic sedimentation of Middle and Upper Pennsylvanian Strata around Winterset, Iowa*. Iowa Department of Natural Resources, Energy and Geological Resources Division, Geological Survey Bureau.

Heckel, P. H., & Weibel, C. P. (1991). Current status of conodont-based biostratigraphic correlation of Upper Pennsylvanian succession between Illinois and Midcontinent. In *Sequence Stratigraphy in Mixed Clastic-Carbonate Strata, Upper Pennsylvanian, East-central Illinois. Great Lakes Section, SEPM, 21st Annual Field Conference* (pp. 60-69).

Herrmann, A. D., Barrick, J. E., & Algeo, T. J. (2015). The relationship of conodont biofacies to spatially variable water mass properties in the Late Pennsylvanian Midcontinent Sea. *Paleoceanography*, *30*(3), 269-283.

Herrmann, A. D., Kendall, B., Algeo, T. J., Gordon, G. W., Wasylenki, L. E., & Anbar, A. D. (2012). Anomalous molybdenum isotope trends in Upper Pennsylvanian euxinic facies: Significance for use of δ 98 Mo as a global marine redox proxy. *Chemical Geology*, *324*, 87-98.

Hoffman, D.L., Algeo, T.J., Maynard, J.B., Joachimski, M.M., Hower, J.C., Jaminski, J., (1998). Regional and stratigraphic variation in bottomwater anoxia in offshore core shales of Upper Pennsylvanian cyclothems from the Eastern Midcontinent Shelf (Kansas), USA. In: Schieber, J., Zimmerle, W., Sethi, P.S. (Eds.), Shales and Mudstones, vol. 1. Schweizerbart'sche, Stuttgart, pp. 243–269.

Holterhoff, P., Cassady, K., (2012). Late Pennsylvanian and Early Permian black shale-limestone bed-set couplets of the Eastern Shelf, Midland Basin (Texas): climate-driven redox cycles of the inner platform realm. American Association of Petroleum Geologists Annual Meeting, Search and Discovery Article #90142.

Horton, D. E., Poulsen, C. J., Montañez, I. P., & DiMichele, W. A. (2012). Eccentricity-paced late Paleozoic climate change. *Palaeogeography, Palaeoclimatology, Palaeoecology*, *331*, 150-161.

Houseknecht, D., Wood, G., Jaques, R., & Gresham, A. (1993). Influence of Ozark uplift on Pennsylvanian sediment dispersal patterns. In Geological Society of America, Abstracts with Programs; (United States) (Vol. 25:3). United States.

Joachimski, M. M., von Bitter, P. H., & Buggisch, W. (2006). Constraints on Pennsylvanian glacioeustatic sea-level changes using oxygen isotopes of conodont apatite. Geology, 34(4), 277-280.

Joachimski, M. M., & Lambert, L. L. (2015). Salinity contrast in the US Midcontinent Sea during Pennsylvanian glacio-eustatic highstands: Evidence from conodont apatite δ 18 O. *Palaeogeography, Palaeoclimatology, Palaeoecology*, *433*, 71-80.

Joeckel, R. M. (1995). Paleosols below the Ames marine unit (Upper Pennsylvanian, Conemaugh Group) in the Appalachian Basin, USA: variability on an ancient depositional landscape. *Journal of Sedimentary Research*, *65*(2).

Joeckel, R. M. (1999). Paleosol in Galesburg Formation (Kansas City Group, Upper Pennsylvanian), northern Midcontinent, USA: evidence for climate change and mechanisms of marine transgression. *Journal of sedimentary research*, *69*(3).

Kasten, S., & Jørgensen, B. B. (2000). Sulfate reduction in marine sediments. In *Marine geochemistry* (pp. 263-281). Springer Berlin Heidelberg.

Kennish, M. J. (2001). Coastal salt marsh systems in the US: a review of anthropogenic impacts. *Journal of Coastal Research*, 731-748.

Klapper, G., & Barrick, J. E. (1978). Conodont ecology: pelagic versus benthic. *Lethaia*, *11*(1), 15-23.

Klein, G.D., & Willard, D. A. (1989). Origin of the Pennsylvanian coal-bearing cyclothems of North America. *Geology*, *17*(2), 152-155.

Kluth, C. F. (1986). Plate Tectonics of the Ancestral Rocky Mountains: Part III. Middle Rocky Mountains.

Kolata, D. R., & Nelson, J. W. (1990). Tectonic history of the Illinois Basin. *AAPG Bulletin (American Association of Petroleum Geologists);(USA)*, *74*(CONF-900605--).

Kolata, D. R., & Nelson, W. J. (1997). Role of the Reelfoot rift/Rough Creek graben in the evolution of the Illinois basin. *SPECIAL PAPERS-GEOLOGICAL SOCIETY OF AMERICA*, 287-298.

Kvale, E. P., Fraser, G. S., Archer, A. W., Zawistoski, A., Kemp, N., & McGough, P. (1994). Evidence of seasonal precipitation in Pennsylvanian sediments of the Illinois Basin. *Geology*, *22*(4), 331-334.

Lyons, P. C., Outerbridge, W. F., Triplehorn, D. M., EVANS, H. T., Congdon, R. D., Capiro, M., ... & Nash, W. P. (1992). An Appalachian isochron: a kaolinized Carboniferous air-fall volcanic-ash deposit (tonstein). *Geological Society of America Bulletin*, *104*(11), 1515-1527.

Malinky, J. M., & Heckel, P. H. (1998). Paleoecology and taphonomy of faunal assemblages in gray" core"(offshore) shales in Midcontinent Pennsylvanian cyclothems. *Palaios*, *13*(4), 311-334.

Maughan, E. K. (1993). The Ancestral Rocky Mountains in Wyoming. *Geology of Wyoming. Geol. Surv. Wyoming Mem*, *5*, 188-207.

Merrill, G. K., & Von Bitter, P. H. (1976). *Revision of conodont biofacies nomenclature and interpretations of environmental controls in Pennsylvanian rocks of eastern and central North America*. Royal Ontario Museum.

Meyers, P. A., Bernasconi, S. M., & Yum, J. G. (2009). 20My of nitrogen fixation during deposition of mid-Cretaceous black shales on the Demerara Rise, equatorial Atlantic Ocean. *Organic Geochemistry*, *40*(2), 158-166.

Miller, E. L., Miller, M. M., Stevens, C. H., Wright, J. E., & Madrid, R. (1992). Late Paleozoic paleogeographic and tectonic evolution of the western US Cordillera. *The Cordilleran Orogen: Conterminous US: Geological Society of America, The Geology of North America*, *3*, 57-106.

Miller, K. B., & West, R. R. (1993). Reevaluation of Wolfcampian cyclothems in northeastern Kansas: significance of subaerial exposure and flooding surfaces. *Kansas Geological Survey Bulletin*, *235*, 1-26.

Nelson, W. J., Elrick, S. D., & Ames, P. (2010). “Merging” Pennsylvanian limestones in Illinois basin: formation at highstand. In *Geological Society of America, Abstracts with Programs* (Vol. 42, No. 2, p. 51).

Olszewski, T. (1996). Sequence stratigraphy of an Upper Pennsylvanian, midcontinent cyclothem from North America (Iola Limestone, Kansas and Missouri, USA). Facies, 35(1), 81-103.

Opluštil, S., Pšenička, J., Libertín, M., & Šimůnek, Z. (2007). Vegetation patterns of Westphalian and Lower Stephanian mire assemblages preserved in tuff beds of the

continental basins of Czech Republic. *Review of Palaeobotany and Palynology*, *143*(3), 107-154.

Patchett, P. J., Ross, G. M., & Gleason, J. D. (1999). Continental drainage in North America during the Phanerozoic from Nd isotopes. *Science*, *283*(5402), 671-673.

Perlmutter, M. A., & Matthews, M. D. (1989). Global Cyclostratigraphy: effects on the timing of sediment delivery to continental margins relative to sea level. In *Chapman Conf. on Long Term Sea Level Changes, Abstr. Progr.*.

Peyser, C. E., & Poulsen, C. J. (2008). Controls on Permo-Carboniferous precipitation over tropical Pangaea: a GCM sensitivity study. *Palaeogeography, Palaeoclimatology, Palaeoecology*, *268*(3), 181-192.

Poulsen, C. J., Pollard, D., Montañez, I. P., & Rowley, D. (2007). Late Paleozoic tropical climate response to Gondwanan deglaciation. *Geology*, *35*(9), 771-774.

Pratt, L. M. (1984). Influence of paleoenvironmental factors on preservation of organic matter in Middle Cretaceous Greenhorn Formation, Pueblo, Colorado. *AAPG Bulletin*, *68*(9), 1146-1159.

Prokopenko, M. G., Sigman, D. M., Berelson, W. M., Hammond, D. E., Barnett, B., Chong, L., & Townsend-Small, A. (2011). Denitrification in anoxic sediments supported by biological nitrate transport. *Geochimica et Cosmochimica Acta*, *75*(22), 7180-7199.

Read, J. F. (1995). Overview of Carbonate Platform Sequences, Cycle Stratigraphy and Reservoirs in Greenhouse and Icehouse Worlds.

Rimmer, S. M., Rowe, H. D., Taulbee, D. N., & Hower, J. C. (2006). Influence of maceral content on δ 13 C and δ 15 N in a Middle Pennsylvanian coal. *Chemical Geology*, *225*(1), 77-90.

Robinson, R. S., Kienast, M., Luiza Albuquerque, A., Altabet, M., Contreras, S., De Pol Holz, R., ... & Ivanochko, T. (2012). A review of nitrogen isotopic alteration in marine sediments. *Paleoceanography*, *27*(4).

Rosenau, N. A., Tabor, N. J., Elrick, S. D., & Nelson, W. J. (2013a). Polygenetic history of paleosols in middle–upper Pennsylvanian cyclothems of the Illinois basin, USA: Part I. Characterization of paleosol types and interpretation of pedogenic processes. *Journal of Sedimentary Research*, *83*(8), 606-636.

Rosenau, N. A., Tabor, N. J., Elrick, S. D., & Nelson, W. J. (2013). Polygenetic history of paleosols in middle–upper Pennsylvanian cyclothems of the Illinois basin, USA: Part II. Integrating geomorphology, climate, and glacioeustasy. *Journal of Sedimentary Research*, *83*(8), 637-668.

Rosenau, N. A., Tabor, N. J., & Herrmann, A. D. (2014). Assessing the Paleoenvironmental Significance of Middle–Late Pennsylvanian Conodont Apatite δ18O Values in the Illinois Basin. Palaios, 29(6), 250-265.

Ross, C. A., & Ross, J. R. (1985). Late Paleozoic depositional sequences are synchronous and worldwide. *Geology*, *13*(3), 194-197.

Ross, C.A., and Ross, J.R.P. (1988). Late Paleozoic transgressive-regressive deposition, in Wilgus, C.K., Hastings, B.S., Kendall, C.G.St.C., Posamentier, H.W., Ross, C.A., and Van Wagoner, J.C., eds., Sea-Level Changes; An Integrated Approach, Society of Economic Paleontologists and Mineralogists, Special Publication 42, p. 227-247.

Rosscoe, S. J., & Bader, J. D. (2010). A comparison of Idiognathodus faunas from the Upper Salesville Shale of north-central texas and the Hushpuckney Shale of Oklahoma, Kansas, and Nebraska: Geological Society of America. In *Abstracts with Program* (Vol. 42, No. 2, p. 72).

Rosscoe, S. J., & Barrick, J. E. (2013). North American species of the conodont genus Idiognathodus from the Moscovian-Kasimovian boundary composite sequence and correlation of the Moscovian-Kasimovian stage boundary. *The Carboniferous-Permian Transition.─ New Mexico Museum of Natural History and Science, Bulletin*, *60*, 354-371.

Schenk, P. E. (1967). Facies and phases of the Altamont Limestone and megacyclothem (Pennsylvanian), Iowa to Oklahoma. *Geological Society of America Bulletin*, *78*(11), 1369-1384.

Schultz, R. B., & Coveney, R. M. (1992). Time-dependent changes for Midcontinent Pennsylvania black shales, USA. *Chemical geology*, *99*(1-3), 83-100.

Schutter, S. R., & Heckel, P. H. (1985). Missourian (early Late Pennsylvanian) climate in midcontinent north America. *International Journal of Coal Geology*, *5*(1), 111-140.

Scotese, C. R. (1998). Continental drift (0-750 million years), a Quicktime computer animation. *PALEOMAP Project, University of Texas at Arlington, Arlington, Texas*.

Seddon, G., & Sweet, W. C. (1971). An ecologic model for conodonts. *Journal of Paleontology*, 869-880.

Sigman, D. M., Karsh, K. L., & Casciotti, K. L. (2009). Ocean process tracers: nitrogen isotopes in the ocean. *Encyclopedia of ocean science, 2nd edn. Elsevier, Amsterdam*.

Speed, R. C., Sharp, W. D., & Foland, K. A. (1997). Late Paleozoic Granitoid Gneisses of Northeastern Venezuela and the North America‐Gondwana Collision Zone. *The Journal of Geology*, *105*(4), 457-470.

Soreghan, G. S., & Giles, K. A. (1999). Amplitudes of late Pennsylvanian glacioeustasy. *Geology*, *27*(3), 255-258.

Stamm, R. G., & Wardlaw, B.R. (2003). Conodont faunas of the late Middle Pennsylvanian (Desmoinesian) lower Kittanning cyclothem, USA.

Swade, J. W. (1985), Conodont Distribution, Paleoecology, and Preliminary Biostratigraphy of the Upper Cherokee and Marmaton Groups (upper Desmoinesian, Middle Pennsylvanian)

From Two Cores in South-Central Iowa, Iowa Geological Survey, Technical Information Series, vol. 14, 71 pp., Iowa Geological Survey, Iowa City

Tabor, N. J., & Poulsen, C. J. (2008). Palaeoclimate across the Late Pennsylvanian–Early Permian tropical palaeolatitudes: a review of climate indicators, their distribution, and relation to palaeophysiographic climate factors. *Palaeogeography, Palaeoclimatology, Palaeoecology*, *268*(3), 293-310.

Tandon, S. K., & Gibling, M. R. (1994). Calcrete and coal in late Carboniferous cyclothems of Nova Scotia, Canada: Climate and sea-level changes linked. *Geology*, *22*(8), 755-758.

Teo, W. S. (1991). *ELEMENTAL GEOCHEMISTRY OF SHALES IN PENNSYLVANIAN CYCLOTHEMS. MIDCONTINENT NORTH AMERICA* (Doctoral dissertation, Texas Tech University).

Thiede, J., & Suess, E. (Eds.). (1983). *Coastal upwelling, its sediment record: Part B: Sedimentary records of ancient coastal upwelling*. Plenum Press.

Veevers, J. T., & Powell, C. M. (1987). Late Paleozoic glacial episodes in Gondwanaland reflected in transgressive-regressive depositional sequences in Euramerica. *Geological Society of America Bulletin*, *98*(4), 475-487.

Voss, M., Dippner, J. W., & Montoya, J. P. (2001). Nitrogen isotope patterns in the oxygen-deficient waters of the Eastern Tropical North Pacific Ocean. *Deep Sea Research Part I: Oceanographic Research Papers*, *48*(8), 1905-1921.

Wanless, H. R., & Shepard, F. P. (1936). Sea level and climatic changes related to late Paleozoic cycles. *Geological Society of America Bulletin*, *47*(8), 1177-1206.

Wanless, H. R., & Weller, J. M. (1932). Correlation and extent of Pennsylvanian cyclothems. *Geological Society of America Bulletin*, *43*(4), 1003-1016.

Warning, B., & Brumsack, H. J. (2000). Trace metal signatures of eastern Mediterranean sapropels. *Palaeogeography, Palaeoclimatology, Palaeoecology*, *158*(3), 293-309.

Watney, W. L., French, J. A., Doveton, J. H., Youle, J. C., & Guy, W. J. (1995). Cycle hierarchy and genetic stratigraphy of Middle and Upper Pennsylvanian strata in the upper Mid-Continent.

Watney, W. L., French, J. A., & Franseen, E. K. (1989). Sequence Stratigraphic Interpretations and Modeling of Cyclothems in the Upper Pennsylvanian (Missourian), Lansing and Kansas City Groups in Eastern Kansas: Guidebook, 41st Annual Field Conference.

Wells, M. R., Allison, P. A., Piggott, M. D., Gorman, G. J., Hampson, G. J., Pain, C. C., & Fang, F. (2007). Numerical modeling of tides in the late Pennsylvanian midcontinent seaway of North America with implications for hydrography and sedimentation. *Journal of Sedimentary Research*, *77*(10), 843-865.

Wenger, L. M., & Baker, D. R. (1986). Variations in organic geochemistry of anoxic-oxic black shale-carbonate sequences in the Pennsylvanian of the Midcontinent, USA. *Organic geochemistry*, *10*(1), 85-92.

Whiticar, M. J. (1996). Stable isotope geochemistry of coals, humic kerogens and related natural gases. *International Journal of Coal Geology*, *32*(1), 191-215.

Wignall, P. B. (1994). *Black shales* (Vol. 30, p. 144). Oxford: Clarendon Press.

Willman, H. B., Atherton, E., Buschbach, T. C., Collinson, C. W., Frye, J. C., Hopkins, M. E., ... & Simon, J. A. (1975). Handbook of Illinois stratigraphy. *Bulletin no. 095*.

Witzke, B. J. (1987). Models for circulation patterns in epicontinental seas applied to Paleozoic facies of North America craton. *Paleoceanography*, *2*(2), 229-248.

Yancey, T. E. (1986). Controls on the deposition of mixed carbonate and siliciclastic sediments on the Eastern Shelf of the Midland basin, Pennsylvanian of Texas.

Yancey, T. E., & Cleaves, A. W. (1990). Carbonate and Siliciclastic Sedimentation in Late Pennsylvanian Cycles, North-Central Texas.

Ye, H., Royden, L., Burchfiel, C., & Schuepbach, M. (1996). Late Paleozoic deformation of interior North America: the greater Ancestral Rocky Mountains. *AAPG bulletin*, *80*(9), 1397-1432.

Youle, J. C., Watney, W. L., & Lambert, L. L. (1994). Stratal hierarchy and sequence stratigraphy—Middle Pennsylvanian, southwestern Kansas, USA. *Geological Society of America Special Papers*, *288*, 267-286.

Zangerl, R., and Richardson, E.S. (1963). The paleoecological history of two Pennsylvanian black shales: Fieldiana Geology Memoir 4, 1-352 p.

Zonneveld, K. A. F., Versteegh, G. J. M., Kasten, S., Eglinton, T. I., Emeis, K. C., Huguet, C., ... & Mollenhauer, G. (2010). Selective preservation of organic matter in marine environments; processes and impact on the sedimentary record.

APPENDIX: GEOCHEMICAL DATA

Table 1: TX-3027 dataset for Upper Salesville Shale outcrop (i.e. Hushpuckney Shale equivalent) in north-central Texas. Elemental concentrations were acquired using LA-ICP-MS analysis and measured in counts-per-second (cps). Facies acronyms: DGS=Dark Grey Shale, LGS=Light Grey Shale, and UTS=Upper Tan Shale.

Sample Height (cm)	Facies	$\delta^{15}N$ (‰)	TN (%)	TOC (%)	TIC (%)	TS (%)	Al (cps)	Fe (cps)	U (cps)	Mo (cps)
2.5	DGS	3.90	0.09	0.16	0.00	0.02	47854997	1224916	23136	
7.5	DGS	4.41	0.09	0.14	0.16	0.04	46477476	1293437	21844	
12.5	DGS	4.63	0.11	0.39	0.17	0.04	43680916	944125	29990	
17.5	DGS	4.52	0.11	0.46	0.11	0.03	42955948	876850	24196	
22.5	DGS	4.23	0.10	0.31	0.15	0.03	42217260	920377	22820	
27.5	DGS	4.71	0.09	0.14	0.00	0.03	54937952	1747851	25869	
32.5	DGS	4.20	0.09	0.14	0.00	0.04	44264058	1413016	20369	
37.5	DGS	4.13	0.10	0.18	0.00	0.03	45876337	1181708	20081	
42.5	DGS	4.07	0.10	0.19	0.00	0.03	39473317	1109883	16767	
47.5	DGS	4.33	0.10	0.18	0.00	0.03	36471075	932735	14942	
52.5	DGS	3.85	0.10	0.17	0.00	0.03	53249116	1741503	24414	
57.5	DGS	4.05	0.10	0.22	0.00	0.02	55001317	1523533	26080	
62.5	DGS	3.84	0.10	0.27	0.00	0.03	48863935	1289253	25412	
67.5	DGS	4.01	0.10	0.25	0.00	0.02	42297916	1119225	19964	
72.5	DGS	3.79	0.10	0.23	0.00	0.02	39713430	1123817	19382	
77.5	DGS	3.80	0.09	0.21	0.00	0.02	37420352	863949	15174	
82.5	DGS	3.55	0.10	0.25	0.00	0.02	32065337	724972	13373	
87.5	DGS	3.62	0.10	0.29	0.00	0.02	34307098	781528	13421	
92.5	DGS	4.14	0.10	0.24	0.00	0.04	33658054	831721	13716	
97.5	DGS	3.88	0.10	0.17	0.07	0.03	32536069	715209	12291	
102.5	DGS	3.34	0.10	0.28	0.00	0.02	61938569	1666000	30123	
107.5	DGS	4.23	0.11	0.33	0.00	0.02	59163912	1353821	25295	
112.5	DGS	4.05	0.10	0.31	0.00	0.02	52341824	1121607	25681	
117.5	DGS	4.09	0.10	0.35	0.00	0.01	45740250	999848	21556	
122.5	DGS	4.10	0.10	0.36	0.00	0.01	41662023	1039203	22945	

Table 1 (Continued)

127.5	DGS	3.60	0.09	0.47	1.74	0.02	65604270	1554322	36171	
132.5	DGS	3.91	0.11	0.38	2.10	0.02	53410917	1297839	31365	
137.5	DGS	3.47	0.09	0.40	2.00	0.01	50589594	1182843	29575	
142.5	DGS	3.49	0.09	0.45	2.24	0.02	44366259	1015241	22810	
147.5	DGS	4.10	0.09	0.42	2.77	0.02	38450312	812790	19941	
152.5	LGS	4.45	0.09	0.16	0.15	0.03	69807954	1985160	27898	
157.5	LGS	4.06	0.09	0.17	0.13	0.01	47519038	1337163	22887	
162.5	LGS	4.30	0.09	0.15	0.15	0.01	50029702	1376658	21340	
167.5	LGS	4.14	0.09	0.14	0.17	0.01	45223235	1211695	16546	
172.5	LGS	4.15	0.09	0.14	0.12	0.01	39259665	1063713	13039	
177.5	LGS	4.38	0.09	0.13	0.07	0.01	66241017	1864021	23182	
182.5	LGS	3.78	0.09	0.12	0.03	0.01	51430728	1536066	15716	
187.5	UTS	3.93	0.09	0.14	0.06	0.01	49773310	1276159	15013	
192.5	UTS	3.95	0.09	0.15	0.08	0.01	40595332	1083052	12117	
197.5	UTS	3.83	0.09	0.13	0.09	0.01	41932407	1001555	12257	
202.5	UTS	4.18	0.09	0.15	0.09	0.01	52962409	1485264	16147	
207.5	UTS	4.19	0.09	0.15	0.08	0.01	37816230	1089434	11060	

Table 2: Clarkson dataset for Hushpuckney Shale in southeast Kansas. Elemental concentrations were acquired using XRF analysis and measured in weight percent (wt%) for major elements and parts per million for trace elements (ppm). Facies acronyms: LBS=Lower Black Shale, MBS=Middle Black Shale, UBS=Upper Black Shale, and UGS=Upper Grey Shale.

Sample Height (cm)	Facies	$\delta^{15}N$ (‰)	TN (%)	TOC (%)	TIC (%)	TS (%)	Al (wt%)	Fe (wt%)	U (ppm)	Mo (ppm)
0.0	LBS	7.06		6.56	2.44	0.76	0.40	4.26	11.53	10.25
1.7	LBS			9.64	0.97	0.74	8.94	4.28	12.31	12.27
3.0	LBS	6.57		6.74	1.34	1.04	6.52	2.72	55.27	10.75
4.5	LBS			6.80	0.39	1.16	9.44	4.88	26.08	17.79
5.7	LBS			7.04	0.00	1.07	8.84	4.65	57.22	20.07
7.0	LBS	8.13		6.19	0.86	1.59	8.21	4.22	43.09	23.70
8.5	LBS			7.95	0.30	1.83	9.71	5.79	30.21	35.88
9.0	LBS			13.59	0.78	1.72	8.52	4.73	30.96	43.94
10.5	LBS	12.24		10.73	0.36	1.66	9.22	5.78	144.84	210.78
11.1	LBS			11.90	0.37	1.59	9.59	5.73	143.34	174.51
12.1	LBS			16.33	0.34	1.77	7.84	4.68	130.21	260.44
13.0	MBS	13.77		23.49	1.60	1.84	6.60	4.95	182.37	366.26
14.0	MBS			15.08	3.00	0.64	8.67	6.31	80.81	624.62
15.5	MBS	10.21		18.20	1.48	2.13	6.41	5.69	151.22	218.27
16.5	MBS			16.04	1.30	1.94	7.50	5.21	129.83	155.83
17.5	MBS			21.94	1.32	2.62	6.44	6.16	122.14	204.28
18.5	MBS	8.17		26.31	2.20	2.78	5.31	6.48	161.92	240.11
19.5	MBS			31.40	1.70	1.87	5.77	5.26	173.17	243.62
20.7	MBS			20.04	1.06	1.79	7.67	4.74	199.63	357.64
21.8	MBS	7.73		18.91	1.06	1.78	7.82	4.81	177.11	278.90
22.9	MBS			30.94	1.09	2.76	5.79	6.27	142.22	283.40
24.0	MBS	6.58		24.36	2.55	2.59	5.08	6.19	160.79	138.97
25.3	MBS			27.11	0.82	2.30	5.67	5.88	115.95	122.94
26.6	MBS			31.17	0.98	2.72	5.57	6.01	116.70	212.08
27.5	MBS	6.34		31.80	1.17	2.49	5.17	5.96	124.95	268.71

Table 2 (Continued)

28.5	MBS			30.07	0.12	2.55	8.05	8.17	150.85	242.58
30.0	MBS			27.73	1.16	2.91	8.42	8.91	70.17	143.48
31.3	MBS			22.12	1.09	2.34	8.35	7.66	67.36	98.63
32.5	UBS			26.73	0.60	2.69	8.55	8.36	58.73	103.26
34.0	UBS			16.52	0.46	2.29	7.43	6.86	36.77	78.74
36.0	UBS			11.07	1.45	1.75	6.59	6.62	39.96	84.28
38.0	UBS			5.67	4.14	15.21	7.25	23.11	3.93	144.82
39.5	UBS			10.33	1.14	8.09	7.72	10.50	49.64	31.16
40.5	UBS	5.79		11.33	1.13	4.23	8.49	9.04	11.00	43.39
41.7	UBS			12.24	1.36	2.89	8.54	7.57	14.93	34.28
42.8	UBS	6.09		17.21	0.67	2.23	8.59	7.10	12.57	46.19
44.0	UBS	5.95		21.87	1.42	3.24	8.45	8.95	9.95	68.94
45.0	UBS			22.86	1.50	2.60	6.25	5.78	74.79	42.96
46.0	UBS			20.87	0.39	2.95	7.53	6.42	19.52	38.49
47.0	UBS	6.39		10.79	0.69	1.74	9.39	6.22	7.99	22.60
48.5	UBS					1.47	9.39	5.69	10.61	22.68
50.0	UBS	5.29		14.35	1.48	1.35	4.95	2.87		9.95
51.5	UBS			12.69	1.60	2.57	7.77	6.43	6.16	19.18
53.0	UBS			7.78	1.44	2.75	9.18	7.33	5.50	23.86
54.0	UBS	5.23		8.25	1.03	2.23	9.24	6.95	7.33	24.50
55.0	UBS			9.96	1.52	3.19	8.68	7.75	5.89	27.74
56.0	UBS			12.94	1.11	2.39	7.66	5.68	17.03	26.52
57.5	UBS	6.68		16.39	1.16	2.24	8.79	6.88	6.16	30.68
58.5	UBS			9.07	1.86	1.88	1.65	2.31		18.00
60.0	UBS	6.21		15.05	1.01	4.01	5.56	7.13	*8.13*	26.59
61.0	UGS			2.36	1.47	4.97	6.74	5.73	20.17	23.36
62.5	UGS	4.21		5.52	0.54	0.69	9.95	4.54	8.25	5.86
64.5	UGS			5.48	0.69	1.56	9.25	6.22	4.85	5.02

Table 2 (Continued)

66.3	UGS			4.03	0.70	1.31	9.44	5.91	4.06	6.32
68.0	UGS			3.80	0.59	0.80	9.56	5.02	4.98	5.69
68.8	UGS			3.48	0.89	0.76	9.51	4.94	4.85	4.60
70.0	UGS			3.69	0.44	0.93	9.51	5.21	4.19	5.90
71.0	UGS			3.49	0.27	0.81	9.46	4.93	4.58	5.48
71.7	UGS			2.98	0.55	0.75	9.51	4.84	5.37	5.69
72.3	UGS			2.54	0.50	0.70	9.16	4.80	5.11	6.75
73.0	UGS			2.79	0.50	0.78	9.91	4.43	4.45	5.14
73.8	UGS			3.09	0.41	0.88	9.36	4.99	3.54	7.04
74.4	UGS			3.03	0.29	0.97	9.41	5.24	3.67	7.25
75.1	UGS			2.71	0.40	0.87	9.33	4.97	5.11	7.25
75.8	UGS			2.98	0.59	0.89	9.45	5.05	4.98	7.38
76.5	UGS			2.97	0.51	0.77	9.14	4.88	3.80	5.23
77.3	UGS			2.87	0.47	0.70	9.92	4.42	5.50	5.90
78.0	UGS			3.07	0.36	0.83	10.08	4.55	4.85	5.61
78.8	UGS			3.36	0.61	0.74	9.08	4.90	5.11	6.41
79.8	UGS			3.73	0.48	0.83	9.04	4.98	6.03	7.51
81.0	UGS			3.56	0.63	0.66	9.52	4.95	4.19	6.96
81.8	UGS			2.75	0.39	0.84	9.74	4.62	4.19	7.34
82.6	UGS			2.70	0.38	0.73	9.80	4.97	4.85	6.11
83.5	UGS			3.14	0.64	0.68	9.07	4.92	4.58	6.79
84.3	UGS			3.42	0.82	0.71	9.59	4.50	3.27	7.00
85.2	UGS			3.00	0.80	0.77	9.50	5.04	5.11	6.49
86.0	UGS			3.48	0.48	0.74	9.98	4.35	4.58	3.20
87.2	UGS			3.04	0.68	0.66	10.01	4.09	6.94	4.43
88.0	UGS			3.27	0.69	0.66	9.67	3.96	6.94	5.02
89.0	UGS			2.81	0.72	0.45	9.60	3.67	8.51	5.40
90.5	UGS			2.70	0.76	0.60	9.66	3.91	6.81	6.11
91.5	UGS			2.85	0.86	0.45	9.48	3.65	7.73	6.24

Table 2 (Continued)

93.0	UGS			2.99	0.80	0.44	9.84	3.78	6.55	6.24
94.5	UGS			3.38	0.43	0.41	9.32	4.26	6.03	7.46
96.0	UGS			4.17	0.64	0.56	9.81	4.30	5.89	8.18
96.9	UGS			4.12	0.56	0.68	9.70	4.29	3.67	5.99
97.8	UGS			3.60	0.60	0.65	9.41	4.71	5.50	6.37
98.8	UGS			3.52	0.62	0.60	9.53	4.17	4.06	6.20
99.7	UGS			2.94	0.57	0.61	9.66	4.27	4.32	4.93
100.7	UGS			2.70	0.51	0.64	9.72	4.83	4.19	7.80
101.3	UGS			2.87	0.63	0.53	9.72	4.17	3.93	5.65
102.0	UGS			3.48	0.67	0.56	9.51	4.76	2.75	5.65
103.5	UGS			3.89	0.65	0.63	9.97	4.21	4.19	2.61
104.7	UGS			3.83	0.50	0.49	9.67	3.98	5.24	3.54
105.5	UGS			3.59	0.51	0.51	9.60	3.92	6.68	2.99
106.2	UGS			3.59	0.81	0.55	9.61	3.86	5.11	4.38
107.1	UGS			3.34	0.71	0.57	9.60	3.90	3.67	2.53
108.0	UGS			3.01	0.87	0.49	8.95	4.20	5.76	2.49
108.8	UGS			2.81	0.79	0.43	9.33	3.67	4.19	3.16
110.0	UGS			2.98	0.58	0.38	9.54	4.10	4.85	4.34
112.0	UGS			2.86	0.78	0.42	9.37	3.66	4.72	3.75
113.0	UGS			2.77	0.87	0.42	9.39	3.73	5.76	3.71
114.0	UGS			2.77	1.03	0.43	9.00	3.63	6.68	3.88
115.0	UGS			2.85	1.05	0.55	8.79	3.79	4.58	4.93
116.3	UGS			2.77	1.03	0.54	9.15	4.36	6.29	3.63
117.3	UGS			2.74	1.12	0.53	9.16	4.44	4.45	2.91
118.3	UGS			2.65	1.22	0.46	8.87	3.76	6.03	3.33
119.5	UGS			2.61	0.96	0.50	8.98	3.78	4.32	4.13
120.5	UGS			2.40	1.12	0.50	8.89	3.78	3.80	3.29
121.3	UGS			2.37	1.16	0.55	9.18	4.47	4.32	3.84
122.5	UGS			2.36	1.19	0.55	8.79	3.90	3.80	4.81

Table 2 (Continued)

123.5	UGS			2.22	1.18	0.55	8.98	3.77	4.32	4.09
124.5	UGS			1.97	1.22	0.57	9.10	3.92	5.37	4.34
125.5	UGS			2.00	1.28	0.62	9.01	3.84	3.41	2.87
126.5	UGS			2.05	1.29	0.62	8.63	3.90	2.62	4.98
127.3	UGS			1.93	1.37	0.63	8.74	3.82	3.54	3.50
128.5	UGS			1.94	1.46	0.66	8.65	3.81	3.01	2.23
129.5	UGS			2.12	1.40	0.76	8.64	3.99	2.49	3.20
130.5	UGS			2.04	1.27	0.68	8.74	3.88	4.45	3.75
132.1	UGS			1.95	1.38	0.54	8.54	3.67	3.27	1.73
133.7	UGS			2.02	1.37	0.51	8.68	3.72	3.80	1.77
134.4	UGS			1.99	1.33	0.54	8.63	3.64	3.67	2.70
135.2	UGS			1.83	1.36	0.59	8.67	3.88	3.67	3.50
136.0	UGS			2.01	1.41	0.62	8.76	3.82	2.88	2.53
136.8	UGS			2.15	1.21	0.61	8.66	3.86	3.27	2.45
137.6	UGS			1.97	1.56	0.64	8.66	3.78	5.37	2.78
138.4	UGS			1.91	1.42	0.49	8.83	3.66	3.54	1.73
139.2	UGS			1.96	1.36	0.61	9.09	3.77	3.27	1.69
141.5	UGS			1.90	1.35	0.59	8.32	4.28	4.19	1.81
144.5	UGS			2.02	1.25	0.49	8.34	4.19	2.49	1.48

Table 3: KEX dataset for Hushpuckney Shale in northeast Kansas. Elemental concentrations were acquired using XRF analysis and measured in weight percent (wt%) for major elements and parts per million for trace elements (ppm). Facies acronyms: LBS=Lower Black Shale, MBS=Middle Black Shale, UBS=Upper Black Shale, and UGS=Upper Grey Shale.

Sample Height (cm)	Facies	$\delta^{15}N$ (‰)	TN (%)	TOC (%)	TIC (%)	TS (%)	Al (wt%)	Fe (wt%)	U (ppm)	Mo (ppm)
1.0	LBS	7.16	0.42	8.43	0.99	1.84	7.56	3.23	34.60	33.50
3.0	LBS	10.15	0.48	9.65	0.34	1.70	7.67	3.23	37.89	52.95
4.0	LBS	10.87	0.49	12.94	0.37	1.97	3.89	2.37	83.37	58.03
5.2	LBS	12.86	0.58	14.77	0.40	2.26	4.58	2.97	138.76	226.28
6.6	MBS	13.39	0.90	20.97	0.31	2.60	5.37	3.45	63.50	689.93
7.9	MBS	11.66	1.12	25.67	0.17	2.31	4.92	3.06	171.26	699.64
9.3	MBS	9.87	0.56	11.10	0.26	2.06	7.27	3.55	119.83	275.18
10.8	MBS	9.20	0.66	15.39	0.00	2.26	5.70	3.33	223.37	247.40
12.3	MBS	9.34	0.98	20.86	0.37	2.68	5.74	3.32	121.25	333.91
13.8	MBS	8.49	0.57	13.00	0.37	2.62	5.91	3.59	189.35	267.65
15.3	MBS	8.07	0.90	21.68	0.37	2.17	4.17	2.97	256.22	387.96
16.7	MBS	7.46	1.17	27.54	0.37	2.27	3.83	2.53		384.78
17.7	MBS	7.41	0.81	18.11	0.37	1.61	7.50	3.14	148.23	318.54
18.6	MBS			30.85	0.37	1.71	4.08	1.96	303.17	382.62
19.3	MBS	6.45	1.09	23.59	0.37	2.12	4.01	2.58	286.50	360.44
20.0	MBS			25.15	0.37	1.98	3.97	2.40		244.07
20.7	MBS	5.80	1.05	26.59	0.37	2.09	2.17	1.65		256.13
21.5	MBS			29.07	0.37	3.21	2.96	1.81	179.29	282.01
22.2	MBS	4.90	1.73	38.13	0.37	2.18	5.00	2.99	46.58	497.95
22.8	MBS			26.55	0.37	2.19	5.24	3.29	151.31	302.46
23.5	MBS	5.03	0.97	21.44	0.37	1.97	4.38	3.20	225.78	242.60
25.2	UBS	4.43	1.72	36.47	0.37	2.67	3.75	3.07	49.40	542.08
26.5	UBS			21.10	0.37	2.18	5.53	3.23	122.78	325.57
27.5	UBS	4.62	0.94	23.75	0.37	2.23	4.79	3.14	124.66	322.05
28.5	UBS	4.87	0.66	14.03	0.37	2.21	6.37	3.67	60.00	203.05

Table 3 (Continued)

29.5	UBS	5.18	0.61	13.19	0.37	2.40	5.98	3.27	97.04	196.92
30.7	UBS	5.23	0.91	21.47	0.37	2.24	3.40	2.57		283.37
32.0	UBS	4.38	0.81	17.10	0.37	1.94	6.72	3.62	23.39	285.05
33.3	UBS	4.23	1.03	23.47	0.37	2.12	5.36	2.92	75.90	114.09
34.7	UBS	4.93	0.56	11.61	0.37	2.43	7.07	3.65	36.69	46.65
36.0	UBS	5.32	0.49	7.50	0.37	1.72	7.21	3.77	40.26	41.71
37.0	UBS	4.87	0.42	6.84	0.55	2.53	7.72	4.24	21.73	39.80
38.0	UBS	5.03	0.52	10.40	0.00	1.93	7.52	3.68	35.71	47.34
39.0	UBS			17.62	0.00	1.30	6.77	2.77	43.90	77.39
40.5	UBS	5.32	1.05	23.54	0.00	1.36	4.66	2.71	75.89	108.34
42.0	UBS	5.06	0.99	25.21	0.00	1.94	5.12	2.95	72.34	93.10
43.5	UBS	4.58	0.58	11.85	2.02	1.83	7.21	3.87	8.93	50.07
44.5	UBS	5.08	0.66	13.31	0.37	1.27	6.95	3.16	29.76	53.72
45.7	UBS	4.63	0.92	16.93	0.00	1.67	5.91	3.36	36.63	95.20
47.0	UBS	5.01	0.65	13.10	0.37	1.32	6.65	3.16	34.97	80.12
49.0	UBS	5.87	0.71	14.51	0.37	1.89	6.83	4.01	37.94	175.72
50.5	UBS	5.42	0.55	11.73	0.37	1.87	7.31	3.76	14.88	136.41
52.0	UGS	5.10	0.29	4.91	0.37	1.53	9.03	3.90	0.74	56.25
54.0	UGS	4.05	0.21	3.33	0.37	1.44	9.35	3.76	0.74	48.08
57.0	UGS	5.51	0.16	2.15	0.37	1.56	9.60	3.83	0.74	44.25
60.0	UGS	4.50	0.15	1.94	0.37	1.53	9.32	3.55	0.74	38.89
62.5	UGS	5.07	0.14	1.47	0.37	1.36	9.58	3.35	0.74	32.75
65.5	UGS	4.88	0.13	1.26	0.37	1.50	9.47	3.56	0.74	30.80
67.0	UGS	4.88	0.13	1.34	0.37	1.95	9.22	3.40	0.74	28.41
69.0	UGS	6.14	0.14	1.50	0.37	1.65	8.98	3.73	0.74	28.65
73.0	UGS	5.54	0.12	1.35	0.37	1.37	8.92	3.48	0.74	26.62

Table 4: ILH dataset for Hushpuckney Shale in southwest Iowa. Elemental concentrations were acquired using XRF analysis and measured in weight percent (wt%) for major elements and parts per million for trace elements (ppm). Facies acronyms: LBS=Lower Black Shale, MBS=Middle Black Shale, and UBS=Upper Black Shale.

Sample Height (cm)	Facies	$\delta^{15}N$ (‰)	TN (%)	TOC (%)	TIC (%)	TS (%)	Al (wt%)	Fe (wt%)	U (ppm)	Mo (ppm)
0.0	LBS	6.04		1.39	7.21	0.83	3.21	1.09	30.34	10.36
1.5	LBS	7.98		7.73	0.20	0.85	8.53	2.60	87.79	68.13
2.4	LBS			8.76	0.00	1.23	7.60	3.67	80.14	118.31
3.4	LBS			12.36	1.66	1.26	6.48	2.68	59.90	189.86
4.3	LBS	11.83		13.59	2.63	1.37	4.82	2.22	60.00	206.54
4.9	LBS			12.42	1.82	1.24	5.01	1.90	94.63	301.57
5.6	LBS			12.23	2.90	1.27	4.98	1.94	70.50	243.53
6.4	LBS			10.72	2.33	1.13	5.79	2.07	123.65	334.55
7.0	LBS	13.45		11.96	2.45	1.05	5.77	2.01	169.58	540.69
7.6	LBS			13.62	2.28	1.15	5.02	1.92	216.66	736.62
8.2	LBS			14.27	1.95	1.23	5.17	2.04	236.77	738.26
9.4	MBS	14.60		14.74	1.96	1.25	5.34	2.15	243.63	833.17
10.1	MBS			15.18	1.73	1.03	4.77	1.67	245.62	912.69
10.7	MBS			17.23	1.21	1.18	5.12	2.17	222.24	760.69
11.3	MBS	12.37		21.48	1.05	1.26	5.00	1.79	229.28	785.99
12.2	MBS			12.34	0.46	1.52	6.67	3.36	160.19	546.31
12.8	MBS	10.45		12.51	0.00	1.52	6.70	3.36	175.63	553.11
13.4	MBS			16.79	0.05	1.44	6.20	3.23	184.91	683.23
14.0	MBS	8.90		13.53	0.46	1.45	6.56	3.30	191.01	603.16
14.6	MBS			22.67	0.61	1.45	5.21	3.09	209.87	870.16
15.5	MBS			19.92	2.33	1.43	4.61	2.81	202.74	718.75
16.2	MBS	9.07		13.52	2.09	1.78	4.84	3.10	212.90	500.36
16.8	MBS			11.63	2.67	1.80	5.23	3.30	219.99	443.72
17.7	MBS			9.96	1.86	1.63	5.86	3.16	254.89	517.12
18.6	MBS	8.28		9.50	1.57	1.57	5.70	3.07	221.92	434.09

Table 4 (Continued)

19.5	MBS			10.63	1.31	1.55	5.69	3.11	231.44	488.28
20.4	MBS	7.80		13.03	1.33	1.39	6.01	2.98	230.51	539.04
21.0	MBS			17.31	1.46	1.39	5.14	3.12	225.32	571.35
21.6	MBS	6.60		19.40	1.60	1.36	5.40	3.03	435.10	499.48
22.2	MBS			26.80	0.00	1.47	5.15	2.82	374.84	568.42
23.2	MBS			20.23	0.00	1.29	5.87	2.89	213.11	824.25
24.4	MBS	5.91		29.47	0.00	1.42	4.52	2.86	229.28	1100.34
25.6	MBS			18.81	2.05	1.39	5.13	2.85	250.80	714.23
27.1	MBS			19.20	0.47	1.28	5.54	2.80	274.32	676.86
28.0	MBS	5.36		24.00	0.00	1.46	4.72	2.43	298.35	830.97
29.3	MBS			25.29	0.00	1.34	4.48	2.32	301.94	970.35
30.2	MBS	4.33		29.37	0.47	1.30	4.36	2.23	259.91	983.02
31.4	MBS			28.45	0.00	1.28	4.55	2.55	218.15	895.67
32.0	MBS	4.07		22.81	0.65	1.33	4.48	2.66	228.56	750.17
32.6	MBS			19.06	1.65	1.50	5.45	2.88	237.05	677.45
33.2	MBS			16.33	2.45	1.29	5.67	2.85	231.34	567.30
33.8	MBS			19.75	0.29	1.39	5.26	2.87	220.84	605.94
34.4	MBS			21.13	1.02	1.42	4.77	2.89	198.61	600.16
35.1	MBS			24.88	0.00	1.43	4.83	2.82	162.34	640.87
35.7	MBS	3.41		34.08	1.22	1.62	3.75	2.78	169.58	998.98
36.6	MBS			25.52	0.00	1.26	5.21	3.39	139.25	1198.50
37.2	UBS	3.13		31.85	1.44	1.48	4.21	3.04	108.91	1333.69
38.1	UBS			22.58	2.34	1.48	4.96	3.06	93.52	876.33
38.7	UBS	3.41		19.84	0.00	1.24	5.27	3.32	94.19	698.48
39.3	UBS					1.58	6.17	3.37	95.79	461.92
39.9	UBS			10.37	1.59	1.47	6.60	3.52	96.31	364.58
40.8	UBS	4.15				1.59	6.54	3.62	127.84	376.42
41.5	UBS			7.90	1.41	1.73	6.86	4.17	184.20	301.86
42.1	UBS			10.37	1.12	1.78	6.17	3.78	134.58	298.95

Table 4 (Continued)

42.7	UBS	4.27		10.00	1.54	1.67	6.10	3.59	116.93	325.74
43.6	UBS			12.24	1.49	1.51	5.69	3.35	129.04	359.11
44.2	UBS	2.32		16.83	0.88	1.64				
44.8	UBS			20.37	1.83	1.47	4.96	3.11	125.74	578.91
45.4	UBS	1.50		20.73	1.11	1.62	5.08	3.07	121.05	545.63
46.0	UBS			24.18	1.36	1.67	4.31	3.00	129.66	631.62
46.6	UBS			31.22	2.07	1.44	4.02	2.83	102.34	793.34
47.2	UBS	2.64		36.50	2.95	1.70	3.94	2.86	81.64	950.71
47.9	UBS			31.11	4.72	1.62	4.37	3.40	73.09	1184.77
48.5	UBS			24.57	0.48	1.53	5.81	4.00	72.63	1221.01
49.1	UBS	-0.56		18.27	0.00	1.71	5.98	4.35	58.11	1062.67
49.7	UBS			15.63	1.54	1.85	5.71	4.50	55.85	1092.70
50.3	UBS	0.53		23.85	0.00	1.69	5.57	4.35	54.15	1334.87
50.9	UBS			26.32	1.64	1.33	4.79	3.89	55.42	1152.17
51.5	UBS	2.03		1.42	24.30	1.49	4.89	3.13	47.87	301.34
52.1	UBS			31.59	4.02	1.47	4.69	3.04	49.64	655.53
52.7	UBS			14.71	1.85	1.55				
53.3	UBS			8.26	3.69	1.88	6.14	3.58	37.79	139.74
53.9	UBS					1.62	6.34	3.62	41.85	140.86
54.9	UBS			6.30	0.80	1.53	6.06	3.39	71.66	140.93
55.8	UBS	4.59		5.41	0.88	1.69	7.13	3.52	53.50	113.67
56.4	UBS			4.29	3.00	2.76	7.09	4.52	46.38	86.13
57.0	UBS			7.25	0.00	2.21	6.29	3.82	52.08	85.28
57.6	UBS			6.65	1.64	2.18	6.17	3.80	42.90	80.76
58.2	UBS	2.22		6.89	1.59	1.55	6.52	3.24	89.75	66.86
59.1	UBS			7.41			5.68	2.86	173.91	49.11
59.7	UBS			10.10	1.34	1.52	6.81	2.65	65.96	76.23
60.7	UBS			13.04	1.28	1.55	5.43	3.10	40.46	98.99
61.9	UBS			15.32	1.19	1.39	6.22	3.42	58.33	125.18

Table 4 (Continued)

63.1	UBS			17.60	1.05	1.45	6.69	3.47	37.74	168.54
64.3	UBS	4.68		20.88	0.73	1.35	5.39	3.11	126.44	162.61
65.5	UBS			20.71	0.89	1.60	5.64	3.22	29.99	207.61
66.4	UBS			20.49	0.51	1.60	6.05	3.49	27.16	217.44
67.4	UBS			21.68	0.56	1.50	5.94	3.25	26.29	243.25

Table 5: ELY-1 dataset for Hushpuckney Shale and underlying Womac Coal in southeast Illinois. Elemental concentrations were acquired using LA-ICP-MS analysis and measured in counts-per-second (cps). Facies acronyms: LBS=Lower Black Shale, MBS=Middle Black Shale, UBS=Upper Black Shale, and UGS=Upper Grey Shale.

Sample Height (cm)	Facies	$\delta^{15}N$ (‰)	TN (%)	TOC (%)	TIC (%)	TS (%)	Al (cps)	Fe (cps)	U (cps)	Mo (cps)
0.0	Coal	4.29	1.73	63.49	8.27	1.62	13947249	500251	181793	
1.2	Coal	4.71	1.65			1.77	14530330	621367	269231	
2.4	Coal	4.20	1.43	56.14	3.38	1.60	20875108	767377	253958	
3.7	Coal	4.71	1.58			2.93	13679098	1446603	514618	
4.9	Coal	4.88	1.44			3.04	14521575	1218252	366714	
6.4	Coal	5.13	1.57			2.68	14072508	939958	469710	
7.9	Coal	5.00	1.46			3.38	17450346	1600102	320202	
9.4	Coal	4.68	0.67	25.04	0.00	3.08	30074706	1753931	250488	
11.0	Coal	5.56	1.62	62.28	1.23	3.54	10423727	1249441	192391	
12.2	LBS	6.33	0.21	4.11	2.45	1.43	26953251	982966	115097	
13.4	LBS	11.89	0.65	14.99	1.95	1.30	24447096	988113	234250	
14.6	LBS	14.92	1.19	25.93	1.52	1.43	33743331	1510815	514529	
16.2	MBS	15.33	1.30	29.92	0.64	1.50	33009248	1479434	824728	
17.4	MBS	12.45	1.65	36.71	2.60	1.41	35339559	1645686	1482058	
18.6	MBS	10.76	1.30	30.24	0.00	1.35	22077991	873012	310202	
19.8	MBS	8.41	0.40	6.89	0.54	1.80	31118867	1096318	91379	
21.0	MBS	7.69	0.37	6.33	0.55	1.48	40090081	1484125	102880	
22.3	MBS	7.08	0.35	5.98	0.34	1.67	41998125	1562583	100107	
23.2	MBS	7.39	0.38	6.06	1.06	1.87	53178082	1912956	172798	
24.4	MBS	7.55	0.41	7.15	0.55	1.64	38846754	1377657	108311	
25.6	MBS	6.93	0.43	7.28	1.17	1.52	39217381	1304168	248151	
26.8	MBS	7.09	0.54	9.70	0.72	1.56	39430673	1384292	179488	
28.0	MBS	7.43	0.75	14.25	1.63	1.41	39082056	1417550	1578427	
29.3	MBS	8.45	1.45	30.98	0.88	1.38	34022969	1434417	1139391	
30.5	MBS	6.91	1.01	19.53	1.24	1.37	31723585	1170710	138824	

Table 5 (Continued)

32.0	MBS	6.66	1.05	21.32	0.23	1.39	32452817	1282306	126610
33.2	MBS	6.52	1.64	36.50	0.28	1.58	28815227	1271149	947650
34.4	MBS	6.70	1.45	33.76	0.87	1.56	29975682	1278101	3454847
35.7	MBS	3.97	0.67	13.24	0.00	1.68	52084266	1950852	451088
36.9	MBS	5.08	0.55	9.70	0.69	1.58	39184887	1359543	401585
37.8	MBS	5.91	1.37	28.74	1.96	1.80	29260376	1236895	1826696
38.7	MBS	5.46	1.34	29.19	1.62	1.34	22807270	1116724	3504889
39.6	MBS	6.18	1.62	33.47	0.78	1.56	31634713	1344973	214531
40.8	MBS	4.64	1.68	36.78	0.02	1.40	34027272	1420102	269304
41.8	MBS	3.51	1.56	33.65	0.79	1.33	16881364	757160	815763
42.7	MBS	3.78	1.73	39.04	0.00	1.51	27314817	1116319	1177900
43.6	MBS	3.92	1.75	38.62	0.96	1.50	24681478	1102826	1430037
44.5	MBS	4.73	1.60	33.43	1.93	1.41	27972732	1089123	179123
46.0	UBS	2.80	1.68	34.32	1.40	1.44	33841354	1363964	120193
47.5	UBS	4.21	1.59	34.75	2.85	3.58	19263261	1125298	1315693
49.1	UBS	3.66	0.73	14.72	1.00	2.23	32364411	1392928	426812
50.6	UBS	3.23	0.45	8.04	0.41	1.49	45016247	1666681	97015
51.2	UBS	3.09	1.58	30.73	2.40	1.33	35002929	1396773	126397
54.9	UBS	4.71	1.67	37.83	1.81	3.66	25886189	1586185	1638605
57.0	UBS	4.23	0.75	14.87	0.77	1.96	30132991	1223967	149187
58.8	UBS	4.24	0.46	8.15	0.51	1.48	40702265	1504923	91081
60.7	UGS	5.12	0.17	2.35	0.58	0.97	37746393	1213469	48850
62.5	UGS	5.18	0.15	1.86	1.00	2.25	38567730	1568390	39257
64.6	UGS	5.16	0.16	2.34	0.61	1.22	48607010	1822323	53371
66.4	UGS	5.18	0.15	2.06	0.73	1.14	30688197	1055968	32220
68.3	UGS	5.01	0.14	1.70	1.17	1.06	36538879	1246624	32056
70.1	UGS	4.97	0.13	1.74	0.62	1.08	40831831	1416754	40892
72.2	UGS	5.09	0.12	1.48	0.76	1.35	38861721	1473620	32074
74.1	UGS	4.56	0.12	1.40	0.87	0.72	51545788	1689397	41158

Table 5 (Continued)

78.0	UGS	5.22	0.10	0.86	2.50	2.10	34873454	1397149	27054	
82.6	UGS	4.05	0.11	1.05	1.56	0.90	42125205	1410381	18837	
89.3	UGS	4.17	0.12	1.15	0.58	0.31	50784323	1496446	21048	
90.8	UGS	3.47	0.11	1.04	0.00	0.10	46176256	1247631	15576	
92.0	UGS	4.03	0.12	1.05	0.00	0.09	56607359	1762470	16955	
95.1	UGS	3.87	0.12	1.06	0.00	0.09	46153327	1368457	14419	
96.3	UGS	4.14	0.12	1.06	0.82	0.22	48581474	1841369	22302	
97.8	UGS	4.14	0.11	1.09	0.91	0.10	49079403	2324711	17465	
100.9	UGS	3.91	0.12	1.03	0.48	0.10	48220042	1740553	14743	
113.1	UGS	4.02	0.12	1.04	0.26	0.08	51658211	1553541	12719	
120.7	UGS	3.90	0.12	1.04	0.28	0.10	45152172	1266930	11893	
129.8	UGS	3.49	0.10	1.11	0.42	0.22	43526003	1821555	11436	
140.5	UGS	3.76	0.11	1.13	0.49	0.19	46064068	1859015	12314	
150.9	UGS	3.60	0.11	1.14	0.49	0.16	48656745	2066469	14217	
158.8	UGS	3.44	0.11	1.11	0.52	0.15	54850215	2478460	17595	
169.5	UGS	3.38	0.10	1.12	0.40	0.14	38370152	1356783	9578	
180.7	UGS	3.56	0.11	1.13	0.46	0.17	42481074	1641719	13424	
191.4	UGS	3.64	0.11	1.26	0.46	0.21	45158178	1832568	12978	
205.7	UGS	3.79	0.10	1.14	0.48	0.15	47025439	2131996	12364	
219.8	UGS	3.12	0.09	1.16	0.00	0.13	55576630	2314569	14343	

VITA

Bryce Mathis was born and raised in Odessa, Texas where he grew up around the oil field environment of the Permian Basin. His passion for the great outdoors and natural science combined with knowledge of the petroleum industry, led him to pursue a career as a petroleum geologist. After graduating from Permian High School in 2009, he attended Texas Tech University where he received a Bachelor of Science in Geosciences in December of 2012.

In August 2013, Bryce entered the master's degree program at Louisiana State University in the Department of Geology and Geophysics where he received the Applied Depositional Geosystems Fellowship. Working with his advisor, Dr. Achim Herrmann, Bryce researched the geochemical properties and environmental mechanisms responsible for ancient black shale deposits, which serve as important petroleum source rocks and unconventional reservoirs. During his time at LSU, Bryce also participated in the American Association of Petroleum Geologists Imperial Barrel Award Program.